APPLYING A STATISTICAL APPROACH TO DEVELOP A SUSTAINABLE TECHNOLOGY FOR CAPTURING PHOSPHOROUS FROM AN AGRICULTURAL TILE DRAINAGE SYSTEM USING BY-PRODUCT PHOSPHOROUS SORBING MATERIALS (PSM)

by

Amir Kordijazi

A Dissertation Submitted in

Partial Fulfillment of the

Requirements for the Degree of

Doctor of Philosophy

in Engineering

at

The University of Wisconsin-Milwaukee

May 2021

ABSTRACT

APPLYING A STATISTICAL APPROACH TO DEVELOP A SUSTAINABLE TECHNOLOGY FOR CAPTURING PHOSPHOROUS FROM AN AGRICULTURAL TILE DRAINAGE SYSTEM USING BY-PRODUCT PHOSPHOROUS SORBING MATERIALS (PSM)

by

Amir Kordijazi

The University of Wisconsin-Milwaukee, 2021

Under the Supervision of Dr. Hamid Seifoddini

Due to nutrient pollution, agriculture is one of the major sources of pollution in water bodies. Every time it rains, fertilizers, pesticides, and animal waste wash nutrients and pathogens—such as bacteria and viruses—into waterways. As rainfall increases due to climate change, the water problem will worsen. One of the nutrients that extensively contributes to the degradation of water quality is phosphorous (P). In this research, the performance of electric arc furnace (EAF) steel slag was investigated as a P sorbing materials (PSM) according to the conditions present in a P removal structure designed for treating water discharge from an agricultural tile drainage system. Unlike the successful trials of removing P from water runoff, this promising PSM has not been successfully applied for removing phosphorous from water discharge from an agricultural tile drainage system. Consequently, this research aims to study the applicability of this material for this specific application. A simulated flow-through experiment was used to evaluate the P removal efficiency of the slag in different conditions. The effects of slag particle size distribution, presence of bucarbonate in inflow solution, incubation in an anaerobic condition, and chemical treatment on the adsorption capacity of the steel slag were studied**.** A statistical approach was used to determine the significant predictor variables, the empirical models of the design curves according

to each condition, and the type of correlation among the predictor variables and the response variable, namely, maximum removal capacity (mgP/Kg). The results show that reducing the slag particle size distribution and the presence of bicarbonate decrease the P removal capacity of the slag, while the aluminum treatment increases the P removal capacity and reduces the negative effect of bicarbonate on the P removal. Additionally, incubation in water with or without alkalinity does not seem to affect the P removal of the regular steel slag. The result of this study shed light on the reasons and potential solutions for the challenges regarding the application of the P removal structure filled with by-product PSM for treating water discharge from agricultural tile drainage systems.

TABLE OF CONTENTS

LIST OF FIGURES

LIST OF TABLES

ACKNOWLEDGMENTS

Pursuing my PhD degree was a long journey with many ups and downs. If it were not for God's mercy by giving me perseverance, wisdom and placing many wonderful supportive people along the way, I could not be where I am today. I would like to acknowledge some of those people who helped me along the way.

First, I wanted to thank Dr. Timothy Patrick, my former faculty advisor. Unfortunately, he is no longer with us, but following his supervision and guidance I was able to defend the proposal of this project. Second, I would like to thank Dr. Hamid Seifoddini, who kindly accepted to be my new advisor after Dr. Patrick passed away. Because of his mentorship, I was able to prepare this project for the defense. Third, special thanks to Dr. Chad Penn, my external committee member from the National Soil Erosion Research Laboratory at Purdue University. If he had not generously offered me the opportunity to conduct experiments in his lab, provided supervision along the way, and funded the project, I would have not been able to complete and defend the project. I learned a lot from him academically and personally, for which I am forever grateful. I wanted to thank few of his students and staff, specially Andre Defente, Rhonda Graef, and Isis Chagas, who helped me with the experimental works. I also wanted to thank my other committee members Dr. Benjamin Church, Dr. Matthew Petering, and Dr. Wilkistar Otieno for being a part of my committee, and providing their time, consideration, and insightful feedback to improve my dissertation. I first started conducting research about protecting water bodies from agricultural pollution especially phosphorous pollution in 2018 when I was working as a Research Assistant on a project funded by the Great Lake Protection Fund at Water Technology Accelerator of UWM directed by Dr. Marcia Silva. That experience helped me to learn about the importance of this issue specially in the Midwest area and the knowledge gap in the filed which led me to carry out the current project.

Last but not least, I would like to express my deepest gratitude to my wonderful support system of family and friends. If it were not for my mom and dad's continuous encouragement and support throughout my academic pursuit, I would not stand where I am standing now. Additionally, I would like to thank my dear sister and brother-in-law who I have looked up to many times and have tried to learn from their advice and experiences. Finally, I would like to thank Isamar Mayol Claderon, who has been very supportive during the hardest period of my PhD, which made stepping through this difficult path much easier.

1. Introduction

Due to nutrient pollution, agriculture is one of the major sources of pollution in water bodies, including rivers, streams, wetlands, and lakes [1]. Every time it rains, fertilizers, pesticides, and animal waste from farms and livestock operations wash nutrients and pathogens—such as bacteria and viruses—into our waterways. As rainfall increases due to climate change, the water problem will worsen [2]. Discharging excessive nutrients into water bodies leads to a phenomenon called eutrophication that has a detrimental effect on water quality by decreasing the dissolved oxygen levels and, in some cases, producing toxins [3, 4]. One of the nutrients that extensively contributes to eutrophication is phosphorous (P). Conventional Best Management Practices (BMP) have been used to prevent transportation of P to water bodies; however, they are ineffective in precluding losses of dissolved P, a form of P that is dissolved in water and is 100% bioavailable to aquatic ecosystem [3, 5]. The P removal structure, a new BMP that can decrease dissolved P loading, consists of P sorbing materials (PSM) and a structure that contains PSM. It can be applied to treat water discharged from agricultural runoff and subsurface drainage. As high P water flows through the PSMs, dissolved P is sorbed onto the materials, allowing low P water to continue to the outlet [5]. The P removal structure has been successfully used to remove P from water runoff [5, 6]; however, the feasibility of this practice for removing P from subsurface drainage has not been thoroughly examined.

The main research question of the current project is to determine the feasibility of removing P from agricultural subsurface drainage using by-product PSM. Research objectives will include a study of the effect of important parameters present in a tile drainage system on P removal efficiency of EAF by-product. These parameters are as follows:

- PSM particle size distribution
- Presence of competing ions in the discharged water (bicarbonate)
- Incubation time and solution, specific for the bottom-upward P removal structure
- Modification of PSM using chemical treatment

The overall goal of this project is to find solutions for the challenges of applying the P removal structure for subsurface drainage. To reach this goal, the first step is to estimate how much P a PSM can remove in each condition. This can be done by running a flow-through experiment that includes the use of an inflow P solution that is representative of drainage water and measure the P removal percentage by analyzing the outflow solution from a PSM column. Then, additional experiments such as buffer index, pH measurement, and Inductively Coupled Plasma Atomic Emission Spectroscopy (ICP AES) were conducted to investigate the mechanism of P removal of the PSM in each condition. Additionally, a chemical treatment of PSM was applied to change the P removal mechanism of PSM and its effect on the P removal capacity for different conditions was studied. This approach gives us valuable information about the effect of each parameter on the P removal performance of PSM. Using flow-through experiments results, an empirical model was developed for each condition. The model was used to estimate how much P a PSM can remove before it becomes exhausted. By using this information, the total mass of PSM and the footprint required for the P removal structure can be estimated. Finally, recommendations will be provided regarding what measures should be taken in order to make the application of PSM in removing P from subsurface drainage possible.

2. Background

2.1. Importance of the Great Lakes

The Great Lakes are the world's largest surface freshwater resource, 20% of the world and 85% of U.S. water [7]. The Lakes are not only vital for the ecosystem but also are central to the U.S. economy as well. Over 1.5 million jobs are water-dependent in the Great Lakes, generating $62 billion in wages [8]. Moreover, because it is a transboundary water source, between the U.S. and Canada (**Figure 1**), it can be considered as a national security issue if it gets overused or over-polluted. As Elhance [9] stated, "transboundary waters are one of the most urgent, complex, and contentious issues that the developing world and the international community will have to face and resolve in the next century." Therefore, preserving this valuable source of freshwater from overusing and polluting is essential from environmental, economic, and security points of view.

Figure 1. The Great Lakes [10]

There have been previous examples in history when the Great Lakes was in danger. One of the famous ones is over-pollution of Lake Erie (**Figure 2**) in the late 1960s when many people stated that "Lake Erie is dead." The reason for this belief was that factory pollutants and sewer waste were significantly polluting Lake Erie. Without many governmental restrictions, factories disposed of their pollutants into the lake and other waterways that flowed into it, such as the Cuyahoga River that caught on fire on various occasions. Soon, fish began to turn up dead along the shorelines of Lake Erie. In case a lake starts disappearing, millions of tons of dust, containing salt and chemical agriculture pesticides and fertilizers, blow off the lakebed each year that leads to migration of people from the area [11].

Figure 2. Lake Erie

2.2. Agriculture: the main source of water pollution

Seventy percent of water consumption worldwide are caused by agriculture [12]. According to the United States Environmental Protection Agency (U.S. EPA), agriculture is the main source of

pollution in rivers and streams, the second main source in wetlands, and the third main source in lakes [1]. **Figure 3** shows discharge of water from a farm into a river.

Figure 3. Discharge of water from a farm into a river [13]

The main reason agriculture is one of the major sources of water pollution is the lack of regulation. In 1972 the Clean Water Act was designed and passed to preserve water sources. The Act was a response to toxic pollution causing five major rivers to catch on fire: Cuyahoga (over 15 times), Buffalo, Rouge, Detroit, and Chicago. This Act was successful in terms of reducing general residential water use, reducing point source pollution, increasing funding for research, remediation, technology improving water treatment systems, and improving the health of many rivers and lakes. However, it was not successful in reducing nonpoint source pollution.

2.3. Point source and non-point source pollution

Point source pollution refers to contamination that derives from one source. Examples of point source pollution are wastewater/effluent discharged by a manufacturer, an oil refinery, and a wastewater treatment facility. In an attempt to control point source pollution, the EPA regulates what and how much can be discharged by a facility directly into a body of water.

Nonpoint source pollution refers to contamination that originates from multiple sources. Examples of non-point pollutions are agricultural, or stormwater runoff and debris blown into waterways from land. Nonpoint source pollution is the primary cause of water pollution in the U.S. However, it is difficult to regulate, as it comes from different sources and there is no single entity to regulate [2].

2.4. Nutrient pollution

Every time it rains, fertilizers, pesticides, and animal waste from farms and livestock operations wash nutrients and pathogens—such as bacteria and viruses—into our waterways. As rainfall increases due to climate change, the water problem will worsen [2]. Natural resource professionals consider phosphorus and total suspended sediment (TSS) to be the most harmful components of nonpoint or runoff pollution. Having too many nutrients impacts the water quality by contributing to excessive plant growth primarily in rivers and lakes. Phosphorus is the nutrient that most significantly promotes macrophyte and algae growth. **Figure 4** shows the spread of algae blooms in the Great Lakes.

Figure 4. A satellite image of algal blooms around the Great Lakes

Algal blooms are a toxic soup of blue-green algae. Some of the causes of algal growth (excess algae) include too many nutrients, warm water temperatures, and reduced flow. Algae blooms can cause damage to aquatic life by reducing oxygen levels, clogging fish gills, and suffocating streams, lake beds, and underwater vegetation. Some algae blooms can produce toxins that are detrimental to humans, pets, wildlife, and livestock when consumed [1]. **Figure 5** shows the spread of algae blooms that caused the death of fishes in Lake Erie.

Figure 5. Algal bloom in Lake Erie causing the death of fishes

Excessive algae growth is induced when a water body becomes excessively enriched with minerals and nutrients, which is called eutrophication. There are two types of eutrophication: natural and cultural. In natural eutrophication, there is an accumulation of nutrients, sediments, and plant material for many lakes as they age over decades that gradually fill the lake basin. On the other hand, human-induced freshwater eutrophication, also known as cultural eutrophication, is largely due to increased inputs of phosphorus from sources such as agricultural fertilizers or partially treated sewage. **Figure 6** depicts the difference between natural vs. cultural eutrophication [14].

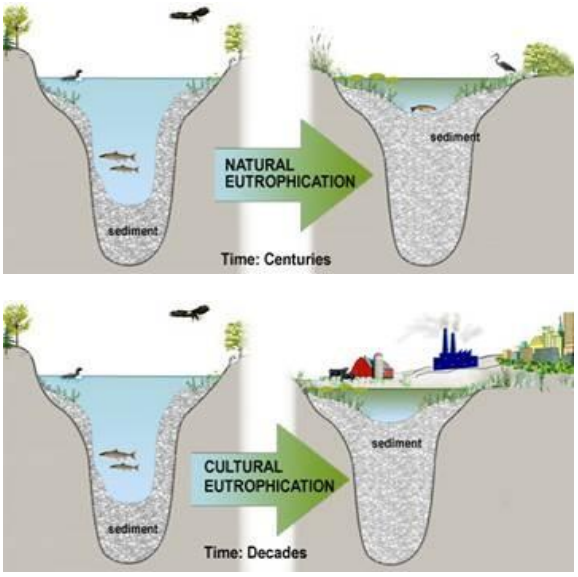

Figure 6. Natural eutrophication vs. cultural eutrophication [14]

2.5. Tile drainage system

Nutrient from agricultural farms transports to water bodies through either water runoff or subsurface tile drainage system [15]. Since the focus of this study is removing P from the tile drainage system, it is necessary to explain this system. Tile drain, as shown in **Figure 7**, is buried perforated corrugated pipe that removes excess subsurface water from the soil. Contrary to irrigation that provides additional water for the soil when it is too dry, drainage reduces the

moisture in soil, which in turn increases the air in the pores to improve soil conditions for optimal growth of crops. Artificial drainage improves crops for farmers by allowing the work to be done in a timely manner and with adequate root aeration [1, 16].

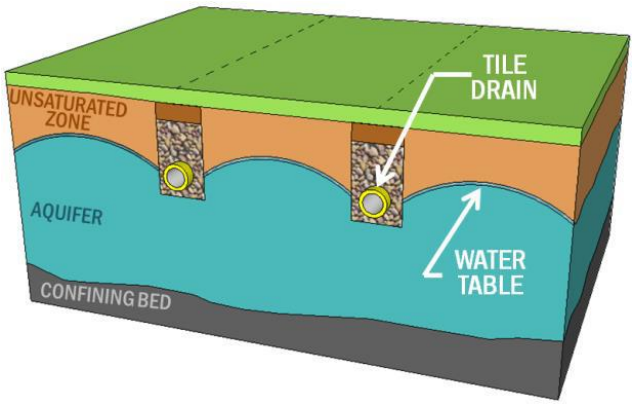

Figure 7. Subsurface drain tile [17]

The tile drainage system, as shown in **Figure 8**, is a network of below-ground pipes that allow water beneath the surface to flow from between soil particles into the tile line. Often, the water that flows through tile lines ends up in surface water points such as lakes, streams, and rivers that are at a lower elevation than the source. The tile drainage system is extensive in flat regions with poor drainage such as the glaciated Midwest. In the U.S., agricultural drainage is greater than 76 million acres, mostly in the upper Midwest Corn Belt that covers more than 50% of the land available to 114 counties [17]. Most phosphorous transported to the water bodies is coming from the tile drainage system.

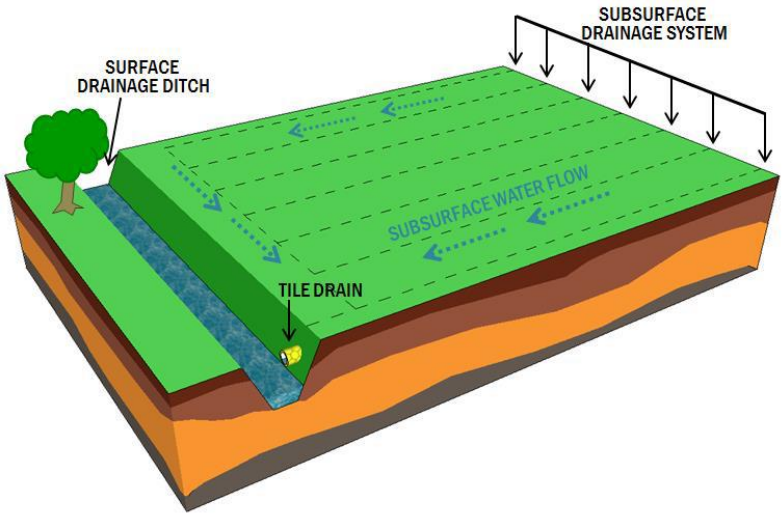

Figure 8. Subsurface tile drain system [17]

3. Literature review

3.1. Current best management practices (BMP)

There are two main sources of non-point P, incidental and legacy P. If the source of P transported is a non-soil P source, i.e., fertilizer or organic compounds such as compost and manure, it is called incidental P. When this applied P reacts with soil, it becomes part of the soil P pool that is called legacy P. This term is used to describe the P "build-up" within soils due to prior management. [18].

Phosphorous transported to water bodies has two different forms: particulate P and dissolved P. Dissolved P, which simply means dissolved P in water, is 100% biologically available to aquatic life. It is often in the form of the phosphate polyatomic anion or PO_4^{3-}, whereas particulate P is the P that is bound to soil and in the composition of different minerals [18].

Best management practices (BMP) have been applied to control the transportation of legacy P to water bodies. These practices can be classified in three main stages: prevention of legacy P, containment of the P on-site, and remediation of the legacy P. The goal of the first stage is

preventing soils from becoming a legacy P source, whereas the second stage is applied when the practices in the first stage failed to prevent P build up in soil. The main goal of the second stage is to reduce the loss of P in runoff and drainage water. Since 100% of phosphorous containment is not possible by the second stage, the third stage needs to be applied to reduce P transportation [19, 20]. These three stages and the practices used for each stage are shown in **Figure 9**.

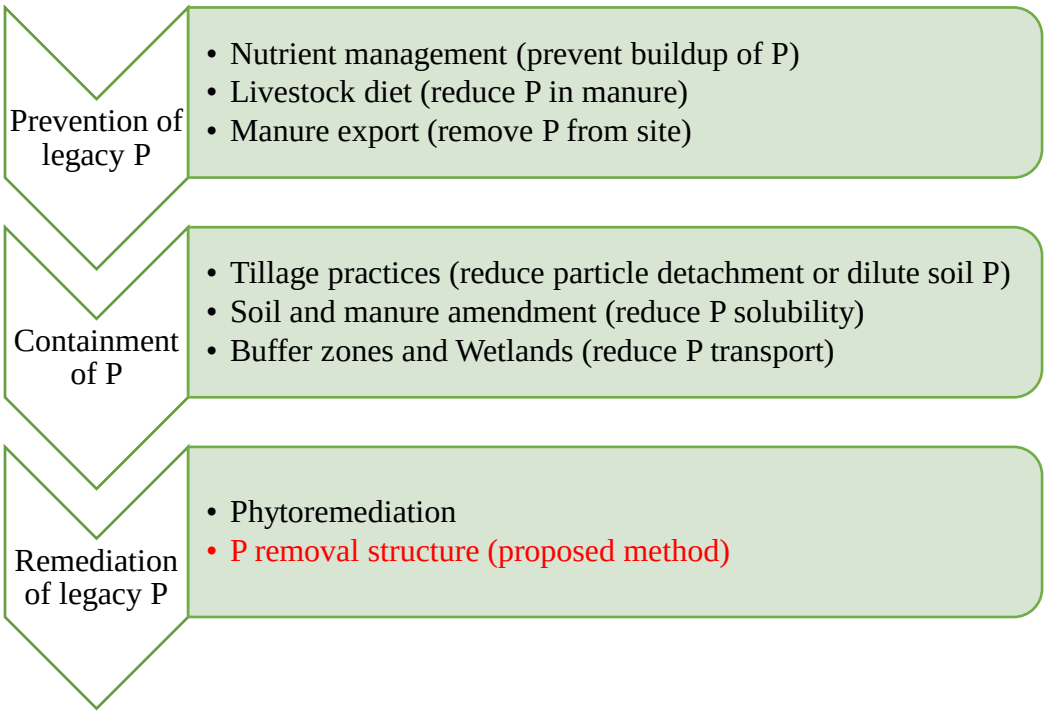

Figure 9. Three stages of legacy P management

Although current BMPs are effective in reducing particulate P transport, they appear to be mostly ineffective for dissolved P loss from legacy P pools. This is because most BMPs focus on decreasing erosion or adding fertilizer underneath the surface [5].

3.2. P removal structure: new BMP

P removal structure filled with PSM is a new BMP that can be used as a relatively fast method to remove the problem of excessive dissolved P losses in drainage water [21].

Any P removal structure should have four components in order to be effective: (1) an effective PSM in a sufficient quantity, (2) containment of the PSM, (3) the ability to replace the PSM when necessary, and (4) passive drainage via gravity at sufficient flow rates suitable for the site [18]. Based on the application of the P removal structure, it can take different forms such as a modular box, a surface-confined bed, cartridges, a blind surface inlet, etc. **Figure 10** is an illustration of the basic premise of a P removal structure and **Figure 11** shows different forms of P removal structures.

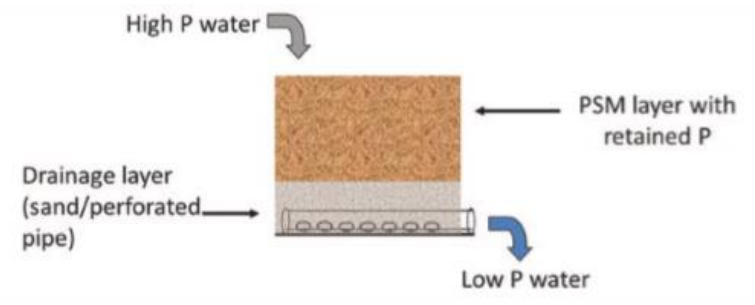

Figure 10. Three stages of legacy P management [20]

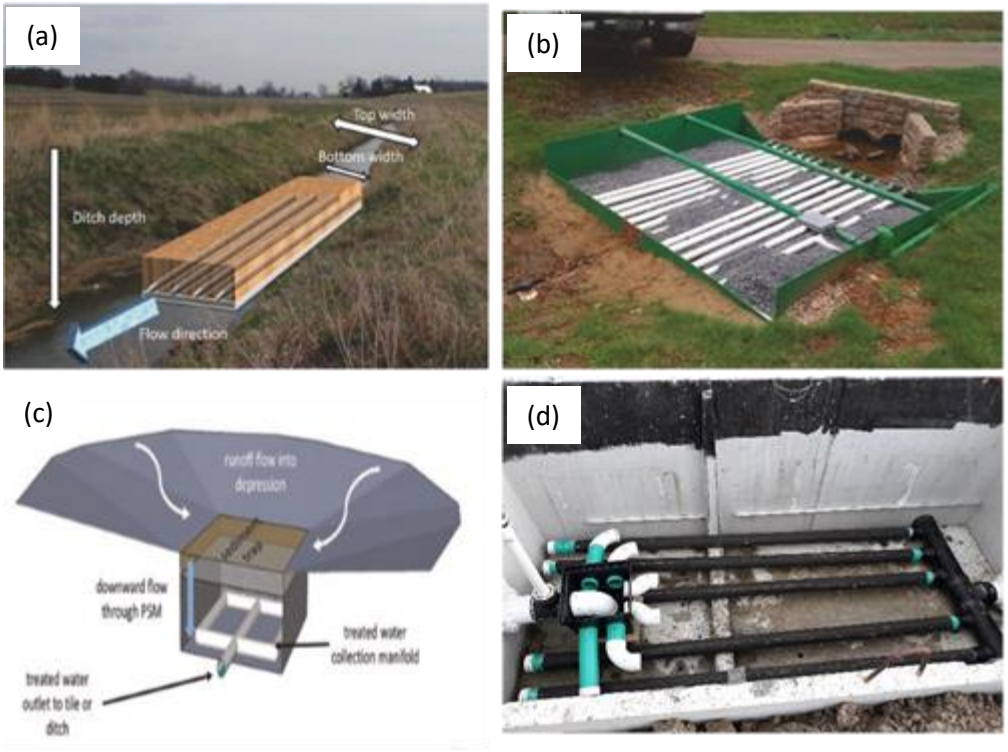

Figure 11. P removal structures used for removal of P from (a) ditch, (b) golf course, (c) poorly drained soil, and (d) subsurface tile drain [20]

For the design of the P removal structure three important considerations should be taken, as follows: (1) site hydrology and water quality characteristics; (2) target P removal and lifetime; and (3) PSM characteristics. The size of the P removal structure (i.e., mass and volume of PSM) is mainly determined by the P adsorption capacity of PSM in the field condition. In order to estimate the P removal ability of PSM, a design curve should be obtained. The design curve is a mathematical relationship between the P removal percentage and the P added to the structure. This will be discussed more in detail in the methodology section. According to the design curve, it will be estimated how much PSM is needed to meet a specific P removal target. The footprint and consequently the cost of the P removal structure is mostly dictated by the volume and mass of PSM required.

Error! Reference source not found. lists a chronological order of different P removal structures, t heir application, and the PSM used for each structure. As the table shows, the P removal structure can be utilized for treating any dissolved P sources, including urban, agricultural, golf course, horticultural, and wastewater. However, feasibility of this new BMP for treating the agricultural drainage water system needs to be more investigated.

Table 1. Chronological order of P removal structure

Year	**Structure**	**PSM**	**Application**	**References**
1997	Confined bed	Marvel gravel	Swine farm wastewater	[22]
2003	Confined bed	Calcite	Municipal water	[23]
2005	Confined bed	Shell sand	Domestic wastewater	[24]
2006	Confined bed	Melter slag	Municipal wastewater	[25]
2006	Confined bed	Filtralite-P™	Municipal wastewater	[26]
2007	Confined bed	EAF slag	Dairy effluent	[27]
2007	Confined bed/ditch filter	AMDR	Agricultural runoff	[6]
2009	Confined bed	AMDR	Municipal wastewater	[28]
2010	Confined bed/large cartridge filter	Ca-rich hydrated oil shale ash	Municipal wastewater	[29]
2011	Cartridge filter	Blast furnace slag	Golf course drainage	[30]
2011	Pond filter	EAF	Recirculating urban pond	[31]
2012	Confined bed	EAF	Golf course and residential runoff	[21]
2012	Ditch filter	FGD gypsum	Agricultural runoff	[32]

2012	Runoff interception trenches (confined bed)	Burnt lime, spent lime by-product, mixed lime	Agricultural runoff	[33]
2013	Bio-retention cell	WTR	Urban stormwater runoff	[34]
2014	Runoff interception trenches (confined bed)	EAF	Turfgrass runoff	[35]
2014	Confined bed	EAF	Golf course and residential runoff	[36]
2015	Recirculating domestic wastewater	EAF	Recirculating domestic wastewater	[37]
2015	Confined bed	Sachtofer PR®	Agricultural runoff	[38]
2015	Bio-retention cell	Fly-ash	Urban runoff	[39]
2016	Confined bed	AMDR	Fish hatchery effluent	[40]
2016	Modular box	EAF	Agricultural runoff	[41]
2016	Ditch filter	EAF and FGD	Agricultural runoff	[41]
2017	Constructed wetland	thermally-treated calcium-rich attapulgite (TCAP)	Municipal wastewater	[42]
2018	Confined bed	Fe-coated sand (-glauconite)	Agricultural drainage water	[43]

3.3 P Sorbing Materials (PSM)

PSMs are unconsolidated solids that have a strong affinity to bond with dissolved phosphorous and can be considered as the heart of the P removal structure. An effective PSM should be able to sorb an acceptable level of P in a timely fashion, conduct water through it at a flow rate acceptable for field application, and be safe for the environment. In general, these materials are rich in aluminum, iron, calcium, magnesium, and some rare earth elements such as lanthanum. Being unconsolidated is necessary for PSM because it allows water to pass through the materials. This leads to direct contact between liquid with high dissolved P concentration and PSM [20].

In one classification, PSM can be categorized into two main classes: by-product and manufactured PSM. Many PSMs are by-products from the waste stream of several industries such as steel production, mining operations, the coal-fired power industry, wastewater treatment plants, and the metal casting industry. By-products from steel production are mainly known as steel slag and are usually rich in Fe, Al, Ca, and Si. The main types of steel slag are blast oxygen furnace (BOF), electric arc furnace (EAF), and melter slag. BOF and EAF are usually rich in Ca. **Figure 12** shows a sample of EAF that is used in this study. Acid amine drainage residual (AMDR) is another type of PSM that is a by-product of mining operations, specifically from coal mines. These materials also tend to be rich in Ca. Several by-products of coal-fired power industries also can be used as PSM, such as flue gas desulfurization (FGD) gypsum, fly-ash, and bottom ash. These materials can remove P through a reaction between Ca and phosphate. The main disadvantages of these materials are that they have very small particle size that limits their ability to convey water. Water treatment residual (WTR), the sediment resulted from reactions occurring in wastewater treatment plants (WWTP), have a strong affinity to P and also can serve as PSM. Their sorption capability is higher compared with other PSM; however, their major disadvantage is their poor ability to conduct water through them. Finally, in certain types of metal casting, sand, known as “foundry

sand," is used as a mold for the molten metal. After continuous use this sand becomes rich in Al and Fe, which makes it a potential PSM. Due to the sandy texture, the sand molds have a superior ability to conduct water. However, the disadvantages of these types of PSM is that sometimes they contain trace metals and organic compounds that were used as binders during the casting process making them unsafe for the environment [20]. **Table 2** lists a chronological order of different potential PSM and their main metal sorbing element.

Figure 12. EAF steel slag as a potential PSM

Table 2. Chronological order of different potential PSM and their main metal sorbing element

Year	PSM	Main P sorbing element	References
1998	Bauxite waste	Ca, Mg, Al, and Fe; varies	[44]
1999	Wollastonite	Ca	[45]
2000	Crushed seashells/marl	Ca	[46]
2002	Fly ash	Ca, Mg, Al, and Fe; varies	[47]
2005	Melter Slag	Ca, Mg, Al, and Fe; varies	[48]
2006	Serpentine	Mg	[49]
2008	Fe-coated sand	Fe	[50]
2008	Biotite	Al and Fe	[51]
2009	AMDR	Ca, Al, Fe; varies	[52]

2010	Oil shale ash	Ca	[29]
2011	FGD	Ca	[53]
2012	WTR	Ca, Mg, Al, and Fe; varies	[54]
2015	Blast furnace slag	Ca, Mg, Al, and Fe; varies	[55]
2015	Crushed concrete	Ca	[55]
2016	Electric arc furnace slag	Ca, Mg, Al, and Fe; varies	[41]
2017	$Ca(OH)_2$ treated zeolite	Ca	[56]
2018	Fe-coated sand - glauconite	Fe	[43]
2019	Fe oxide-coated diatomite	Fe	[57]

The second type of PSM is manufactured PSM. These materials have almost the same composition compared with by-products and are rich in Al and Fe. Beside high adsorption capacity, one main advantage of this type of PSM is that they are created with ideal particle size distribution. This quality causes a high flow rate that can be achieved by using these materials and makes them a perfect choice for P removal structure. **Figure 13** shows a sample of manufactured PSM, activated alumina that has a high adsorption capacity and uniform particle size distribution. However, the main disadvantage of these materials in comparison with by-products is their high cost. The cost of manufactured PSM ranges from eight to forty dollars per pound, while the cost of some by-product is in the range of two to ten dollars per ton [20].

Figure 13. Activated alumina, a manufactured PSM

Based on the P removal mechanism, PSM can be categorized into two classes: Ca-based and Al/Fe-based. Ca-based PSM removes P through "precipitation," while Al/Fe-based PSM removes P by a "ligand exchange" mechanism.

In the precipitation mechanism, dissolved P in solution (i.e., phosphate) reacts with a dissolved metal cation. These two form a new solid by precipitation that takes dissolved P out of the solution. The following reaction shows a simplified generic precipitation:

$$aM^{m+} + bL^{n+} \leftrightarrow M_aL_b \text{ (solid)}$$

Where M is a metal such as Ca and L is a ligand (e.g., phosphate PO_4^{3-}). The Ca-based PSM must be capable of two factors in order to be efficient in removing P from a solution: (1) dissolve enough Ca^{2+} into the solution (2) Maintain and buffer the pH to a high enough level (above 6.5) [58, 59]. The following reaction shows the precipitation mechanism used by Ca-based PSMs to remove dissolved phosphorus from a solution:

$$Ca^{2+} + H_2PO_4^- + 2H_2O \leftrightarrow CaHPO_4.2H_2O_{(solid)} + H^+$$

On the other hand, ligand exchange is a process that happens only on variable charged minerals. The surface charges of these minerals vary as a function of pH. By increasing pH, the surface becomes more negative because of attaching hydroxide ions to the surface. As pH decreases, the surface terminal functional groups become more positively charged. The following reaction shows an example of a ligand exchange reaction for P onto a variable charged functional group

$$\text{---}\ MOH_2^{+0.5} + H_2PO_4^- \longrightarrow MOPO_3H_2^{-0.5} + H_2O$$

Where the line indicates that the functional group is connected to a PSM and where M is Al or Fe are contained in an oxy/hydroxide.

There are different parameters that can affect P removal performance of PSM such as inflow P concentration, retention time (RT), pH, PSM composition, buffer capacity, and co-existing ions. The most important factors affecting adsorption capacity of a PSM, the maximum amount of P that can be sorbed by PSM in each condition, are inflow P concentration and retention time. Retention time is defined as the amount of time that the PSM is in contact with the solution. As a rule of thumb, higher inflow P concentration almost always increases the total amount of P removed. Increasing retention time also increases P sorption, but there are some PSM that are not sensitive to retention time. P sorption capacity can be also dependent on pH, buffer index, etc. For example, Ca-based PSM is highly sensitive to pH; increasing pH causes an increase in sorption capacity [20]. **Table 3** lists a chronological order of studies where the effect of different parameters on P removal performance of specific PSM were investigated.

Table 3. Chronological order of studies where the effect of different parameters on P removal performance of specific PSM were investigated

Year	PSM	Parameters studied	References
2008	La-coated zeolite	pH, competing ions	[60]

2010	Oil shale ash	Ash composition	[29]
2011	La-treated silica	PSM composition, RT	[61]
2011	Fly-ash, Bauxite, WTR, FGD, AMDR	pH, buffer capacity, ionic strength	[53]
2012	Minnesota Filter (Metal fabrication shavings and iron filings)	RT, P concentration, the ratio of PSM and sand	[62]
2012	Electric arc furnace slag	hydraulic head, water velocity, RT, P concentration	[63]
2014	Crushed autoclaved aerated concrete	RT, P concentration	[64]
2015	Blast furnace slag, concrete waste	RT, P concentration, pH	[55]
2016	AMDR, EAF, FGD	Materials characteristics, RT, P concentration	[41]
2017	$Ca(OH)_2$ treated zeolite	pH, P concentration, T, co-existing ions, organic matter	[56]
2018	Fe-coated sand - glauconite	Composition, particle size distribution, bulk density	[43]
2019	Fe oxide-coated diatomite	P concentration, RT, the coating method	[57]

Although PSMs show promising results in removing phosphorus in laboratory-scale experiments, they do not show the same performance for large-scale applications specifically for removing P

from tile drainage water. There are some parameters in the large-scale application that might reduce efficiency of PSM in P removal and not be considered in the lab-scale experiment in the first place. One of the objectives of this project is studying the effect of these parameters in P removal efficiency of PSM. The parameters that were studied in this project are competing ions, particle size distribution, and the effect of aging. A chemical treatment method was used to increase the P sorption capability of a PSM. The current project aims to develop this practice for the treatment of subsurface tile drainage water, since to date it has not been successfully applied for this application. The PSM that was studied for this project is steel slag from EAF, which is a Ca-based PSM. It should be noted that the EAF slags contain an appreciable amount of Fe and Al, but this does not mean they are Al/Fe-based slags. For a material to be able to remove P by a ligand exchange mechanism in addition to containing a considerable amount of Al and Fe, these elements should be in the proper form and "active" [20].

3.3.1 Application of slag materials as PSM

Minable stocks of phosphorus are being reduced and would need to be replaced by the recovery of P that is already depleted from the agricultural system, creating problems with water quality. Agricultural runoff and erosion (46% of mined P globally) and animal waste (40%) are the two main flows of lost P [65]. Since the 1950s, the development of technologies of phosphorus removal has been studied in response to the issue of P loss and consequent eutrophication [66].

In the late 1980s, research was initiated on the possible use of natural and industrial by-products in on-site treatment systems for the removal of P from wastewater, along with the development of constructed wetlands (CW), a low-cost technology for the treatment of point-source pollution [67, 68]. In laboratory and pilot scale studies around the world, over 100 materials have been tested for

P retention capability. The P removal efficacy of many of these materials has been compared by systematic reviews of the published literature. [69–71].

Alkaline granular filters (AGFs) are passive reactive filters with sizes ranging from sand to gravel that are effective in eliminating phosphorus (P) from runoff and wastewater. P removal occurs in AGFs by precipitation of phosphate minerals associated with a pH increase caused by reactive media dissolution (reaching as high as pH 13). Industrial by-products (fly ash, electric arc furnace slag, basic oxygen furnace slag, blast furnace slag), natural media (bauxite, calcite, seashells, apatite), or manmade media are examples of AGF media [71, 72]. To date, several problems have restricted the implementation of AGFs in full-scale applications: long-term phosphorus removal performance, uncertainty about durability estimation, management of used media, alkaline effluent neutralization, capitalization and maintenance costs, and clogging [73]. Steel slags, a co-product of the manufacture of steel, have shown the greatest potential to remove P from a range of waste water sources [31]. Steel slags were primarily used in many areas of application (cement processing, road construction), but there is a promising market for wastewater treatment [74, 75].

One of the factors that make slag a suitable PSM is its environmentally friendliness characteristics. Because of its chemical and physical properties, slag is identified as non-hazardous waste. Low-level emissions of chromium, lead , nickel and molybdenum, below the maximum allowed limits, have been observed [76, 77]. Research into these issues has concluded that the use of slag does not pose any environmental or health threats, as heavy metals are tightly bound within the slag matrix [75, 78, 79]. Toxicity testing showed that slags are unlikely to leach large amounts of potentially harmful elements, exhibiting potential for use as environmental modifications. If used as filtration media for freshwater, other considerations such as the presence of dissolved organic matter are likely to further reduce the toxicity of these slags to the receiving environment [80, 81].

3.3.2 Different types of slags as PSM

Different types of slag, each with its own distinctive composition, may be generated depending on the method from which it is generated. [78]. These include: Electric Arc Furnace steel slag (EAF) from steel production; Blast Furnace iron slag (BFS) from iron production; Basic Oxygen Furnace steel slag (BOF) from steel production; and Melter slag. Iron and calcium have been identified as the primary constituents of EAF [82], while the main components of BFS are silica and alumina. BOF is composed of significant iron- and calcium oxyhydroxide concentrations [78] and melter slag is rich in titanium/aluminum [75, 82].

Another by-product of the manufacturing process that can be used as PSM is argon oxygen decarburization (AOD) slag. For every ton of stainless steel made, 270 kg of AOD slag is produced. This slag is primarily used in the manufacture of cement, road construction, fertilizer production and the regular covering of landfills [83]. However, these applications do not fully utilize the enormous volume of the slag produced and thus there are accumulating volumes of AOD slag. Therefore, alternative uses of AOD slag are being explored. In the form of easily soluble calcium silicate [84–86], AOD slag is stated to have a high alkalinity and to contain more than 35% Ca. Therefore, through calcium phosphate precipitation, it may be a promising wastewater treatment material for P removal and recovery [87].

One of the important sources for the recovery of metals from their waste is the steelmaking industry. The main reaction in the steel industry is the oxidation of these metals by dissolved oxygen in hot metals, as follows [88]:

$Fe + O \rightarrow FeO$,

$Mn + O \rightarrow MnO$,

$C + O \rightarrow CO$,

$Ca + O \rightarrow CaO$,

$Mg + O \rightarrow MgO$,

$Si + O \rightarrow SiO_2$,

$2P + 5O \rightarrow P_2O_5$.

As the gas (CO), elemental carbon is removed while all other impurities are transformed into metal oxides, which are then made to float on the surface of the molten metal during the hot metal to steel refining process. Lighter than molten steel, the floated residues form an immiscible phase on the top of the molten steel [89]. Steel slag is a non-metallic solid residue formed in various types of furnaces during the manufacture of steel and iron and contributes to approximately 10-15 percent of the steel produced. Slag has a lower density than steel in steel manufacturing. Consequently, it floats to the top of the molten steel bath. At temperatures around 1600 ° C, the liquid slag is tapped and solidified by air-cooling or other techniques [76, 78].

3.3.3 EAF slag

During crude steelmaking, EAF slag is produced through the electric arc furnace. Steel scrap, together with limestone or dolomite fluxes, is heated by an electrical current to form a liquid phase. The removal of phosphorus, silicon , manganese and carbon, sulphur, and aluminium from steel is taken into account in the EAF refining process [90]. The removal of silicates and phosphorus chemicals from molten steel is commonly obtained by the addition of lime (CaO) or dolomite [91]. For melting minerals and fluxes, energy is given by an electric arc. The fluxes are combined with the non-metallic scrap components during the melting process. The nonsteel elements form a liquid

slag after the reaction is completed. The primary concern in steelmaking is hydrogen and nitrogen as dissolved gases. During the refining stage, iron oxides react with the carbon present in the bath and carbon monoxide gases are formed. By increasing the amount of CO gases, scrap melt begins to boil, leading to the removal of impurities such as phosphorus, hydrogen, nitrogen and non-metallic compounds. After vaporizing the gaseous impurities, the liquid state survives as slag [92]. Steel is drained from the furnace through a submerged top-hole in the tapping process and the slag is poured out during the superheating phase from the slag door. The molten slag is then solidified into a rock-like substance [76, 93].

EAF is widely employed in construction, cement manufacturing, transportation industry (aggregate in road construction and maintenance), and wastewater and water treatment [75]. It has been also applied as a daily and final landfill cover material [78], Portland cement additive [94], an agricultural fertilizer [95], and in mineral CO_2 sequestration [96, 97]. Moreover, EAF has been applied in wastewater treatment [98] and as an inexpensive material for the remediation of the environment [99]. Slag is known as waste that is non-hazardous and that can be disposed of in suitable landfills. Sealing aggregate (skid resistant), asphalt aggregate, base, sub-base, construction fills, subsoil drains, grit blasting and wastewater treatment are common applications for slags [93].

3.3.4 Field-scale application of slag

There are some challenges that need to be resolved for scaling up P removal structures. These challenges are preferential flow, variability in incoming flow (volume and chemistry), clogging due to suspended and possibly material alterations, as well as decreased retention capacity as a result of organic material contamination or competition from other elements. P exists in inorganic

and organic forms under field conditions, while laboratory experiments use mostly inorganic P, which can also affect outcomes. In the development of P filters, adequate contact time between the filter material and the flow solution is likewise a critical factor. Numerous studies have demonstrated that some materials can remove P from household waste water or agricultural runoff, but further investigations are necessary to optimize the design of filter beds for field conditions [100]. While several slags show promise to extract P from effluent, a few field-scale installations of active slag filters for wastewater treatment have been reported. Active melter slag filters have been developed in New Zealand to treat effluent from a number of waste stabilization ponds [25, 48, 101]. These filters have been highly effective in reducing effluent P levels, with removal efficiencies ranging from 54% to 84%.[101, 102]. Two field-scale applications of slags for P removal from agricultural wastewater are constructed wetland and tile drainage system.

Constructed wetland (CW) technology was introduced as an alternative ecological technology for wastewater treatment in the 1970s. Compared with traditional wastewater treatment plants, CW has many benefits, such as low investment, maintenance and operational costs [103]. The constructed wetland system can be also employed as a low-cost and inexpensive method for phosphorus treatment of wastewater [104, 105]. Adsorption by media, precipitation in the water column, plant absorption, wetland soil accretions and microbial immobilization are the P removal mechanisms in CWs [106–111]. However, removal occurs primarily as a consequence of adsorption and precipitation reactions in the sand, gravel substrate and sediment of CWs with Al , Fe, Ca, and clay minerals [112, 113]. In the late 1980s, research was conducted on the possible use of industrial byproducts for treatment systems to eliminate phosphorus from wastewater. The removal of phosphorus was carried out along with the development of constructed wetlands (CW). In this system, slag plays an important role in the absorption of impurities, in particular,

phosphorus. Steel slag, in combination with small secondary treatment systems (such as CW), has been demonstrated to be an attractive approach compared with other methods [49, 114, 115].

A common practice in the Midwestern United States and many other areas is the construction of subsurface drainage in poorly drained agricultural fields [116]. It is estimated that for 25% of cropland in the United States and Canada, subsurface drainage has made farming possible [117] and enhanced yield by 5 to 25 percent in some areas [118] by reducing shallow water tables to eliminate excess soil moisture. Subsurface drainage, however, provides a clear route for the transport of nutrients into surface waters [116]. The phase of eutrophication can be exacerbated by excess nutrient loading on surface waters, leading to reduced water quality, toxic algal blooms, anoxia, and loss of aquatic life [119]. In surface waters, phosphorus (P) has been commonly established as the limiting nutrient and excess total P concentrations > 0.02 mg / L are also viewed as problematic [120, 121]. In agricultural ecosystems, surface runoff and subsurface flow are the two main routes for transporting P. Owing to reduced concentrations and the capacity of subsoil to bind P, early work identified surface runoff as the primary method of P transport and P contributions from subsurface flow were often considered negligible [122]. Several studies, however, have found subsurface drainage to be an effective pathway for the export of P to water bodies [123–126]. Dissolved P, which is 100 percent biologically accessible for aquatic life, is usually dominated by subsurface drainage [127]. King et al. [124] reported in an eight-year analysis that subsurface drainage is responsible for 48% of the dissolved P transported from a watershed in central Ohio and surpassed the 0.02 mg/L threshold by more than 90% of the measured concentrations. Gentry et al. [123] analyzed dissolved P concentrations in three central Illinois watersheds as high as 1.25 mg/L discharged from subsurface drainage. Management practices must be established to eliminate P from agricultural subsurface drainage in order to

minimize P depletion and avoid further harm to surface water ecosystems [128]. Application of slag has exhibited a low-cost and sustainable method for capturing P discharge from tile drainage [129].

3.3.5 Regeneration of slag

An emerging field of research on phosphorus retention materials is the rejuvenation of spent materials. Rejuvenation, also called regeneration, represents the method of recovering used PSM with reduced potential for phosphorus retention to a state similar to or at best equivalent to the fresh material. Rejuvenation of spent materials with less expensive maintenance results in phosphorus filters becomes even more cost-efficient [130, 131]. In the literature different methods have been reported for regeneration of PSM. One method is to regenerate the material by adding a resting period after the material shows reduced efficiency of phosphorus retention to enable the surface to accumulate reactive content [69, 132, 133]. The second regeneration method is regeneration based on desorption, which is accomplished by adding a chemical solution to desorb the bound phosphorus and make available the adsorption sites for further retention of phosphorus [115, 128, 134, 135]. In order to precipitate new reactive content on the surface, the third approach is to apply a chemical solution to the spent material and thus improve the material's phosphorus retention ability [136].

In a study that investigated the phosphorus retention ability of electric arc furnace (EAF) slag through a column test, Drizo [91] developed a resting regeneration process. When more phosphorus could no longer be absorbed by the EAF slag, the column was drained and the EAF slag rested for four weeks. After the resting time, the slag was fed again for 124 days with the same synthetic solution. The outcome showed that a significant portion of its phosphorus retention

efficiency was recovered by the regenerated slag. A potential mechanism for this process of regeneration is that the solution occupying the pores of the slag was concentrated and supersaturated during the resting time as metal ions continuously dissolved into the solution and water continuously evaporated from the solution, leading to reactive minerals being precipitated in the pores. Therefore, more sites for further phosphorus retention were given by these precipitated reactive minerals. In other literature, this resting regeneration approach is shown to be effective [69, 132], but it was challenged by a study that tested resting, agitation and crushing on spent smelter slags and discovered that only crushing of the three techniques could temporarily increase the phosphorus retention efficiency of spent slags, while resting and agitation did not lead to any increase in efficiency [102].

For adsorption-based PSMs, a desorption-based regeneration framework has been developed. For such products, the solution phosphate is primarily retained by chemisorption, which includes the chemical reaction between the material surface of the metal hydroxide complex and the solution phosphate ion [137]. The metal phosphate complex is formed in the ligand exchange process, resulting in generation of OH^-. In a high pH environment, the direction of the reaction may therefore be reversed in which metal hydroxide is formed and phosphate is released. A high concentration of sodium hydroxide solution or a combination of sodium chloride and sodium hydroxide solution is typically applied to cause the desorption reaction. Desorbed phosphate accounts for more than 70 percent of the absorbed phosphate, although in some cases the ratio can be as high as 95 percent [137–139]. The material regenerated by this process can be reutilized for the retention of phosphorus and the desorbed phosphate can be extracted in the form of calcium phosphate or magnesium ammonium phosphate from the desorbed solution, which can be applied as fertilizer [140]. A potential explanation for the incomplete desorption of phosphate is that the

high pH of the solution of sodium hydroxide causes the formation of the substance of insoluble compounds on the surface that impedes phosphate desorption. In a study, an acid wash treatment was tested before the desorption procedure and the findings show that the hybrid technique could achieve complete regeneration of spent material in multiple adsorption-desorption cycles [141].

A realistic way to attain regeneration is also to precipitate new reactive content on the surface of spent material. This approach is typically paired with the method of desorption regeneration, since a portion of the phosphorus retention content can be dissolved by the desorption solution. In particular, leaching during the desorption process can be very important for materials based on reactive metal compounds such as aluminum and manganese [142, 143]. The solution containing some soluble compounds of the leached metal was fed to the filter for a period of time to compensate for the loss of phosphorus retention material to allow the precipitation of reactive content. Research has shown that the regenerated material retains a high proportion of the phosphorus retention capacity of the initial material [143] and the process of regeneration can be frequently applied. This technique of regeneration also means the regeneration of precipitation-based materials since the consumption of co-precipitating metal ions is followed by phosphorus retention by precipitation [142, 136].

3.3.6 Chronological order of studies about application of steel slag as PSM

In this section the major breakthrough for the application of steel slag materials for removing P are discussed. Yamada et al. [144, 145] introduced steel slag as PSM for the first time. They studied the effect of different parameters, i.e., pH, temperature, competing ions (NaCl), and slag porosity on P removal capacity of slag in batch experiments. They found that the highest adsorption can be achieved at pH 8. They also reported that more porosity and soft granulated materials led to more

removal of P; increasing the temperature from 5 to 30 ^{o}C degrees and decreasing NaCl concentration resulted in greater P removal. At the time, using batch experiments was a common method to study P removal capacity of a PSM [146], but it was Mann [147] who reported for the first time that there is a discrepancy between results generated by batch and flow-through (column) experiments. Following his results, Drizo et al. [91] recommended the use of long-term column experiments as a more representative technique for estimating the P retention capacity of active filters. They also introduced for the first time a physical treatment of resting slag materials in order to regenerate their P removal capacity.

Almost 20 years after steel slag was introduced as a PSM, Shilton et al. [25] reported the first long-term field data for slag filters. They used Melter slag for P removal in a wastewater treatment plant. They showed that Melter slag can provide P removal for a half a decade before filter replacement/rejuvenation is required. Weber et al. [27] reported the first evidence on the efficacy of EAF steel slag material in a field application for P removal from dairy effluents. They suggested that the system would not be sustainable without the exchange of the EAF slag material upon reaching P retention capacity. In another field study, Pratt and Shilton [148] proved the invalidation of predictive analysis based on the batch experiment data by actual long-term data. They claimed that the isotherm is ineffective for prediction of field-scale because the weathering effect, which generates substantial new adsorption sites, is not accounted for by adsorption isotherms. In another study after performing lab and pilot scale experiments, Valero et al. [149] concluded that batch data underestimates the P removal capacity of BFS slag in a pilot-scale. They argued that in the field pilot-scale filter, the sorption capacity of BFS was greater than in the laboratory bench-scale filter, presumably due to changes in the aerated rock filter linked to pH and organic matter and concentrations of dissolved oxygen.

In a long-term study, Pratt and Shilton [115] challenged the regeneration results by Drizo et al. [91], claiming that regeneration of P removal efficiency using physical techniques is ineffective. Instead, they introduced chemical regeneration methods by treating the spent slag with HCl and $Na_2S_2O_4$ as effective methods in the regeneration of P removal efficiency, while the NaOH treatment seems to be ineffective. In their next paper [134] they showed that pre- and post-chemical treatment (after exhaustion) can increase P removal. They argued that chemical reagents can manipulate the pH/Eh of the slag granule surfaces and possibly activate them for further P removal.

Although there have been several studies about field application of slag, no accurate model had been introduced by the time for prediction of the performance of steel slag in a long-term application. Penn and McGrath [31] for the first time started to develop a predictive equation for P removal of steel slag in a filed application. They found that the effect of retention time and P concentration on P removal varied based on material chemical properties, i.e., oxalate extractable aluminum (Al), iron (Fe), and water-soluble (WS) calcium (Ca). They proved that increases in RT and inflow P concentrations increased P removal among materials most likely to remove P via precipitation, whereas RT had little effect on materials likely to remove P via ligand exchange [54]. They used this modeling approach to design of in situ agricultural drainage filters using a ditch filter [150]. Later on, they introduced a universal flow-through model that was able to predict P removal in 23 different scenarios, including a diversity in chemical characteristics, conditions (P inflow concentration and RT), and ranged in scale from laboratory flow-through to 80 Mg ditch filters [41]. This study led to developing a software (Phrog) that can be used for design P removal structures [20, 151]. **Figure S 1.** Data transformation for the effect of bicarbonate concentration on P removal of Al-treated slag

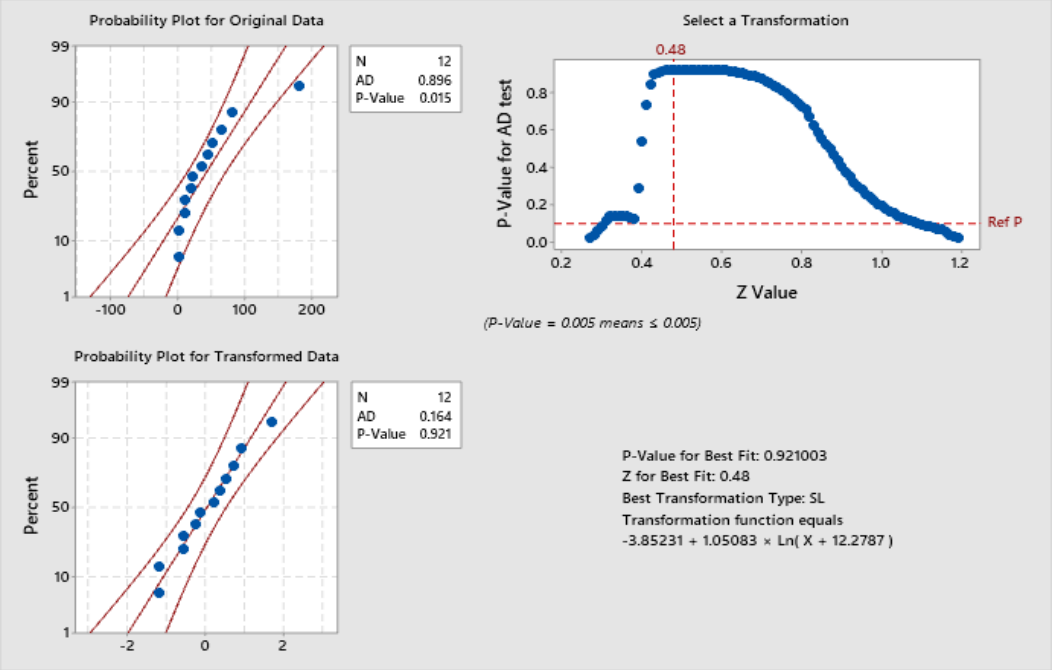

Figure S 2. Data transformation for the effect of Al treatment on P removal of slag for bicarbonate-rich inflow solution

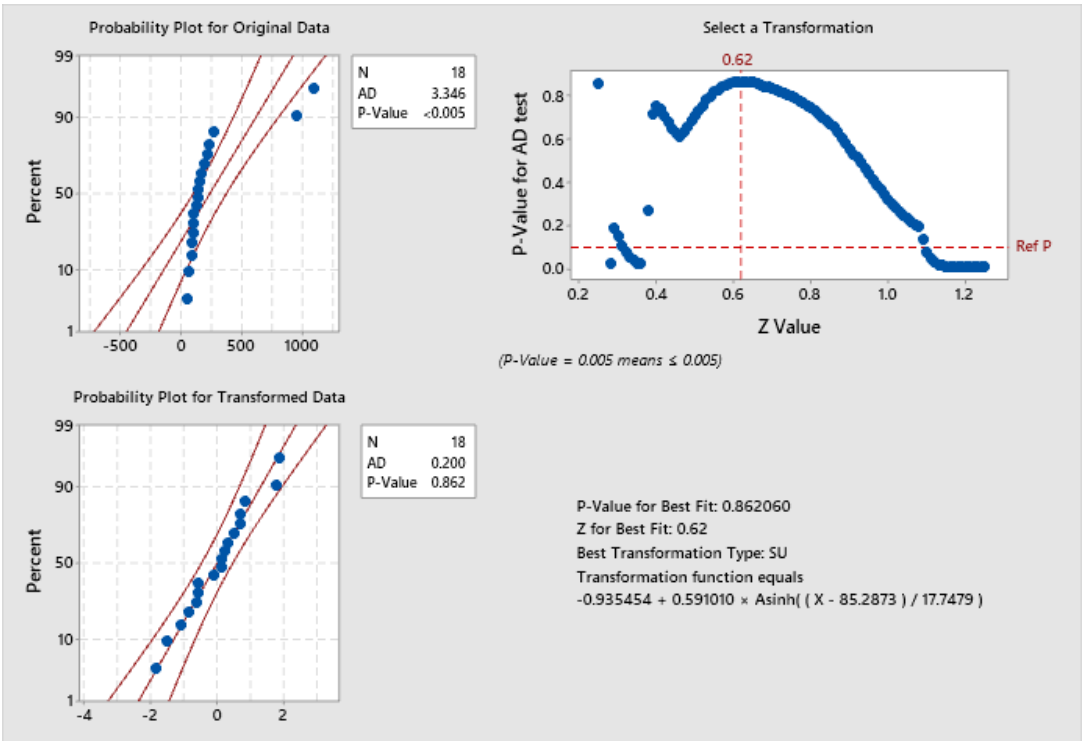

Figure S 3. Data transformation for the effect of incubation time and solution on Al-treated slag

Table S *1* provides a comprehensive list of research about applications of steel slag as PSM in a chronological order.

In summary, EAF slags have been successfully applied for removing phosphorous in various applications such as water runoff ditches, blind inlets, constructed wetlands, and WWP; however, the applicability of this material for treating water discharge from agricultural tile drainage systems has not been fully studied. In this research the aim is to study the effect of important parameters present in a tile drainage system on P removal efficiency of EAF in order to investigate its feasibility for this application. The studied parameters include slag particle size distribution, competing ions' concentration, incubation time and incubation solution, and modification of slag by chemical treatment. The effect of each parameter on P removal efficiency are analyzed using simulated flow-through experiments. Then, it will be recommended whether this material is suitable for this application.

4. Methodology

4.1. Analysis of slag

4.1.1. Flow-through experiment

To study P removal of steel slag in different conditions, flow-through experiments should be performed. These experiments include adding a P solution to the column containing PSM and collecting water samples after it passes through the PSM. The water samples then are analyzed to measure their P concentration that shows the efficiency of the PSM in removing phosphorus. **Figure 14** shows a schematic of flow-through experiment.

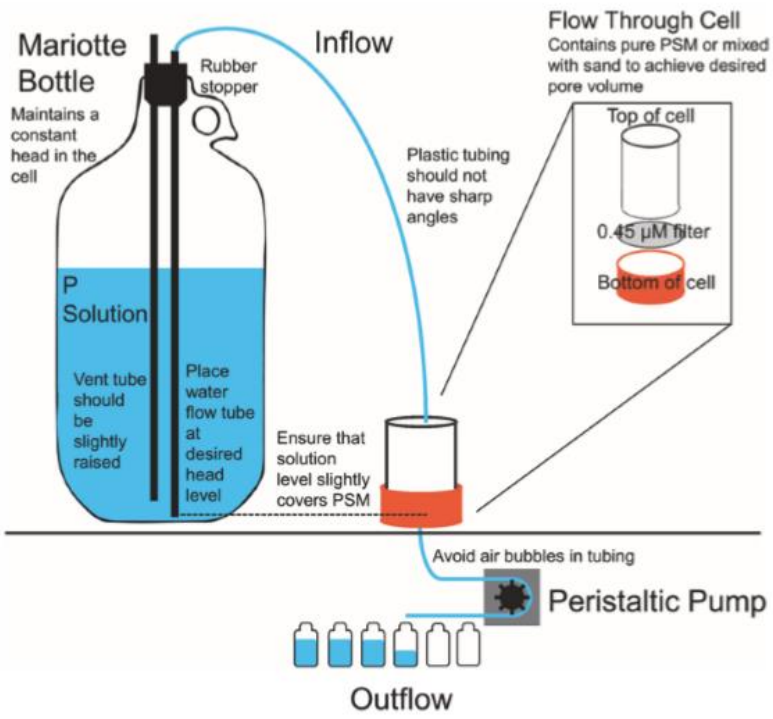

Figure 14. Schematic of the general procedure for conducting a flow-through P sorption test on PSMs [20]

Flow-through cells were constructed as described in DeSutter et al. [152]. In this study 0.5 gr of phosphorus sorption materials were mixed with 4.5 gr of acid-washed, lab-grade sand (pure Si sand, 14808–60–7; Acros Organics, Morris Plains, NJ) to achieve a total pore volume of 1.26 cm^3 (5 g of sand; 40% porosity) and placed in a flow-through cell. A 0.45-µm filter was placed beneath the materials, and the bottom of the cell was connected to a single-channel peristaltic pump (VWR, "low flow" 61161–354 and 54856–070) using plastic tubing. The desired RT (RT [min] = pore volume [mL]/flow rate [$mL.min^{-1}$]) was achieved by varying the pump flowrate, which pulled solution through the cell. A retention time of 10 minutes was used for this study. RT is defined as the amount of time required for the solution to pass through the cell. This RT represents a reasonable amount of time for drainage water to pass through a P removal structure. While excessive RT may be effective at P sorption, it reduces the total amount of drainage water that can

be treated for a given mass of material under high flow conditions. A constant head Mariotte bottle apparatus was used to maintain a constant volume of P solution on the materials [31, 54].

Figure 15 shows a photograph of the actual flow-through experiment setting used for this study. It includes six stations of flow-through experiments that enable the researcher to run three different experiments at the same time. In order to check the reproducibility of the experiments, two stations were assigned for each experiment.

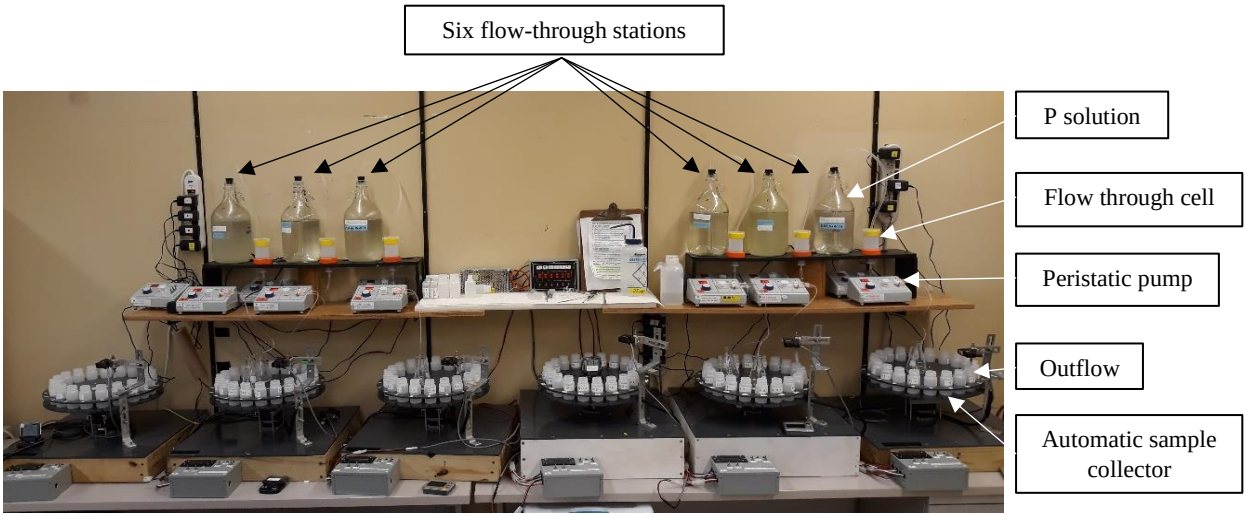

Figure 15. Photograph of six stations for conducting a flow-through experiment

4.1.2. pH measurement

The pH is an important value to measure because the effectiveness of both types of PSM, Ca-based and Al/Fe-based, are dependent on pH values. To measure pH, the following steps should be taken:

1. Add 3 gr of PSM and 15 mL of de-ionized (DI) into a snap vial. The ration between solid to DI should be maintained at 1:5.
2. Shake snap vials for 1 min
3. After waiting for 20 minutes, shake the snap vials for a second time for 1 min
4. After waiting 20 more minutes, pH can be measured [20]

Moreover, the pH of the outflow solution is measured that can be used to investigate the mechanism of P removal.

4.1.3. P and Ca analysis

After collecting outflow samples, the P removal efficiency of PSM was studied using an ascorbic acid method. This method, which is an EPA standard method, includes using reagents for the outflow samples and measuring the P concentration via a spectrophotometer [153].

This method was based on orthophosphate-specific reactions. Ammonium molybdate and antimony potassium tartrate react in an acid medium with dilute solutions of phosphorus to form an antimony-phospho-molybdate complex. This complex is reduced by ascorbic acid to an intensely blue complex. Only the orthophosphate forms a blue color in this test and the color is proportional to the phosphorus concentration. **Figure 16** shows a rack of outflow samples and the spectrophotometer used for this study.

Figure 16. A rack of outflow sample and spectrophotometer used for P analysis

In addition to P, the Ca concentration in the outflow solution was measured using Inductively Coupled Plasma Atomic Emission Spectroscopy (ICP AES). The purpose of this measurement was to study the effect of alkalinity on calcium phosphate precipitation.

4.2. Statistical analysis

4.2.1. Model development:

Results of the flow-through experiment are used to find the design curve. A design curve is a relationship between P sorption onto a PSM with cumulative P loading of the material, under specific conditions of contact time (retention time) and inflow dissolved P concentration. Retention time is defined as the amount of time that the PSM is in contact with the solution. The importance of the design curve is that it shows how much P a PSM removes from water. **Figure 17** shows an example of a design curve for the steel slag resulting from a flow-through test with an inflow P concentration of 0.5 mg/L phosphorous and 10 minutes' retention time. In the figure discrete P removal percentage (DP_{rem}) is plotted as a function cumulative P added (CP_{add}) to the PSM.

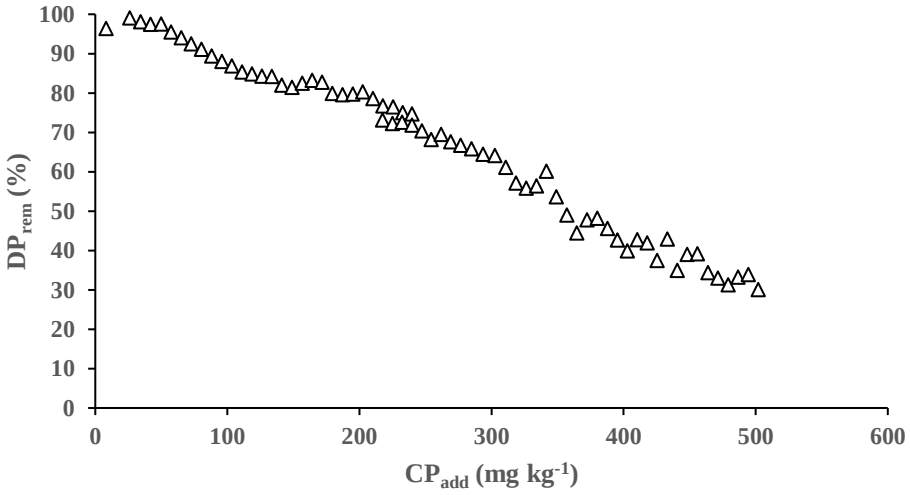

Figure 17. Design curves for the PSM (EAF steel slag) resulting from flow-through P sorption tests with an inflow P concentration of 0.5 mg/L and five minutes retention times

By using experimental values of the design curve, an empirical model will be obtained for the PSM. This can be done using statistical software by finding the best-fitted curves to the experimental design curve. R-squared values will be used to compare fitted-curves (**Figure 18**).

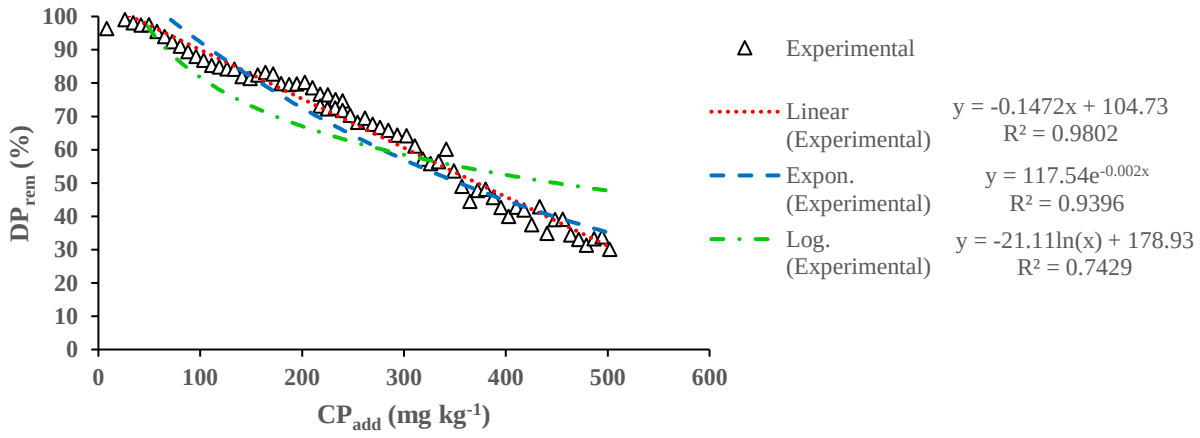

Figure 18. Fitted curves for DPrem (%) vs. CPadd

By finding the best-fitted curve an empirical model will be obtained that relates DP_{rem} (%) to CP_{add}. Essentially, this model allows calculating how much P will be removed or retained by the PSM. **Eq. 1** is integration of a design curve to estimate cumulative P removal for a given P load to the PSM.

$$CP_{rem}\,(\%) = \frac{\int_0^x f(x)dx}{x} \qquad (1)$$

Where *x* is CP_{add} (mg kg^{-1}), DP_{rem} is a function of x as DP_{rem} (%) = *f(x)*, and CP_{rem} (%) is cumulative P removed. Dividing the integrated design curve by 100 instead of CP_{add} results in CP_{rem} in units of mg P kg^{-1} PSM.

$$CP_{rem}\,(mg\ kg^{-1}) = \frac{\int_0^x f(x)dx}{100} \qquad (2)$$

The final loading point is when the PSM's discrete P removal (%) is zero (f(x) = 0), i.e., when the PSM is spent and inflow P equals outflow P concentration. Solving the model when CP_{rem} is zero leads to calculating the maximum P added to the PSM. The input of CP_{add} Max into **Eq. 1** and **2** will result in the maximum CP_{rem} in percent or mg kg^{-1}, respectively.

4.2.2 Analysis of variance and contrast analysis

To quantify the impact of the independent variable on P removal efficiency, a statistical approach was used. The response variable used in the statistical analysis was Maximum Cumulative P removed (mg/kg) for each condition that was calculated using the best fit for design curves. Two statistical techniques, i.e., Analysis of Variance (ANOVA) and contrast analysis, were used to investigate the potential significance of the independent variables on P removal capacity and differences between groups. A contrast analysis is a specific type of analysis that tests for nuanced differences between groups within a dataset, enabling a test for more precise and specific differences among groups of data. SAS 9.4 and Minitab 19 were used for performing statistical analysis. Hypothesis testing was used to interpret ANOVA results. The null hypothesis (H_o) and the alternative hypothesis (H_1) assume no relationship and relationship, respectively. A significance level of 0.05 was used for the statistical analysis. In order to either reject or reject the null hypothesis, the P-value method was used. If the P-value happens to be greater than α, the null hypothesis cannot be rejected. If the P-value was less than or equal to α, the null hypothesis was rejected in favor of the alternative hypothesis [29, 30].

4.3. Competing ions (research objective 1):

One of the factors that can reduce the efficiency of PSM in P removal is the presence of competing ions in the discharged water. The competing ions compete with phosphate ion (PO_4^{3-}) in making a bond with Ca, Al, Fe, and Mg in PSM.

The deployment of the P removal structure for treating subsurface tile drain water has not been successful yet because of the low efficiency of phosphorus removal. One problem that possibly reduces efficiency is the presence of competing ions, specifically carbonate (CO_3^{2-}), in the water discharged from the tile drainage system. Carbonate in soil is provided by atmosphere (carbon dioxide) or from limestone that is used as an amendment to neutralize soil acidity and to supply calcium (Ca) for plant nutrition. The network of the tile drainage system allows water to flow from between soil particles into the tile line located beneath the surface. This flow can lead to the transportation of carbonate or bicarbonate ions to the main tile and consequently to the P removal structure deployed at the end of the network before water discharges to a ditch.

The following reactions show how carbonate ions can compete with phosphate ions in making a bond with the Ca ions present in the composition of PSM. As mentioned before, Ca-based PSM removes P by precipitation of calcium phosphate, as shown below:

Dissolution of $CaOH_2$ from slag

$$CaOH_2 \leftrightarrow Ca^{2+} + 2OH^-$$

P removal by Ca ions:

$$Ca^{2+} + H_2PO_4^- + 2H_2O \leftrightarrow CaHPO_4.2H_2O_{(solid)} + H^+$$

Carbonate ions provided by bicarbonate or carbonic acid and present in outflow tend to react with Ca ions as well. This mechanism is as follows:

$$HCO_3^- \leftrightarrow H^+ + CO_3^{2-}$$

$$H_2CO_3 \leftrightarrow 2H^+ + CO_3^{2-}$$

$$Ca^{2+} + CO_3^{2-} \leftrightarrow CaCO_3$$

As can be seen, alkalinity or carbonate and bicarbonate ions can consume Ca ions of PSM that possibly reduce P removal efficiency of PSM. In this work the effect of carbonate ions on P removal efficiency of PSM will be examined. The study aims to find answers for the following questions: is formation of $CaCO_3$ thermodynamically favorable compared with the formation of $CaHPO_4.2H_2O$? If so, how fast would this reaction be? How much does the efficiency of the PSM in removal of phosphorous decrease because of competing action of the carbonate ion? Four different P solutions with various bicarbonate concentrations (0, 0.25, 0.5, and 0.84 g/L) were used to study the effect of alkalinity on P removal. These concentrations were chosen as Fausey et al. [26] reported these values for bicarbonate concentration in water discharge from tile drainage in Great Lakes states. To study the mechanism of P removal in the presence of alkalinity, ICP experiments will be accomplished that measure the Ca ions present in the outflow from the PSM column.

4.4. Particle size distribution (research objective 2):

Particle size distribution is one of the four main physical properties of PSM that should be considered when designing the P removal structure. The other three factors are hydraulic conductivity, porosity, and bulk density. Particle size distribution is a major factor because, first, the smaller the particles are, the greater surface area they have that generally enhances P removal, and second, particle size distribution has direct impact on the values of three other factors. The total volume and footprint of the structure are generally controlled by bulk density defined as the mass per unit volume of the bulk material. Another important factor is porosity that represents the amount of water that can be held by PSM. Porosity is defined as the total volume of pore space

per unit volume of bulk material. It should be mentioned that removal of P occurs when P-rich water comes into contact with unconsolidated PSM; therefore, the more space the materials provide, the more removal might happen. Hydraulic conductivity assigns how fast water can pass through the PSM; in other words, what would be the maximum flow rate that can be handled by the structure. Hydraulic conductivity is related to the particle size distribution as well. For example, hydraulic conductivity of clayey soils is in the magnitude of 0.0001 cm s^{-1}, for well-sorted sand it is around 0.1 cm s^{-1}, whereas gravel-sized material has a hydraulic conductivity of 1 cm s^{-1}. As can be seen, by increasing particle size hydraulic conductivity increases. Therefore, on the one hand, smaller particles are favorable because they provide more surface area and consequently increase P removal efficiency; on the other hand, greater particles are beneficial because they increase hydraulic conductivity. In the case of slag studied in this work, it was observed that when slag is used in the structure without being sieved, it causes a clog in the system that results in a preferential flow path for P-rich water. This will reduce efficiency of the structure in P removal. Hence, it is necessary to sieve the slag in order to provide a well-sorted material. However, the performance of the sieved slag should be studied to find the answer to whether and how P removal of the slag is affected by sieving. The experiment will include flow-through tests for PSM with different particle size distribution.

4.5. Effect of aging (research objective 3):

The form of a P removal structure that can be used for the treatment of water discharge from a tile drain is a rectangular box containing a buried PSM bed where the tile drain is directly plumbed into the structure and treats the water before it reaches a drainage ditch (**Figure 19**). Two different forms this structure can have include top- downward or bottom-upward flow. In the top-downward form the water enters the structure from top of the box and discharges from the bottom, and in the

bottom-upward form the water flow is from bottom to top. The advantage of a bottom-up flow design is minimizing the structure's footprint by enabling the bed thickness of the PSM to be greater while achieving adequate drainage.

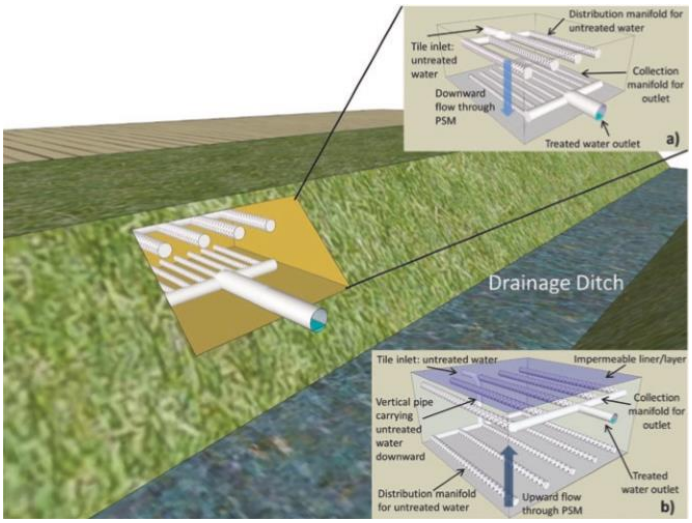

Figure 19. Diagram of a subsurface tile drain P removal structure with top- downward and bottom-upward designs [20]

The footprint is one of the major parameters that affects the total cost of the P removal structure. The footprint is basically controlled by PSM characteristics such as adsorption capacity and hydraulic conductivity. Less mass of materials and consequently less space are required for removing a specific P removal goal using a PSM with high adsorption capacity. This means that less money will be spent on constructing the structure and on transportation of the material. With respect to hydraulic conductivity for a given mass, PSMs with a low value of hydraulic conductivity mean a shallower PSM depth, and hence a bigger footprint for the P removal structure, whereas a smaller footprint is required for materials with higher values of hydraulic conductivity. Moreover, some agricultural fields have a space constraint limiting the area that can be allocated to the P removal structure.

A bottom-upward P removal structure is designed for the cases where there are space limitations in the field, but more mass of materials is required due to low adsorption capacity. This design is shown in **Figure 20**.

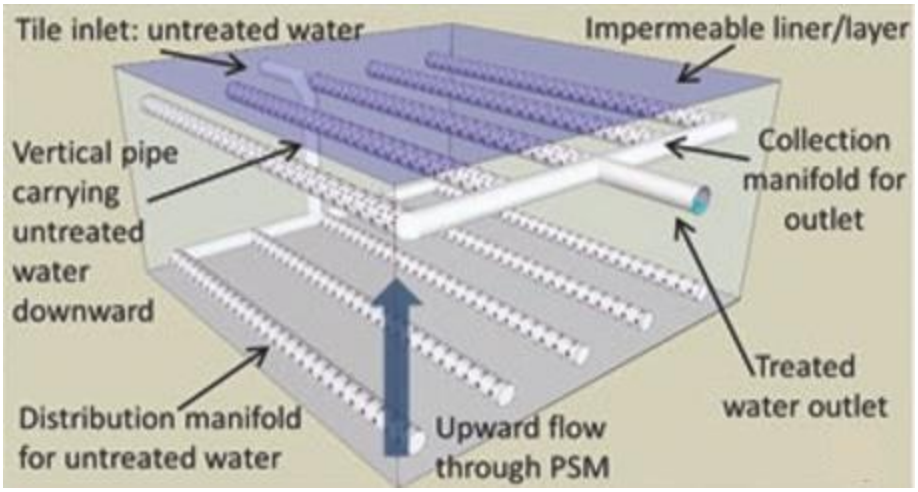

Figure 20. Bottom-upward P removal structure [20]

One potential problem regarding this design is that PSM materials will be soaked into the water between rain events. In a top-downward structure water completely drains after each rain event due to gravity force, but for the bottom-upward structure, draining will stop once the water level comes below to the outlet level that is located at the top of the structure. This means that PSM material will be aged in water in anaerobic conditions. Therefore, it is important to study the effect of aging on P removal efficiency of PSM. The aging may reduce the efficiency because during the soaking period Ca ions may dissolve into water and precipitate in the form with less solubility. As mentioned earlier, soluble Ca is necessary for P removal; hence, this process may reduce P removal efficiency by consuming available Ca. This situation might even worsen if alkalinity (carbonate ions) is present in the water. As discussed earlier, carbonate ions tend to react with Ca, which results in less available Ca for removing phosphorus. Therefore, the effect of aging in water will be studied in this work. The experiment includes aging the PSM in water with different

concentrations of bicarbonate (0, 0.25, 0.5 and 0.84 g/L) for a period of time (3, 7, and 137 days) and then performing flow-through experiments. **Figure 21** shows cups filled with PSM and water used for the incubation experiment.

Figure 21. PSM aged in water with three carbonate concentration (0, 0.5, 0.84 g/L) for incubation experiment

4.6. Modification of PSM (research objective 4):

A viable PSM must be able to remove P at sufficient amounts and relatively quickly. P sorption capacity of PSM is defined as the maximum amount of P that a PSM can sorb under a given condition and can be obtained from a design curve derived from flow-through experiments. The P sorption capacity is a function of inflow P concentration and retention time. Higher P concentration usually increases P sorption capacity and a longer retention time for time-sensitive PSM increases P sorption capacity.

As mentioned earlier, there are two categories for P sorption mechanisms: ligand exchange and precipitation. Ligand exchange is a process that happens only on variable charged minerals. The surface charges of these minerals vary as a function of pH. By increasing pH, the surface becomes more negative because of attaching hydroxide ions to the surface. As pH decreases, the surface terminal functional groups become more positively charged. The following reaction shows an example of a ligand exchange reaction for P onto a variable charged functional group

$$\text{---}\ MOH_2^{+0.5} + H_2PO_4^- \longrightarrow MOPO_3H_2^{-0.5} + H_2O$$

Where the line indicates that the functional group is connected to a PSM and where M is Al or Fe contained in an oxy/hydroxide.

In the precipitation mechanism, dissolved P in solution (i.e., phosphate) reacts with a dissolved metal cation. These two form a new solid by precipitation that takes dissolved P out of the solution. The following reaction shows a simplified generic precipitation:

$$aM^{m+} + bL^{n+} \longleftrightarrow M_aL_b \text{ (solid)}$$

Where M is a metal such as Ca, Al, or Fe, and L is a ligand (e.g., phosphate PO_4^{3-}). The slag studied for this research is Ca-based PSM and removes P by a precipitation mechanism.

PSM can be modified using a chemical treatment to change its P sorption mechanism, when its current sorption mechanism does not result in high P sorption capacity due to the field conditions. We hypothesized that the precipitation mechanism of EAF slag might not produce satisfactory results in the presence of bicarbonate in the inflow solution and decided to study the effect of changing mechanism to ligand exchange in reduction of adverse effect of bicarbonate.

Another advantage of the modification is rejuvenating the slag by changing its removal mechanism, after the slag is spent or after all available dissolved Ca reacts with phosphate ions. After a PSM removes P up to its sorption capacity, it will no longer remove P and is called spent or exhausted PSM. One challenge of a P removal structure is dealing with spent PSM that no longer removes P. The mass of PSM that will be used for the tile drainage structure is in the range of several tons. Therefore, removing this large volume of PSM and replacing it with a new one will be a cumbersome task that increases the cost of the system. One way to tackle this problem is rejuvenating PSM, which enables PSM to revive its adsorption capability. In some modification methods for PSM that removes P using ligand exchange mechanism, phosphorus can be replaced with an OH^-. This method not only removes P from PSM but also efficiently recharges the active functional groups for further P sorption, enabling the materials to serve as a PSM again. This is accomplished by treating PSM with NaOH or KOH solutions. After collecting the leachate that includes phosphate ions in dissolved form, P can be recovered as a fertilizer by adding $CaCl_2$ [140, 154]. In this way both PSM and P can be reused multiple times in the system. Following this method makes this wastewater treatment system a circular economy where waste production can be eliminated, and resources are continually reused [155].

To study modification of the slag with aluminum, the slag was treated by aluminum sulfate solution with concentration of 0.27 M for a period of 48 hours. The treatment process simply includes soaking slag into an aluminum sulfate solution. This leads to the formation of Al oxide/hydroxide on the surface of slag that will later act as new P removal sites. **Figure 22** shows slag before and after the aluminum treatment.

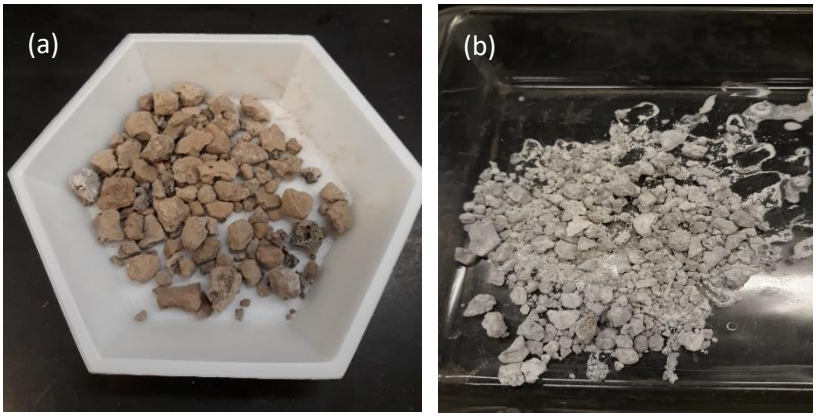

Figure 22. Slag (a) before and (b) after treatment with aluminum sulfate solution

After Al treatment, a flow-through experiment will be performed to study the effect of the treatment on the P removal behavior of the slag. Moreover, the effect of alkalinity on P removal of the treated slag will be investigated.

5. Results and Discussion

5.1. Effect of particle size distribution

Particle size distribution is a major factor to be considered for the selection of PSM. This is because first, the smaller the particles are, the greater surface area they have that generally enhances P removal, and second, particle size has direct impact on the values of three other important physical properties of PSM, including hydraulic conductivity, porosity, and bulk density.

As it was mentioned, smaller particles for PSM are favorable leading to an increase in P removal efficiency. However, smaller particles have less hydraulic conductivity that causes less water flow to be handled by the P removal structure.

The effect of particle size distribution of EAF slag was studied. For that research task, the slag was sieved using a 500 µm sieve.

Figure **Figure 23** shows the slag before and after sieving. Then flow-through experiments were performed for the sieved and non-sieved slags. For the experiment inflow a solution with 0.5 ppm P concentration was used and retention time was adjusted to 10 min. The results of the flow-through experiments are shown in **Figure 24**.

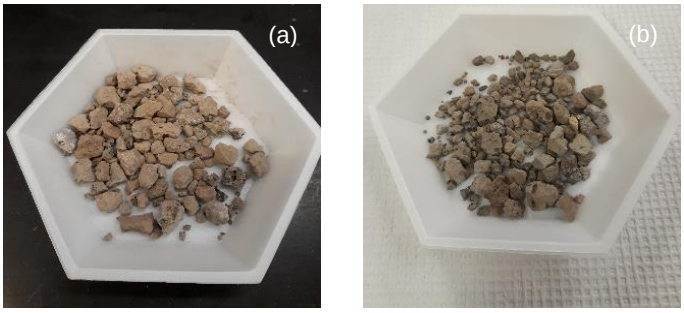

Figure 23. (a) non-sieved EAF slag (b) sieved EAF slag by 500 µm sieve

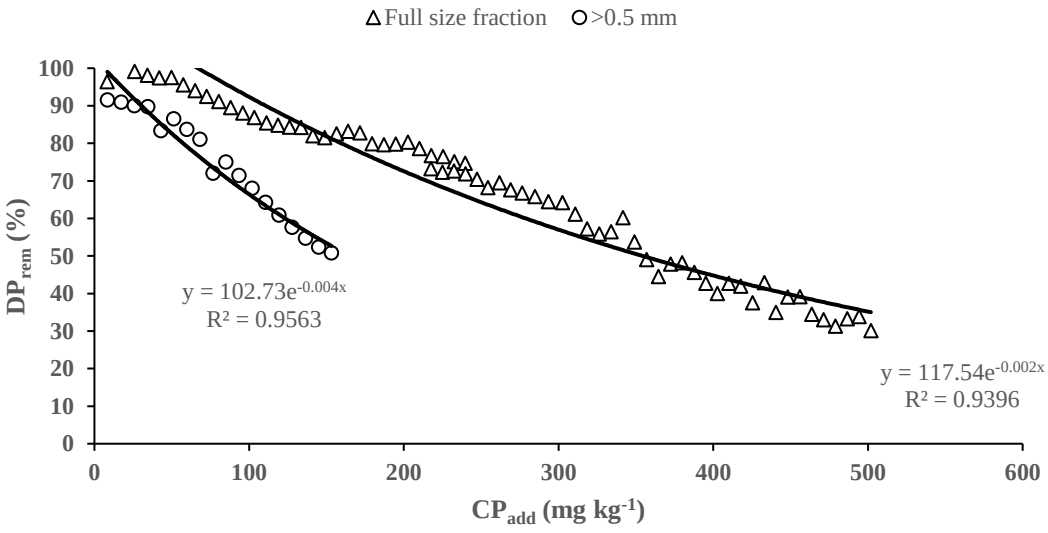

Figure 24. Discrete phosphorus removal (DPrem) design curves and fitted lines for the full size fraction containing particles < 0.5 mm and sieved slag which only contained particles > 0.5 mm.

As can be seen from the figure, P removal of sieved slag noticeably decreases compared with full size fraction slag. To quantify this change, the best-fitted curves should be obtained for the design curves. Using R-squared values, exponential fit was selected as the best-fitted curve. To find the maximum P removed by each slag the following steps were taken:

Estimation of cumulative P removal:

$$CP_{rem}\ (\%) = \frac{\int_0^{CP_{add}} (be^{mCP_{add}})\, dCP_{add}}{CP_{add}} \quad (3)$$

Where CP_{rem} is cumulative P removed, CP_{add} is the cumulative P added per mass of PSM (mg kg^{-1}), and m and b are the coefficients from the exponential equation that describes discrete P removal (i.e., design curve). This formula essentially allows one to determine how much P will be removed and retained by the PSM. Dividing the integrated design curve by 100 instead of CP_{add} results in CP_{rem} in units of mg P kg^{-1} PSM.

$$CP_{rem}\ (mg\ Kg^{-1}) = \frac{\int_0^{CP_{add}} (be^{mCP_{add}})\, dCP_{add}}{100} \quad (4)$$

When DP_{rem} (%) is close to zero, it means that the PSM is spent and inflow P equals outflow P concentration. This is the final loading point and can be calculated using the coefficient of the design curve as shown below:

$$CP_{add}\ \max(mgkg^{-1}) = \frac{\ln(b)}{-m} \quad (5)$$

The input of CP_{add} Max into either **Eq. 4** or **5** for CP_{add} will result in the maximum CP_{rem} in percent or mg kg^{-1}, respectively. This way the total P removed by a PSM can be estimated over its lifetime [20, 31, 41].

According to **Figure 24,** the fitted curves of non-sieved and sieved slags are as follows:

$$DP_{rem}(\%) = 117.54\, e^{-0.002\, CP_{add}}$$

$$DP_{rem}(\%) = 102.73\, e^{-0.004\, CP_{add}}$$

Using **Eq. 5**, the final loading points for full fraction size slag and sieved slag are 2383.38 and 1158.02 mg Kg^{-1}, respectively. By inputting b, m, and the final points in **Eq. 4**, maximum removal capacity of the full fraction size and sieved slag was calculated as 582.7 and 254.3 mgP Kg^{-1}, respectively. As shown in **Figure 25**, by sieving slag with a 500 µm sieve, maximum removal capacity decreases by 56%.

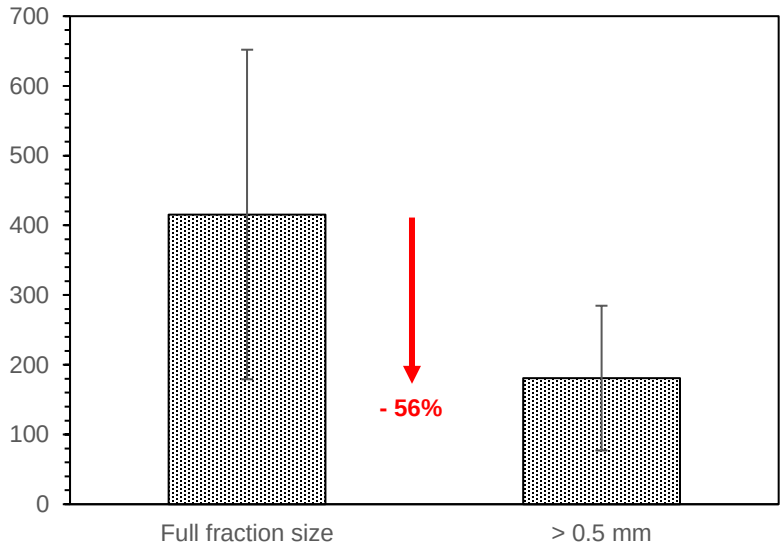

Figure 25. Maximum commutative P removal of non-sieved and sieved slag

The reason the full fraction size slag has higher removal is the fact that the small particles contain greater pH buffer capacity, and a higher degree of soluble Ca [156], as they are extremely soluble in water, which provide more free Ca ions in water compared with sieved slags. The reaction below shows the mechanism of removing P via precipitation.

$Ca^{2+} + H_2PO_4^- + 2H_2O \leftrightarrow CaHPO_4.2H_2O_{(solid)} + H^+$

K value (equilibrium constant) is used to quantify precipitation-dissolution reactions. **Table 4** lists the K value for several different Ca phosphate minerals. During the precipitation mechanism, first the most soluble Ca phosphate mineral will precipitate; then it gradually crystallizes into the least soluble Ca phosphate mineral over time. The concentration of the P (i.e., ligand) and the metal ion (i.e., Ca^{2+}) partly regulate the degree of solid Ca phosphate mineral formation. Enhancing concentrations of P and Ca provide the chemical drive to cause the reaction to occur and transfer from the left side to form the products on the right side of the reaction, i.e., precipitated solid. Therefore, the more that a PSM can dissolve and provide a solution for Ca^{2+}, the more the solution can eliminate P [20]. Decreasing slag size may also cause the specific surface available for HAP crystallisation increases. After precipitation, Ca phosphates may crystallise into the most stable form of hydroxyapatite providing seed crystals for crystallization [14]. smaller sized slag particles contain a higher degree of soluble Ca, greater pH buffer capacity, and therefore superior dissolved P removal via Ca phosphate precipitation [6].

Table 4. K values for several Ca phosphate mineral that can potentially precipitate during P removal by Ca-rich PSMs [20, 157]

Ca phosphate mineral	**Formula**	**Log K of dissolution**
Monocalcium phosphate	$Ca(H_2PO_4)2{\cdot}H_2O$	-1.15
Brushite	$CaHPO_4{\cdot}H_2O$	0.63
Monetite	$CaHPO_4$	0.3
Octacalcium phosphate	$Ca_4H(PO_4)_3{\cdot}2.5H_2O$	11.76
β-tricalcium phosphate	$\beta\text{-}Ca_3(PO_4)_2(c)$	10.18
Hydroxyapatite	$Ca_5(PO_4)_5OH$	14.46

5.2. Effect of alkalinity

Previous research has shown that water discharge from a tile drainage system has a high percentage of alkalinity especially in the form of bicarbonate (HCO_3^-) that can originate from the atmosphere, root respiration, and limestone used as an amendment [116, 158, 159]. In this research we studied whether carbonate ions compete with phosphate ions to react with Ca. Four different P solutions with various carbonate concentration were used to study the effect of alkalinity on P removal of >0.5 mm slags and full-size fraction slags as shown in **Figure 26**. **Table 5** lists the conditions of experiments, the parameters of the exponential fitted line, and the removal capacity for each combination. As can be seen from **Figure 26**, P removal appreciably shifts to lower values at any given cumulative P loading for inflow solutions containing alkalinity for both size fractions, compared with no bicarbonate.

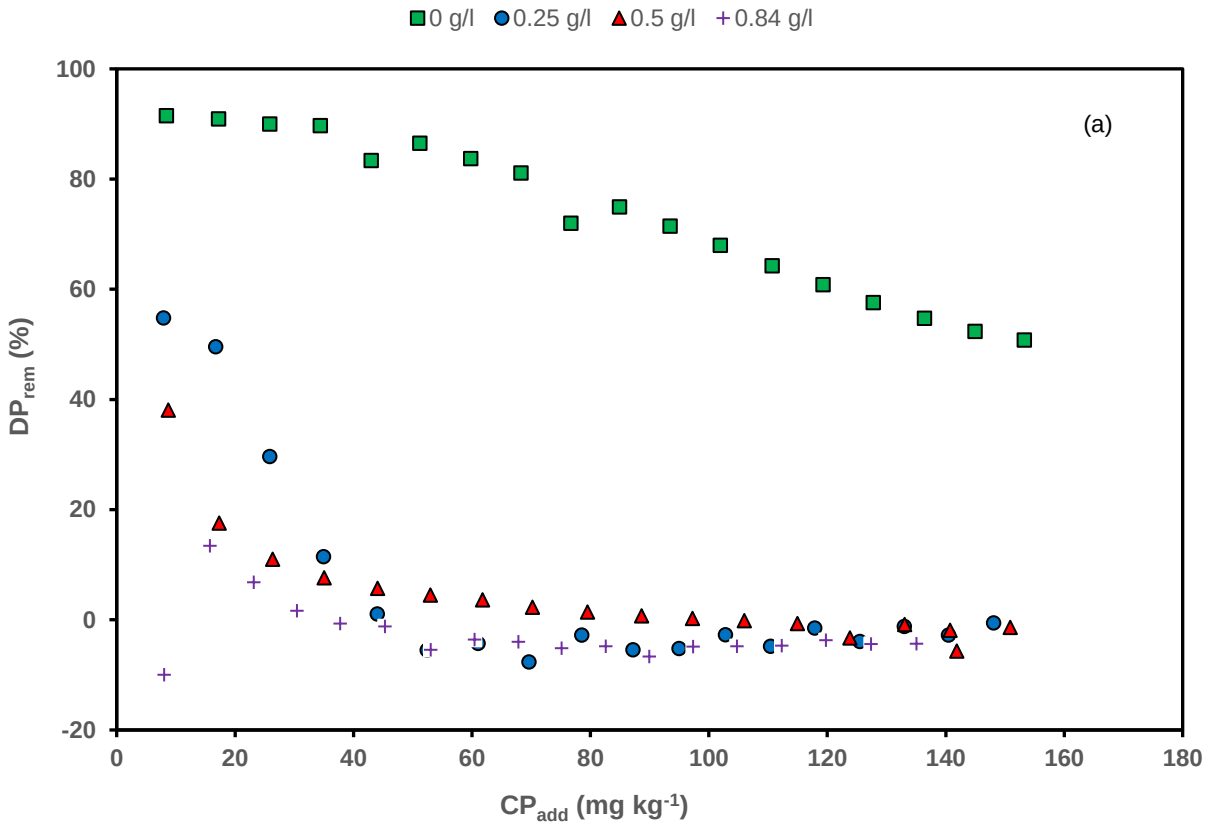
0 g/l
0.25 g/l
0.5 g/l
0.84 g/l
(a)
DP$_{rem}$ (%)
CP$_{add}$ (mg kg^{-1})
100
80
60
40
20
0
-20
0
20
40
60
80
100
120
140
160
180

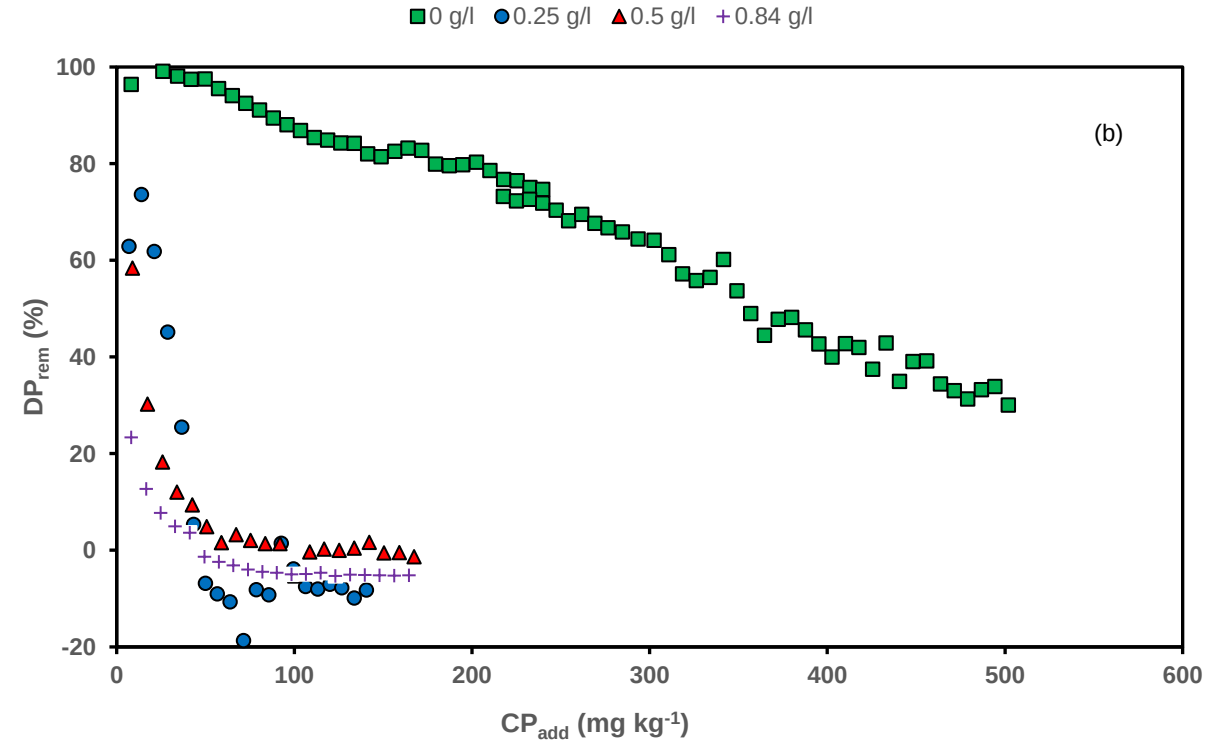
0 g/l
0.25 g/l
0.5 g/l
0.84 g/l
(b)
DP$_{rem}$ (%)
CP$_{add}$ (mg kg^{-1})
100
80
60
40
20
0
-20
0
100
200
300
400
500
600

Figure 26. Discrete phosphorus removal (DPrem) design curves for (a) sieved slag which only contained particles > 0.5 mm and (b) the full size fraction containing particles < 0.5 mm as a function of bicarbonate concentration in inflow solution (0, 0.25, 0.5, 0.84 g/L).

Table 5. Maximum removal capacity for the full size fraction containing particles < 0.5 mm and sieved slag which only contained particles > 0.5 mm as a function of bicarbonate concentration in inflow solution (0, 0.25, 0.5, 0.84 g/L).

Replication	Particle size (mm)	Bicarbonate concentration of inflow (g/L)	b*	m*	R-Squared	Max removal capacity (mg/Kg)
1	Full fraction size	0	117.54	-0.002	0.94	582.7
2	Full fraction size	0	125.23	-0.005	0.94	248.46
1	Full fraction size	0.25	162.74	-0.062	0.73	26.09
2	Full fraction size	0.25	153.96	-0.01	0.84	152.96
1	Full fraction size	0.5	62.187	-0.046	0.92	13.3
2	Full fraction size	0.5	0	0	0	0
1	Full fraction size	0.84	34.239	-0.057	0.99	5.83
2	Full fraction size	0.84	0	0	0	0
1	> 0.5	0	102.73	-0.004	0.96	254.32
2	> 0.5	0	130.01	-0.012	0.9	107.51
1	> 0.5	0.25	232.79	-0.104	0.82	22.28
2	> 0.5	0.25	82.737	-0.044	0.77	18.58
1	> 0.5	0.5	50.06	-0.049	0.96	10.01
2	> 0.5	0.5	0	0	0	0
1	> 0.5	0.84	143.33	-0.142	0.96	10.02
2	> 0.5	0.84	0	0	0	0

*$y = be^{-mx}$

$y = DP_{rem}$

$x = CP_{add}$

To achieve additional insight into group differences, contrast analysis was performed. The results are listed in **Table 5** and a bar chart of removal capacity for each combination is shown in **Figure 27**. From the contrast analysis (**Table 6**) it can be inferred that the difference between P removal capacity when bicarbonate is present compared with no bicarbonate is significant, while the difference between different concentration of bicarbonate is not significant.

Table 6. Contrast analysis between groups

Contrast	DF	Contrast SS	Mean Square	F Value	Pr > F
P removal with zero bicarb matrix vs all those containing bicarb	1	229619.5002	229619.5002	20.45	0.0007
P removal with 0.25 g/l bicarb matrix vs all those containing bicarb	1	6826.3470	6826.3470	0.61	0.4507
P removal with 0.5 g/l bicarb matrix vs all those containing bicarb	1	38466.4957	38466.4957	3.43	0.0889
P removal with 0.8 g/l bicarb matrix vs all those containing bicarb	1	40174.5124	40174.5124	3.58	0.0829
P removal with zero bicarb matrix vs those containing 0.25 g/l bicarb	1	118360.5858	118360.5858	10.54	0.0070
P removal with zero bicarb matrix vs those containing 0.5 g/l bicarb	1	171018.9128	171018.9128	15.23	0.0021

Contrast	DF	Contrast SS	Mean Square	F Value	Pr > F
P removal with zero bicarb matrix vs those containing 0.8 g/l bicarb	1	173207.3224	173207.3224	15.43	0.0020
P removal with 0.25 g/l bicarb matrix vs those containing 0.5 g/l bicarb	1	4831.4450	4831.4450	0.43	0.5242
P removal with 0.25 g/l bicarb matrix vs those containing 0.8 g/l bicarb	1	5205.0604	5205.0604	0.46	0.5089
P removal with 0.5 g/l bicarb matrix vs those containing 0.8 g/l bicarb	1	6.9564	6.9564	0.00	0.9806

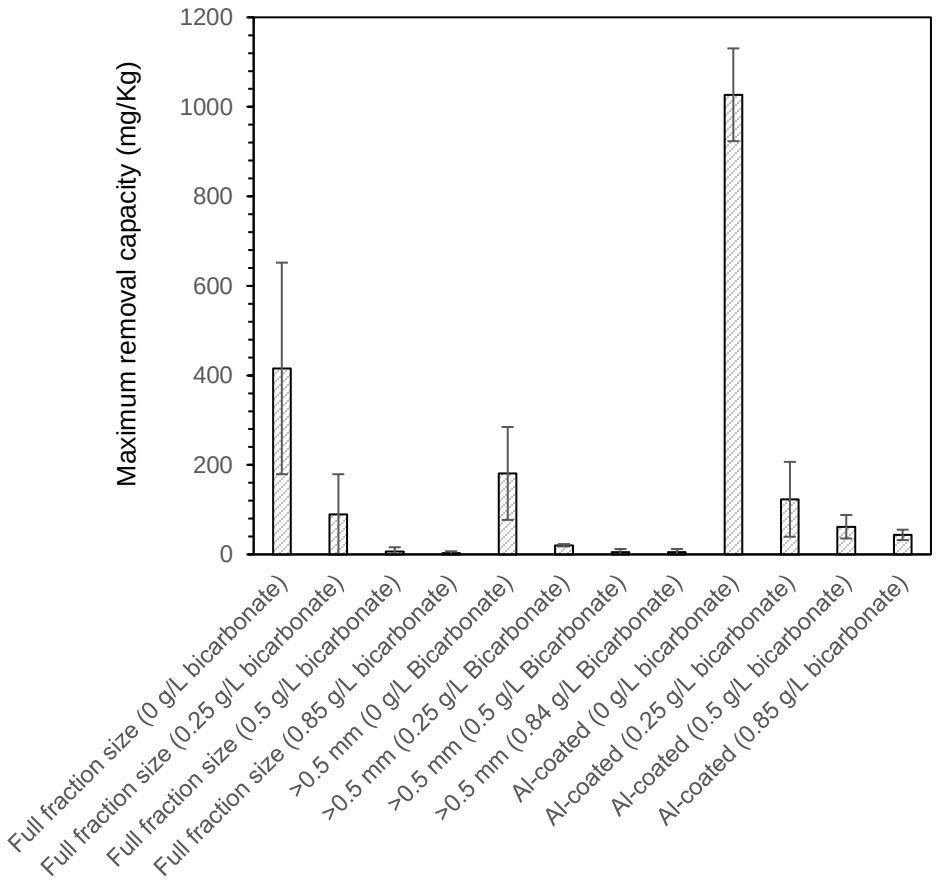

Figure 27. Average maximum removal capacity (mg/Kg) as a function of particle size, bicarbonate concentration, and Al treatment. DP removal determined under inflow conditions of inflow concentrations of 0.5 mg P/L, and 10 min retention time.

This result shows that carbonate ions are strong competitors with phosphate ions in forming a bond with Ca ions present in the composition of PSM. The following reaction shows this process.

Dissolution of $CaOH_2$ from slag

$$CaOH_2 \leftrightarrow Ca^{2+} + 2OH^-$$

P removal by Ca ions:

$$Ca^{2+} + H_2PO_4^- + 2H_2O \leftrightarrow CaHPO_4.2H_2O_{(solid)} + H^+$$

Carbonate ions provided by bicarbonate or carbonic acid and present in outflow tend to react with Ca ions as well. This mechanism is as follows:

$HCO_3^- \leftrightarrow H^+ + CO_3^{2-}$

$H_2CO_3 \leftrightarrow 2H^+ + CO_3^{2-}$

$Ca^{2+} + CO_3^{2-} \leftrightarrow CaCO_3$

As can be seen in the ICP results (**Figure 28**), by increasing bicarbonate concentration, Ca concentration decreases in the outflow solution for each material. This result confirms that carbonate ions present in the solution tends to react with Ca and form calcium carbonate, which is a strong competitive reaction for precipitation of calcium phosphate and halt Ca-based PSM from removing P. Therefore, premature failure of a tile drainage slag filter can be the result of bicarbonate-rich inflow subsurface water. Evidence supported the notion that bicarbonate consumed slag pH buffering capacity by precipitating Ca carbonate, which simultaneously reduced soluble Ca for Ca phosphate precipitation and clogged pore volume with the newly formed carbonate mineral [160].

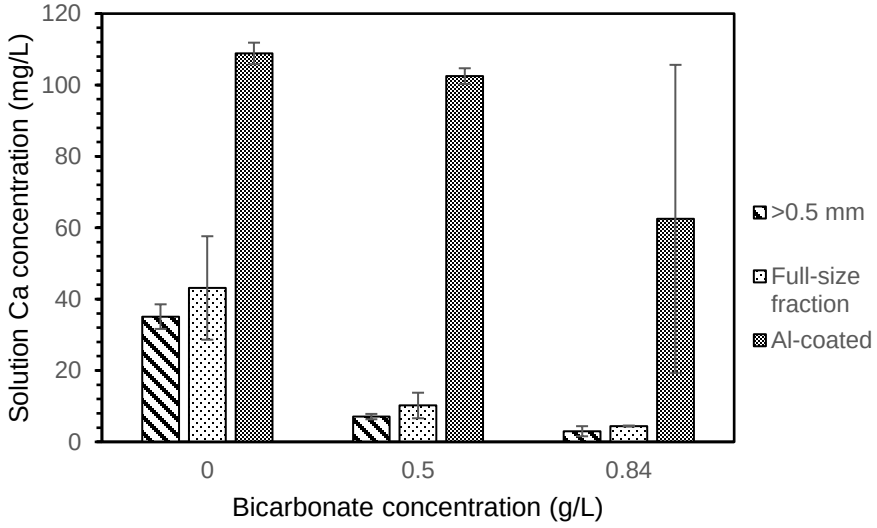

Figure 28. Calcium concentration in outflow solution as a function of PSM type and alkalinity concentration

It can be concluded that formation of $CaCO_3$ is not only thermodynamically favorable compared with $CaHPO_4 .2H_2O$, but also it is kinetically fast enough to make P removal zero during the contact time used in our experiment.

From **Table 5**, the max removal capacity for few replications when 0.5 and 0.84 g/L bicarbonate was present in the inflow solution was assigned to be zero. More accurately, in these solutions instead of P adsorption, P desorption was observed. In other words, P concentration in the outflow solution was higher than the inflow solution. It should be mentioned that the slag already contains P in its composition in the form of Ca-P. This is due to reactions occur during steel making process. One of the main reactions in the steel industry is the oxidation of P by dissolved oxygen in hot metals [31]. During crude steelmaking, EAF slag is produced through the electric arc furnace. Steel scrap, together with limestone or dolomite fluxes, is heated by an electrical current to form a liquid phase. The removal of silicates and phosphorus chemicals from molten steel is commonly obtained by addition of lime (CaO) or dolomite [32]. Therefore, before starting P removal experiment, EAF slag has Ca-P in its composition [3, 33]. Based on the result when bicarbonate concentration is more than 0.5 g/L, it causes Ca-P to dissolve, both “native” P and the P that was previously sorbed.

5.3. Effect of Incubation

The P removal structure can have two different forms, which include top-down or bottom-up flow. In the top-down form the water enters from the top of the box into the system and discharges from the bottom and in the bottom-up form the water flow is from the bottom upwards. The benefit of a bottom-up flow design is to reduce the footprint of the structure by allowing the PSM bed

thickness to be greater while at the same time ensuring sufficient drainage. Bottom-up P removal structure is intended for cases where space constraints are present in the field, but due to the low adsorption efficiency, more material mass is needed.

One concern with this design may be that in rain events PSM materials would be soaked in the water. Since water drains completely after each rain event in the top-down structure due to gravity force, for the bottom-up structure drainage will end as soon as the water level falls below the outlet level at the top of the structure. This means aging of PSM content in anaerobic conditions in water. The effect of aging in water and water with alkalinity was studied on P removal efficiency of the slag. For aging three times were selected, 3 days and 137 days. The first time represents a wet year when the time between two rain events is short; however, the second time is intended to represent a dry year when frequency of having storm events throughout the year is too low. **Figure 29** shows design curves for slag with 0, 3, and 137 days incubation in DI water. DP removal was determined under inflow conditions of inflow concentrations of 0.5 mg P/L, and 10 min retention time without bicarbonate concentration.

Before conducting the experiments, it was hypothesized that equilibration time in DI water may reduce P removal efficiency, because Ca ions can dissolve into water during the equilibration/inundation period and then precipitate into Ca carbonate, which has less solubility in water. As previously stated, soluble Ca is required for the removal of P by EAF slag. In addition, bicarbonate could further reduce the solubility of Ca, as previously discussed. From **Figure 29**, it appears that inundation in DI water does not actually change the P removal capability of the slag. Using an exponential regression fit for the design curves, the removal capacities are listed in **Table 7**. This shows that the P removal efficiency does not significantly change due to equilibration for long periods in DI water.

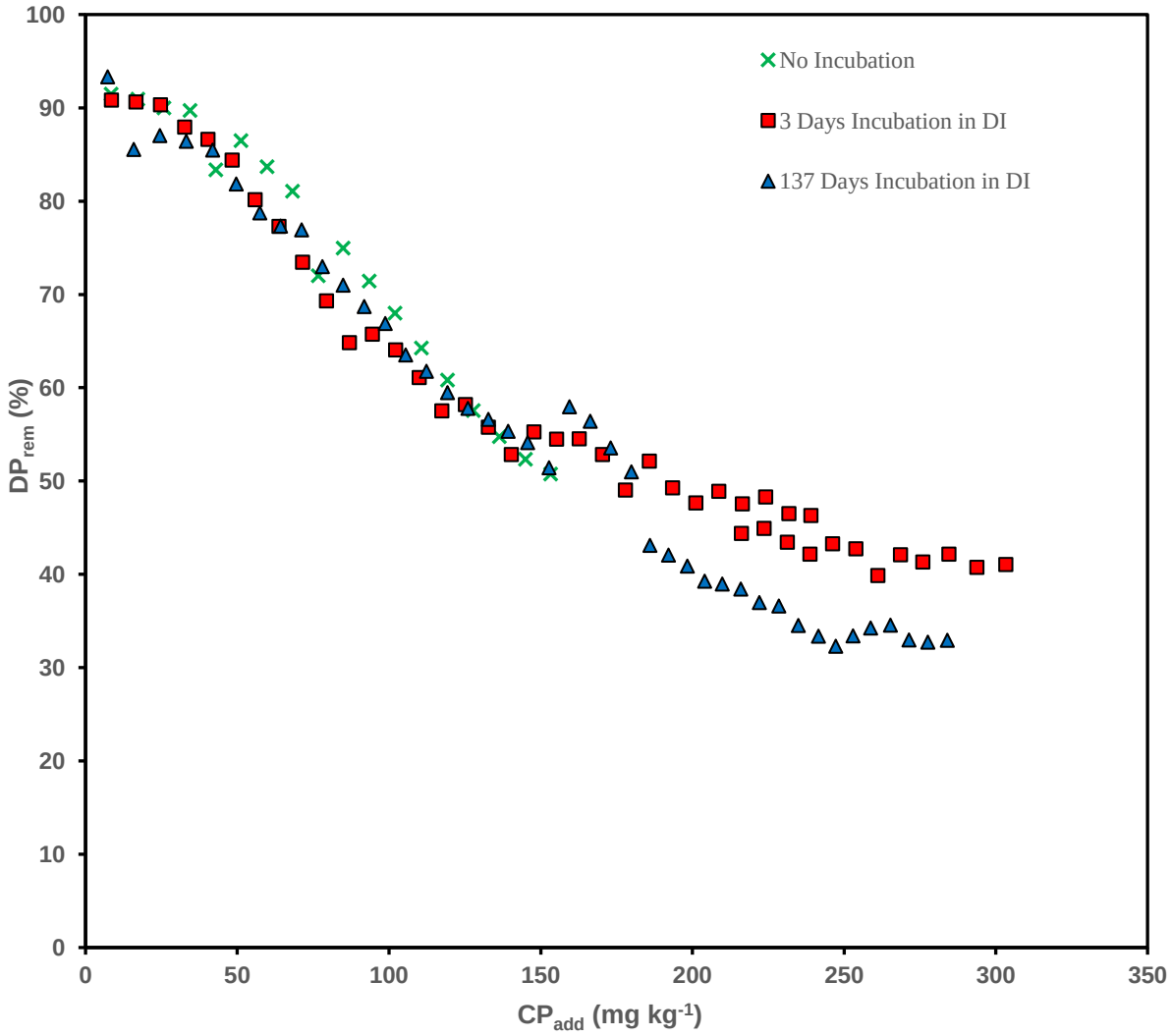

Figure 29. Effect of incubation in DI water on design curve of the slag. DP removal determined under inflow conditions of inflow concentrations of 0.5 mg P/L, and 10 min retention time for the full size fraction EAF slag

Table 7. Maximum removal capacity as a function of incubation time and alkalinity concentration in incubation solution for the full size fraction containing particles < 0.5 mm.

Replication	Incubation time (day)	Alkalinity of solution for incubation (g/L)	b	m	R-squared	Max removal capacity (mg/Kg)
1	0	0	102.73	-0.004	0.96	254.32
2	0	0	130.01	-0.012	0.9	107.51

1	3	0	89.73	-0.003	0.95	295.77
2	3	0	77.39	-0.004	0.9	190.97
1	137	0	99.502	-0.004	0.97	246.25
2	137	0	114.03	-0.007	0.9	161.47
1	3	0.5	57.29	-0.004	0.66	140.72
2	3	0.5	57.29	-0.004	0.66	140.72
1	137	0.5	130.83	-0.008	0.96	162.29
2	137	0.5	105.86	-0.007	0.94	149.8
1	3	0.84	42.619	-0.003	0.84	138.73
2	3	0.84	46.387	-0.002	0.61	226.93
1	137	0.84	108.26	-0.007	0.91	153.22
2	137	0.84	123.37	-0.005	0.92	244.74

The effect of bicarbonate in the incubation solution also was studied during the aging time. Two levels of alkalinity were used 0.5 and 0.84 g/L bicarbonate in DI water. As shown in **Figure 30** and **Figure 31**, P removal efficiencies are affected and reduced during short time; however, the efficiency remained almost unchanged for a long period of time.

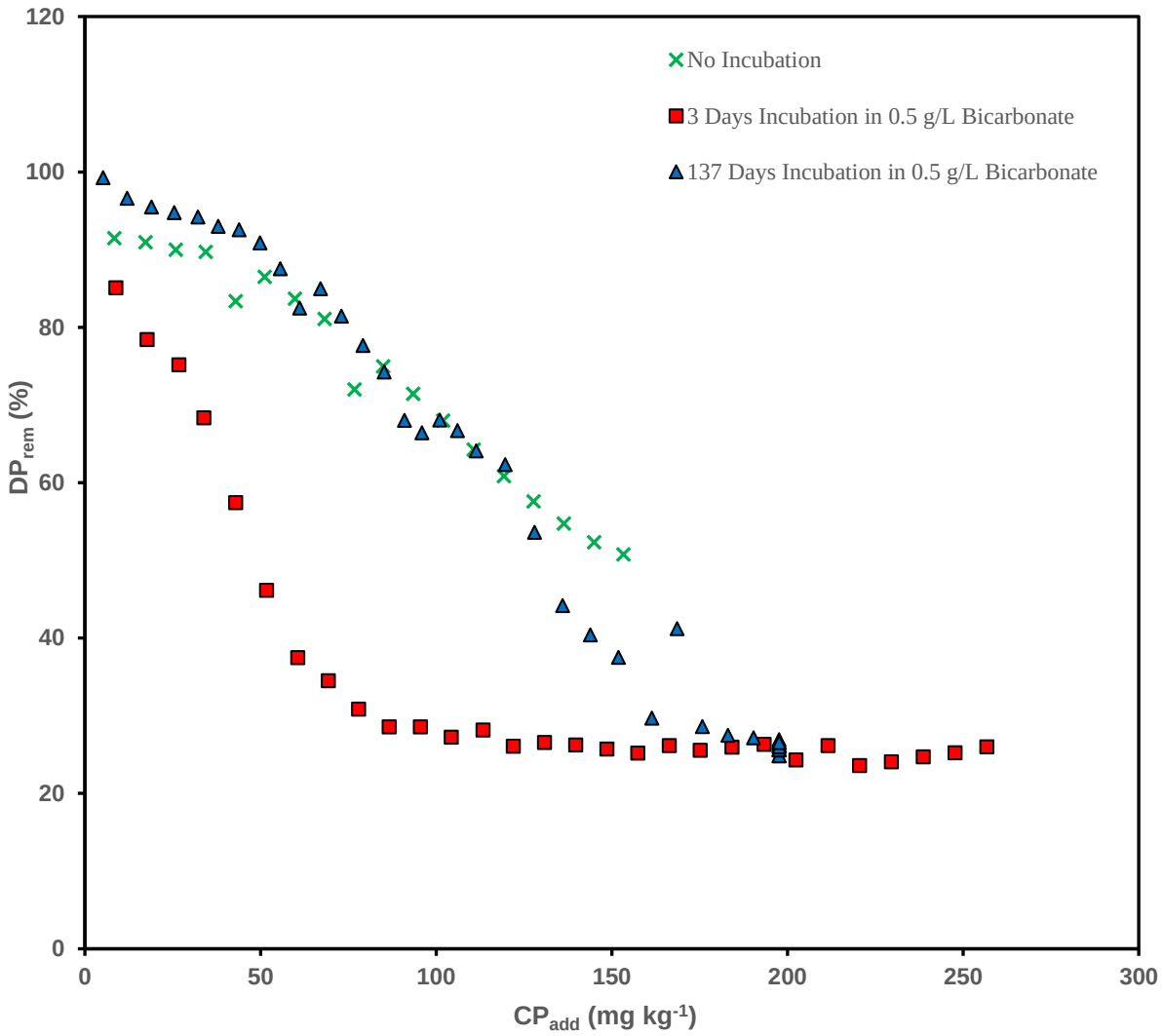

Figure 30. Effect of incubation in 0.5 g/L bicarbonate on design curve of the slag. DP removal determined under inflow conditions of inflow concentrations of 0.5 mg P/L, and 10 min retention time for the full size fraction EAF slag

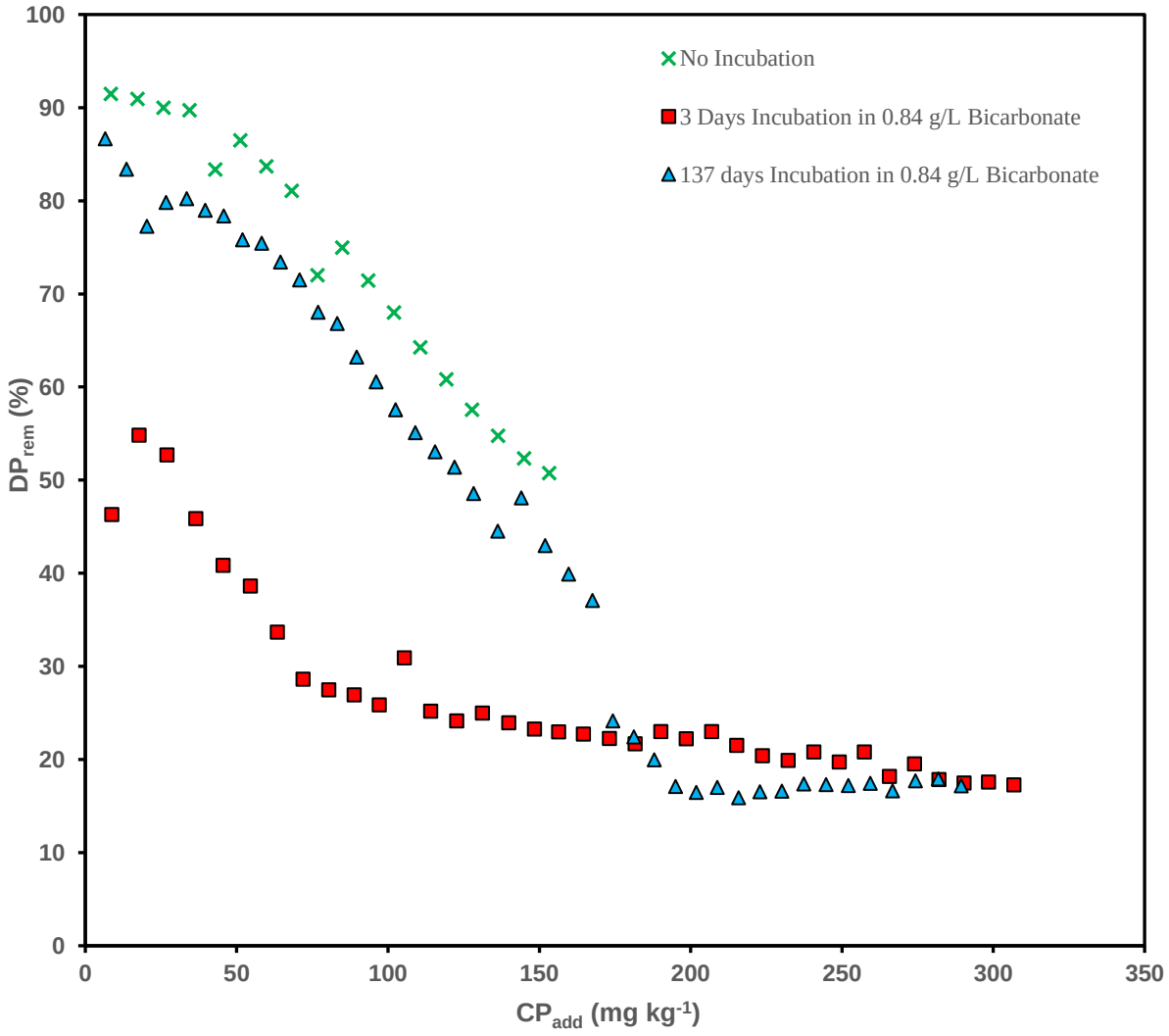

Figure 31. Effect of incubation in 0.84 g/L bicarbonate on design curve of the slag. DP removal determined under inflow conditions of inflow concentrations of 0.5 mg P/L, and 10 min retention time for the full size fraction EAF slag

The reactions below show the three common dissolution reactions of Ca-bearing minerals found in Ca-based PSMs.

$CaCO_3 + 2H^+ \longleftrightarrow Ca^{2+} + CO_{2(g)}$

$CaSO_4 \longleftrightarrow Ca^{2+} + SO_4^{2-}$

$CaO + 2H^+ \longleftrightarrow Ca^{2+} + H_2O$

As these reaction proceeds from left to right, i.e., the mineral dissolves and Ca^{2+} can precipitate with phosphate when the P solution flows through the PSM. Ca minerals differ in their capacity to provide a solution for Ca^{2+}, indicating that some minerals are more soluble than others. These Ca minerals are different in terms of solubility, pH buffering capacity, and pH effects on their solubility. $CaCO_3$ minerals are typically less soluble at a pH of 7 and above, compared with gypsum ($CaSO_4$) [20]. In this experiment EAF steel slag was incubated for various times in solutions with bicarbonate. As previously discussed, bicarbonate, and after de-protonation, carbonate, reacts with a solution Ca that prevents formation of Ca phosphate. Surprisingly, **Figure 30** and **Figure 31** show an inconsistency regarding the effect of incubation time on P removal when slag was incubated with solutions containing bicarbonate. While zero and 137 d of equilibration show minimal differences, three days of equilibration in solutions containing bicarbonate greatly reduced P removal.

Table 8 presents ANOVA results for quantifying the impact of incubation time and bicarbonate concentration on P removal. The results show that incubation of slag while inundated with water, for a given level of bicarbonate concentration in that incubation solution, did not significantly affect P removal after the slag was removed and tested in a flow-through cell with a P solution containing no bicarbonate. Surprisingly, the addition of bicarbonate in the incubation solution also had no impact on subsequent P removal. At first, this appears contradictory to the results from **Figure 26** and **Table 5**, which present the impact of including bicarbonate in the inflow solution matrix for the P removal flow-through tests. Recall that the flow-through tests add many pore volumes of solution to the slag, while on the other hand, the incubation of slag in bicarbonate-rich water was only a single pore volume. This is logical as it confirms the notion that the amount of

bicarbonate added to the slag is what dictates the decrease in P removal ability. pH results (**Figure 32**) also show that incubation does not significantly change the pH level of the outflow solution.

Table 8. ANOVA results

Source	DF	Sum of Squares	Mean Square	F Value	Pr > F
Model	6	13518.16164	2253.02694	0.56	0.7495
Error	7	28017.50750	4002.50107		
Corrected Total	13	41535.66914			

R-Square	Coeff Var	Root MSE	cumrem Mean
0.325459	33.89075	63.26532	186.6743

Source	DF	Type I SS	Mean Square	F Value	Pr > F
Incubation	2	98.91561	49.45780	0.01	0.9877
Bicarbonate	2	11384.04822	5692.02411	1.42	0.3032
Incubation*Bicarbonate	2	2035.19782	1017.59891	0.25	0.7824

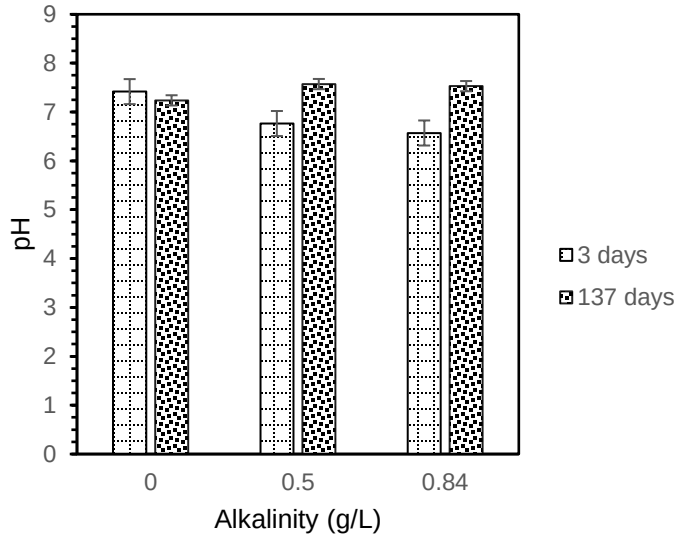

Figure 32. pH values of outflow solution as a function of incubation time.

5.4. Effect of Al treatment

In **Figure 33** design curves of regular EAF slag and Al-treated EAF slags are compared. Final loading points are 5117.08 and 1158.03 for Al-treated and regular slag, respectively.

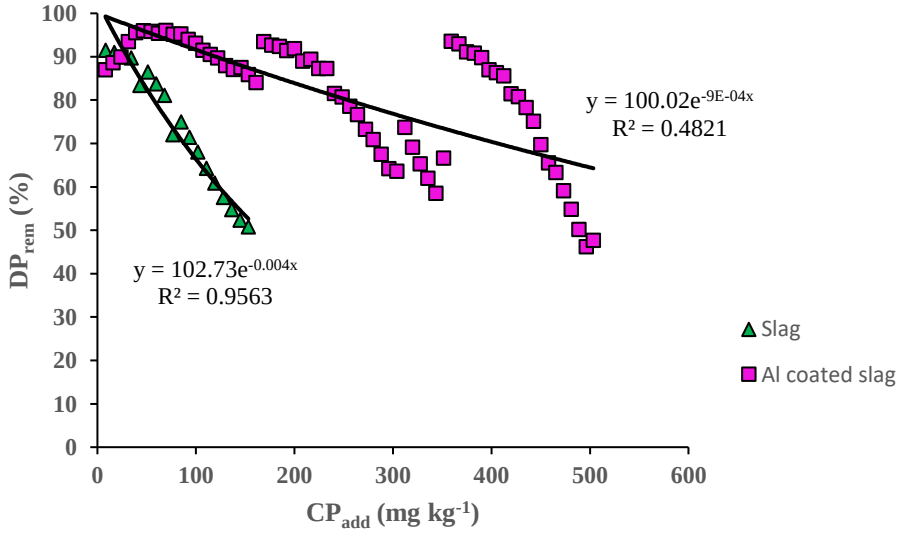

Figure 33. Discrete phosphorus removal (DPrem) design curves for normal EAF slag and Al-treated slag. DP removal expressed as a function of the cumulative P added (CPadd) to PSM.

As aluminum sulfate ($Al_2(SO_4)_3$) solution was used for the Al treatment of EAF slag, the soluble Ca found in Al-coated slag is likely in the form of gypsum ($CaSO_4$), which has been demonstrated to be an effective P sorbent to a certain extent. Additionally, amorphous Al hydroxides formed in the Al-coated surface modified slag would be an effective P sorbent via ligand exchange of P onto terminal hydroxide groups. Therfore, multiple mechanisms can be active for Al-coated EAF slags during P removal. The abrupt increase in P removal at around 400 mg kg^{-1} for Al-coated slag is likely due to re-starting the flow-cell after it had shut off for several hours, or it could be due to a shift in the P removal mechanism as pH changes (**Figure 33**). Regardless, coating slag with Al clearly increased P removal capacity.

To confirm the P removal mechanism followed by the PSM in each condition, ICP analysis was performed on the outflow samples of the P solution from the PSM column. **Figure 28** shows Ca concentration in the outflow solutions for different conditions. As can be seen, Ca concentration is significantly higher for Al-coated slag compared with sieved and non-sieved slags. This result proves that following Al treatment, the P removal mechanism for the EAF slag shifts from precipitation to the ligand exchange. As mentioned earlier, in the precipitation mechanism, soluble Ca reacts with dissolved phosphate ions, which results in precipitation of calcium phosphate. Thus, in the precipitation, more Ca ions in the solution are consumed and consequently less Ca ions would be detected in the solution via ICP. On the other hand, in the ligand exchange, dissolved phosphate ions are removed via a process that happens only on variable charged minerals that are connected to PSM through Al or Fe. In other words, Ca does not play a major role in the P removal in this mechanism, and therefore is more available in the outflow solution [150].

5.4.1. Effect of alkalinity on Al-coated slag

The effects of alkalinity on P removal for Al-treated slag are shown in **Figure 34**. The P removal capacity for each combination, slope and intercept of the exponential fit are listed in **Table 9**. The subsequent ANOVA and contrast analysis for distinguishing the impact of Al-coating and alkalinity are shown in **Table 10** and

Table *11*, respectively. It should be noted normality is one of the assumptions for ANOVA analysis. As the raw data does not follow a normal distribution, it was transformed using Johnson Transformation method (**Figure S 1**). Then, the transformed data was used for the ANOVA analysis.

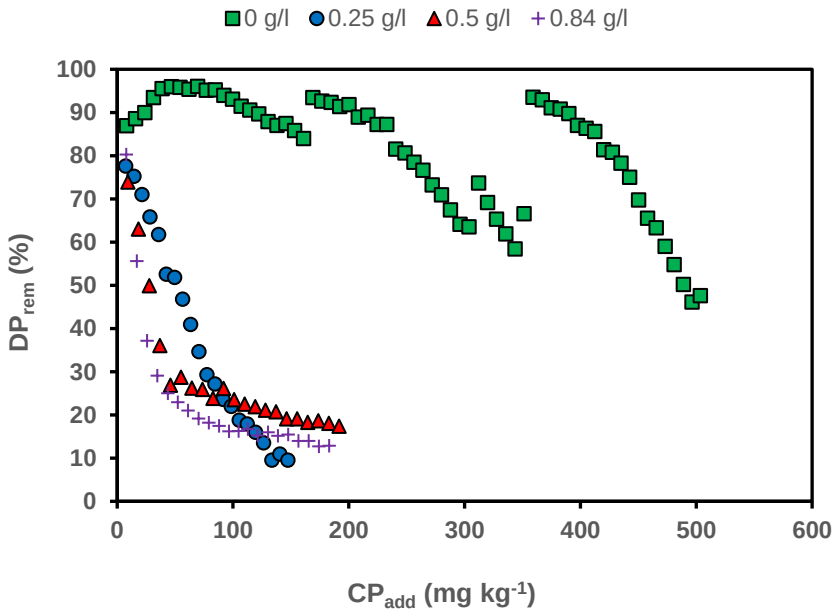

Figure 34. Discrete phosphorus removal (DPrem) design curves for Al-treated slag as a function of bicarbonate concentration (0, 0.25, 0.5, 0.85 g/L). DP removal expressed as a function of the cumulative P added (CPadd) to PSM.

Table 9. Maximum removal capacity for Al-coated slags as a function of bicarbonate concentration of the inflow solution. DP removal determined under inflow conditions of inflow concentrations of 0.5 mg P/L, and 10 min retention time.

Rep	Bicarbonate concentration	b	m	R-Squared	Max removal capacity (mg/Kg)

	of inflow (g/L)				
1	0	100.02	-0.0009	0.48	1100.22
2	0	96.362	-0.001	0.41	953.62
1	0.25	103.39	-0.016	0.98	63.99
2	0.25	55.686	-0.003	0.65	182.29
1	0.5	49.245	-0.006	0.77	80.41
2	0.5	87.732	-0.02	0.9	43.37
1	0.84	42.521	-0.008	0.75	51.9
2	0.84	47.197	-0.013	0.52	35.54

Table 10. ANOVA results for Al-treated slag

Factor	Type	Levels	Values
Bicarbonate concentration (g/L)	Fixed	4	0.00, 0.25, 0.50, 0.84

Source	DF	Adj SS	Adj MS	F-Value	P-Value
Bicarbonate Conc. (g/L)	3	5.202	1.7341	6.67	0.049
Error	4	1.040	0.2601		
Total	7	6.243			

S	R-sq	R-sq(adj)	R-sq(pred)
0.509956	83.34%	70.84%	33.35%

Table 11. Contrast analysis

Contrast	DF	Contrast SS	Mean Square	F Value	Pr > F
P removal with zero bicarb matrix vs all those containing bicarb	1	943215.1480	943215.1480	14.88	0.0023
P removal with 0.25 g/l bicarb matrix vs all those containing bicarb	1	66416.8802	66416.8802	1.05	0.3261
P removal with 0.5 g/l bicarb matrix vs all those containing bicarb	1	119890.0252	119890.0252	1.89	0.1941
P removal with 0.8 g/l bicarb matrix vs all those containing bicarb	1	134855.3210	134855.3210	2.13	0.1703
P removal with zero bicarb matrix vs those containing 0.25 g/l bicarb	1	566329.9951	566329.9951	8.94	0.0113
P removal with zero bicarb matrix vs those containing 0.5 g/l bicarb	1	650872.0418	650872.0418	10.27	0.0076
P removal with zero bicarb matrix vs those containing 0.8 g/l bicarb	1	671762.2005	671762.2005	10.60	0.0069
P removal with 0.25 g/l bicarb matrix vs those containing 0.5 g/l bicarb	1	2939.5278	2939.5278	0.05	0.8331
P removal with 0.25 g/l bicarb matrix vs those containing 0.8 g/l bicarb	1	4497.3128	4497.3128	0.07	0.7945

Contrast	DF	Contrast SS	Mean Square	F Value	Pr > F
P removal with 0.5 g/l bicarb matrix vs those containing 0.8 g/l bicarb	1	164.9836	164.9836	0.00	0.9601

The ANOVA analysis shows that alkalinity can have an impact on dissolved P removal of Al-treated slag. But if the maximum removal capacity of slag for Al-treated and regular slag is compared when bicarbonate is present in the inflow solution using ANOVA analysis (**Table 12**), it can be observed that Al treatment has a statistically significant impact and causes an improvement in the P removal capacity (**Figure 35**). For the ANOVA analysis, data was transformed using Johnson Transformation method as shown in **Figure S 2**.

Table 12. ANOVA result for the effect of Al-treatment on P removal capacity in the presence of bicarbonate in the inflow solution

Factor	Type	Levels	Values
Al treatment	Fixed	2	N, Y

Source	DF	Adj SS	Adj MS	F-Value	P-Value
Al treatment	1	5.869	5.8688	23.77	0.001
Error	10	2.469	0.2469		
Total	11	8.337			

S	R-sq	R-sq(adj)	R-sq(pred)
0.496854	70.39%	67.43%	57.36%

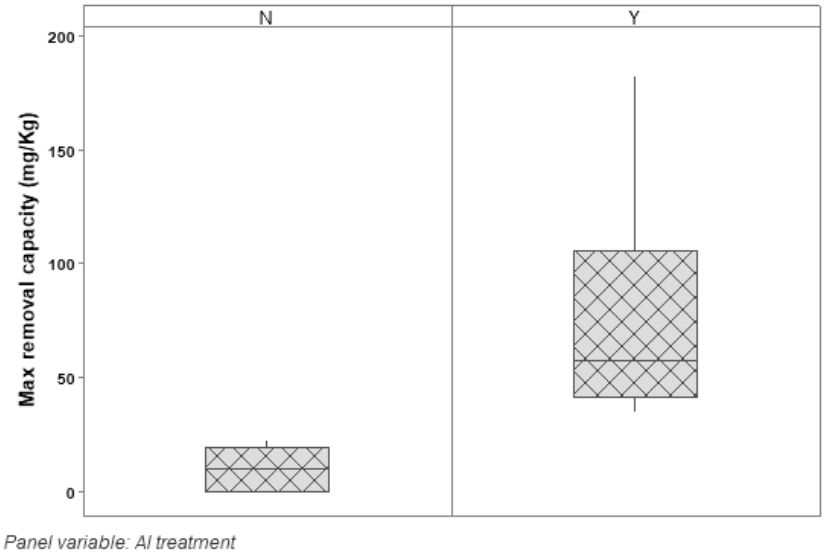

Figure 35. P removal capacity as a function of Al treatment. DP removal determined under inflow conditions of inflow concentrations of 0.5 mg P/L, bicarbonate concentration (0.25, 0.5, 0.84 g/L), and 10 min retention time

pH is a key factor that may affect the efficiency of Al/Fe-based PSM removal. As the pH increases, the P sorption by ligand exchange onto variable charge Al and Fe minerals reduces. This result is due to two reasons: first, the surface charge on the mineral becomes more negative by increasing pH. This change has a detrimental effect on attraction of the negatively charge phosphate ions ($H_2PO_4^-$, HPO_4^{2-}, PO_4^{3-}) by the surface. Second and most important, hydroxide, which is more present in the solution with higher pH, is a strong competitor with phosphate for surface sites. Thus, there is a competition between OH^- and PO_4^{3-} ligands for the same sites on variable charge minerals. Since OH^- is a more effective competitor than PO_4^{3-}, at elevated pH (greater than 8.5) Al/Fe-based materials cannot be used as effective PSM [20]. In this experiment a high concentration of alkalinity in the solution, i.e., bicarbonates, carbonates cause and increase in the pH of the solution. This effect leads to a noticeable shift in P removal efficiency by Al-treated slag to a lower value, as the higher pH reduces the efficiency of the ligand exchange mechanism used for P removal.

Figure 36 show the average pH values of outflow samples in different conditions. From **Figure 36** pH values for full-size fraction and >0.5 mm slags are higher than for Al-coated slag. These data show that the EAF slag was well buffered. It should be noted that one of the main requirements for Ca-based PSM to have acceptable kinetics of the Ca phosphate precipitation reaction is being highly buffered. This requirement is because precipitation of Ca phosphates generates acidity in a solution and if the material was not well buffered, it cannot be used as an efficient PSM [54, 157]. On the other hand, acidification treatment with aluminum sulfate for Al-coated slag is the reason for its low pH value. Moreover, by increasing the alkalinity concentration, the pH values of outflow solutions increase, which is attributed to the buffering ability of carbonate ions in the solution that control the variation of the pH in the solution.

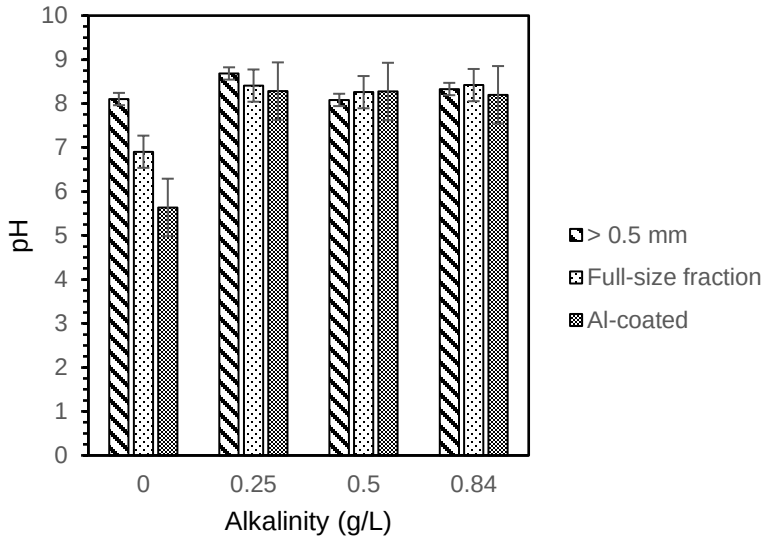

Figure 36. pH values of outflow solution as a function of PSM type and bicarbonate concentration of inflow solution.

Figure 37 (a), **(b)**, and **(c)** compare the P removal capability of treated and un-treated slag in 0.25, 0.5, 0.84 g/L alkalinity solutions, respectively. From the figures in all three alkalinity concentrations, reduction of the P removal efficiency as a function of alkalinity is the least for Al-treated slag, followed by non-sieved and sieved slags. This finding indicates that the effect of CO_3^{2-}

ions in prohibiting P removal through ligand exchange mechanism is less than the precipitation mechanism.

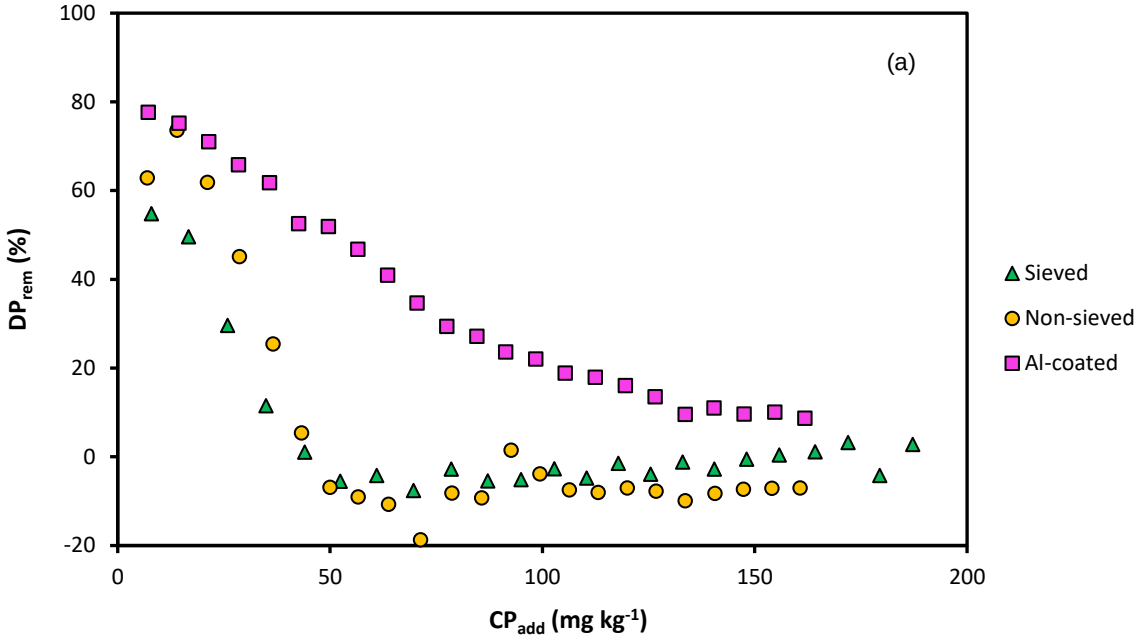

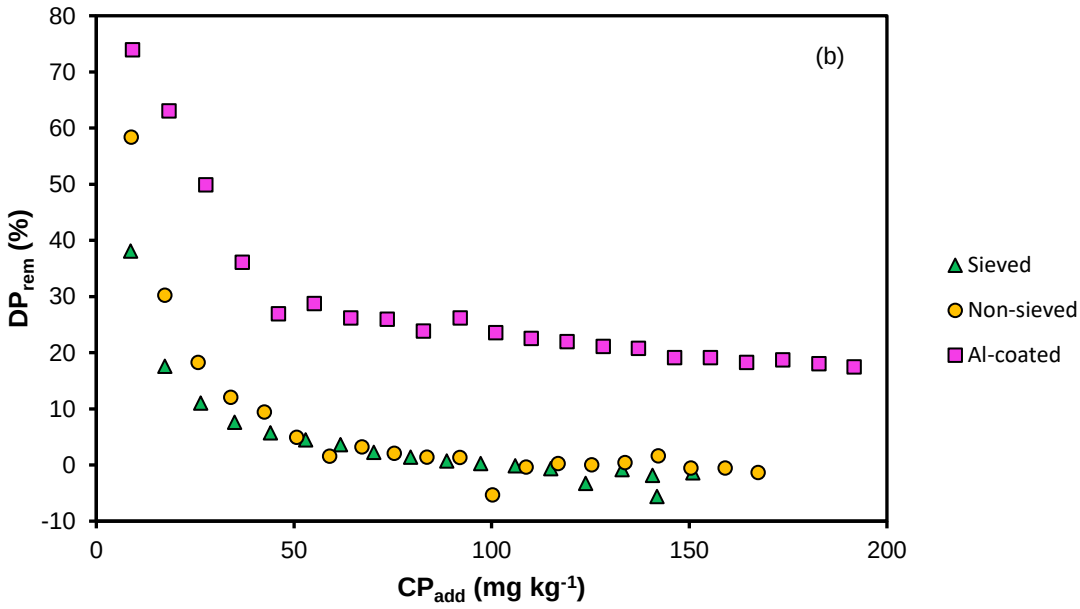

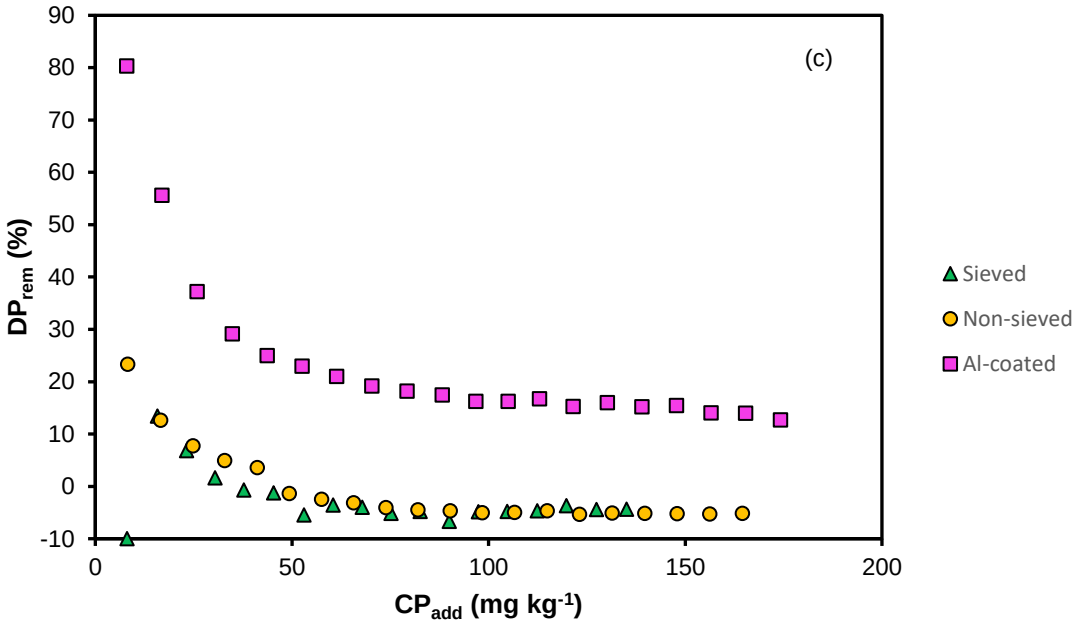

Figure 37. Discrete phosphorus removal (DPrem) design curves for full size fraction, > 0.5 mm, and Al-treated slags in inflow solution with (a) 0.25 g/L, (b) 0.5 g/L, and (c) 0.84 g/L bicarbonate concentration.

5.4.2. Effect of incubation on Al-coated slag

The effect of incubation time and bicarbonate concentration of the incubation solution was studied on Al treated slags. Eight combinations were used for the statistical analysis as listed in **Table 13**. **Figure 38** shows design curves for different combinations. Analysis of Variance (ANOVA) was carried out to investigate if incubation time and alkalinity concentration are statistically significant in variation of P removal efficiency of Al-treated slag. Hypothesis testing was used to interpret ANOVA results. For the ANOVA analysis, data was transformed using Johnson Transformation method as shown in **Figure S 3**. As shown in **Table 14**, only bicarbonate concentration is a slightly significant factor on subsequent P removal. This is somehow consistent with incubation results of the regular slag where neither incubation time nor incubation solution were significant factors. The

slight difference is presumably attributed to the fact that unlike the regular slag, for the Al-treated only short-term incubation was studied.

Hypothesis Test

H_o: $\mu_1=\mu_2=\mu_3=\cdots$

H_1: $\mu_1\neq\mu_2\neq\mu_3=\cdots$

Table 13. Maximum removal capacity as a function of incubation time and bicarbonate concentration in incubation solution for Al-treated slag. DP removal determined under inflow conditions of inflow concentrations of 0.5 mg P/L and 10 min retention time.

Rep	Incubation Time (day)	Alkalinity of solution for incubation (g/L)	b	m	R-Squared	Max removal capacity (mg/Kg)
1	0	0	100.02	-0.0009	0.48	1100.22
2	0	0	96.362	-0.001	0.41	953.62
1	0	0.25	103.39	-0.016	0.98	63.99
2	0	0.25	55.686	-0.003	0.65	182.29
1	0	0.5	49.245	-0.006	0.77	80.41
2	0	0.5	87.732	-0.02	0.9	43.37
1	3	0	102.33	-0.007	0.96	144.76
2	3	0	105.61	-0.004	0.84	261.52
1	3	0.25	112.68	-0.007	0.88	159.54
2	3	0.25	91.873	-0.004	0.92	227.18
1	3	0.5	98.403	-0.007	0.9	139.15
2	3	0.5	110.97	-0.005	0.87	219.94
1	7	0	96.923	-0.007	0.94	137.03
2	7	0	95.242	-0.008	0.79	117.8
1	7	0.25	87.214	-0.009	0.98	95.79

2	7	0.25	53.772	-0.006	0.77	87.95
1	7	0.5	86.454	-0.009	0.99	94.95
2	7	0.5	97.773	-0.01	0.61	96.77

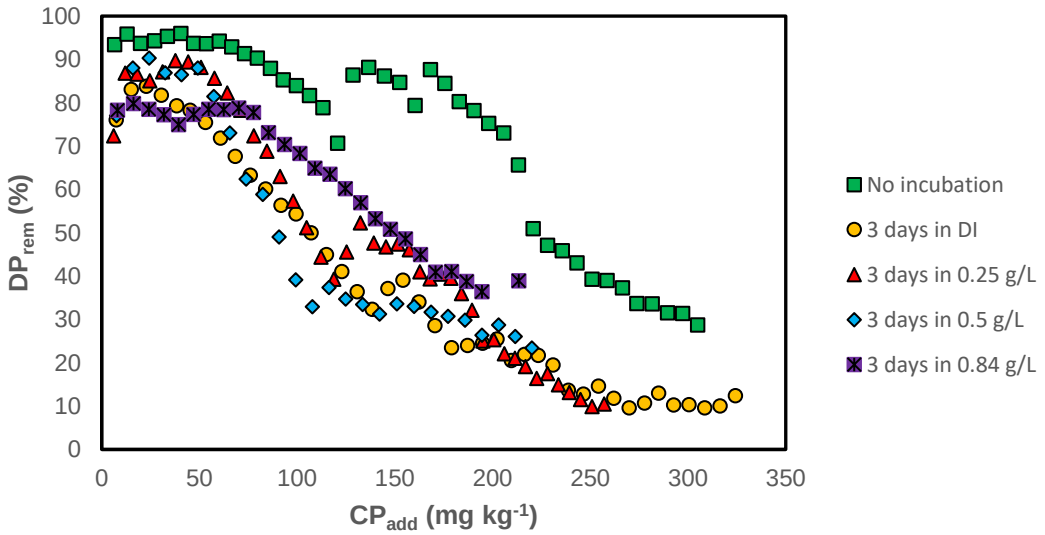

Figure 38. Effect of incubation time and bicarbonate concentration of incubation solution on design curve of the slag. DP removal determined under inflow conditions of inflow concentrations of 0.5 mg P/L, and 10 min retention time for the Al-treated EAF slag.

Table 14. ANOVA result for the effect of incubation time and bicarbonate concentration of incubation solution on P removal of Al-treated slag.

Factor	**Type**	**Levels**	**Values**
Incubation Time (day)	Fixed	3	0, 3, 7
Alkalinity of incubation solution (g/L)	Fixed	3	0.00, 0.25, 0.50

Source	**DF**	**Adj SS**	**Adj MS**	**F-Value**	**P-Value**
Incubation Time (day)	2	2.592	1.2959	1.84	0.197
Alkalinity of incubation solution (g/L)	2	5.869	2.9346	4.18	0.040
Error	13	9.137	0.7028		
Lack-of-Fit	4	6.317	1.5792	5.04	0.021

Pure Error	9	2.820	0.3133
Total	17	17.598	

S	R-sq	R-sq(adj)	R-sq(pred)
0.838348	48.08%	32.10%	0.46%

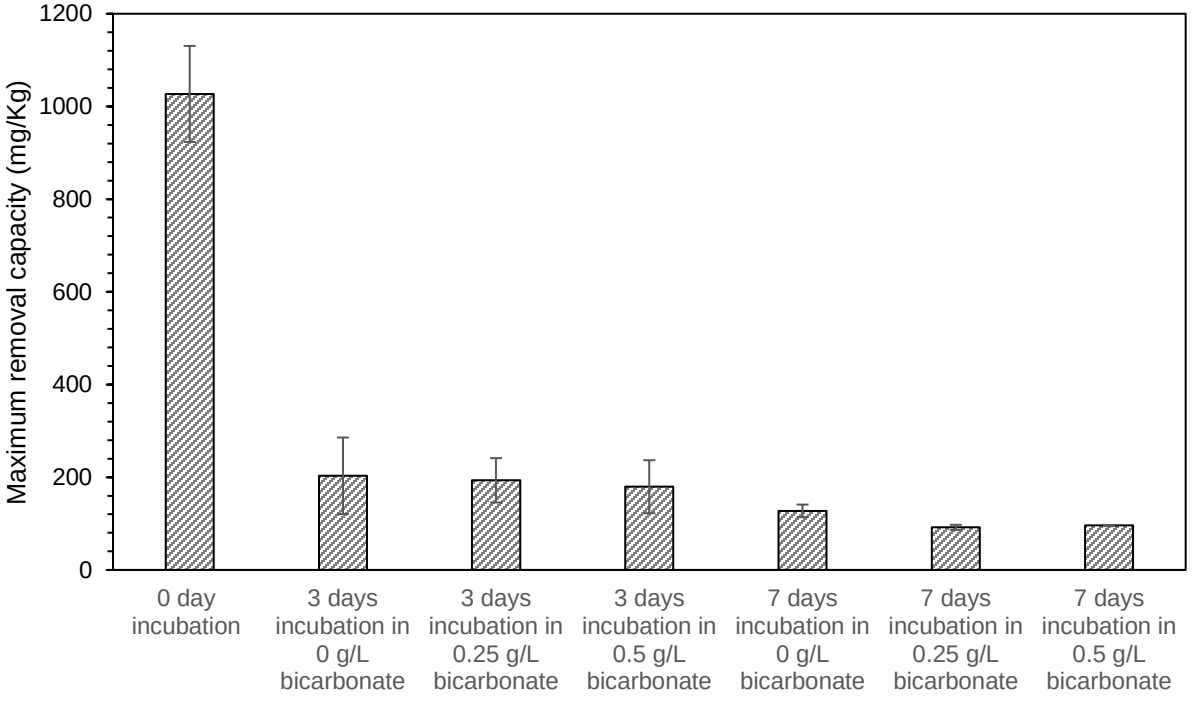

Figure 39. Bar chart for the effect of incubation time and bicarbonate concentration of incubation solution on maximum removal capacity the Al-treated slag.

Results of incubation studies (**Figure 39**) for Al-treated slag show that, unlike regular slag, both incubation time and bicarbonate concentration significantly reduce P removal capacity. This result is presumably due to detaching of some ligand bonds from PSM as a result of incubation, which leads to a decrease in P removal capacity. This finding shows that Al-treated slag should be applied in a top-down P removal structure for removing P from tile drainage systems.

6. Conclusion

A statistical approach was applied to investigate the effect of slag particle size distribution, bicarbonate concentration in inflow solution, incubation in an anaerobic condition, and chemical treatment on the P adsorption capacity of the electric arc furnace steel slag designed for removing P from water discharge in an agricultural tile drainage system. The following items summarize the main results of the present research:

1. Large EAF steel slag (> 500 μm) demonstrates a significant reduction in adsorption capacity compared to as-received slag
2. Presence of bicarbonate in outflow solution leads to zero phosphorous removal by EAF slag. ICP results confirm that bicarbonate is a strong competitor with phosphate ions to react with active Ca cations.
3. Incubation in DI water does not affect the removal efficiency of normal slag. In the presence of bicarbonate, statistical analysis demonstrates that phosphorous removal is not significantly impacted by incubation time and incubation solution
4. Al treatment leads to a shift in sorption mechanism of steel slag from precipitation to ligand exchange which results in a significantly higher P removal efficiency, and more importantly reducing the adverse effects of bicarbonate in inflow solution
5. ICP results confirm that steel slag removes P by precipitation mechanism, while Al-treated slag remove P predominantly via ligand exchange process.
6. Bicarbonate concentration is slightly significant on removal efficiency of Al-treated slag in a short-term incubation period, while incubation time was not found to be significant.

The results of this study can be used to scale up the application of the P removal structure filled by steel slag for a tile drainage system, as it has not been used successfully for this application in the past, unlike the successful trials of removing P from water runoff [41]. In summary, the Al-coated EAF slag, which removes P by ligand exchange onto Al hydroxide minerals, would be better suited to treat bicarbonate-rich tile drainage water than regular EAF slag. These results are also applicable to other types of Ca-based PSM's such as fly-ash, Flue gas desulfurization (FGD) gypsum, marble tailings, Wollastonite, Ca- drinking water treatment residuals (WTR), and sieved limestone [20].

REFRENCES

1. US EPA O (2015) SUMMARIES OF WATER POLLUTION REPORTING CATEGORIES. In: US EPA. https://www.epa.gov/waterdata/summaries-water-pollution-reporting-categories. Accessed 1 Nov 2019

2. May 14, Denchak 2018 Melissa Water Pollution: Everything You Need to Know. In: NRDC. https://www.nrdc.org/stories/water-pollution-everything-you-need-know. Accessed 1 Nov 2019

3. Litke DW (1999) Review of phosphorus control measures in the United States and their effects on water quality. Water-Resources Investigations Report 99:4007

4. Edwards B (2018) Novel porous material for removal of phosphorus from stormwater. UWM Undergraduate Research Symposium

5. Penn C, McGrath J, Bowen J, Wilson S (2014) Phosphorus removal structures: A management option for legacy phosphorus. Journal of Soil and Water Conservation 69:51A-56A

6. Penn CJ, Bryant RB, Kleinman PJ, Allen AL (2007) Removing dissolved phosphorus from drainage ditch water with phosphorus sorbing materials. Journal of Soil and Water Conservation 62:269–276

7. Global Climate Report - Annual 2013 | State of the Climate | National Centers for Environmental Information (NCEI). https://www.ncdc.noaa.gov/sotc/global/201313. Accessed 1 Nov 2019

8. (2011) Study: More than 1.5 million jobs, $62 billion in wages directly tied to Great Lakes. In: University of Michigan News. https://news.umich.edu/study-more-than-15-million-jobs-62-billion-in-wages-directly-tied-to-great-lakes/. Accessed 1 Nov 2019

9. Elhance AP (2000) Hydropolitics: Grounds for despair, reasons for hope. International Negotiation 5:201–222

10. The Eight US States Located in the Great Lakes Region. In: WorldAtlas. https://www.worldatlas.com/articles/the-eight-us-states-located-in-the-great-lakes-region.html. Accessed 3 Nov 2019

11. LCV M (2018) #OurLegacy: The near-death of Lake Erie and its uncertain future. In: Medium. https://medium.com/@MichiganLCV/ourlegacy-the-near-death-of-lake-erie-and-its-uncertain-future-e86c6deb682d. Accessed 3 Nov 2019

12. FAO - News Article: Global Report on Food Crises: acute hunger still affecting over 100 million people worldwide. http://www.fao.org/news/story/en/item/1187744/icode/. Accessed 1 Nov 2019

13. Mateo-Sagasta J, Zadeh SM, Turral H, Burke J (2017) Water pollution from agriculture: A global review. Executive summary. Rome, Italy: FAO Colombo, Sri Lanka: International Water Management Institute (IWMI). CGIAR Research Program on Water, Land and Ecosystems (WLE)

14. (2012) What is the difference between natural and cultural eutrophication?

15. Kordijazi A, Silva M (2018) Advancing Systematic and Fundamental Changes in Agricultural Water Resources Management. In: 2018 IEEE Conference on Technologies for Sustainability (SusTech). pp 1–2

16. Mante AA, Ranjan RS, Bullock P (2018) Subsurface drainage for promoting soil strength for field operations in southern Manitoba. Soil and Tillage Research 184:261–268

17. Sheler RJ (2013) The impact of agricultural drainage systems on hydrologic responses

18. Penn C, Chagas I, Klimeski A, Lyngsie G (2017) A Review of Phosphorus Removal Structures: How to Assess and Compare Their Performance. Water 9:583. https://doi.org/10.3390/w9080583

19. Qin Z, Shober AL, Scheckel KG, et al (2018) Mechanisms of Phosphorus Removal by Phosphorus Sorbing Materials. Journal of environmental quality 47:1232–1241

20. Penn CJ, Bowen JM (2017) Design and Construction of Phosphorus Removal Structures for Improving Water Quality. Springer

21. Penn CJ, McGrath JM, Rounds E, et al (2012) Trapping phosphorus in runoff with a phosphorus removal structure. Journal of Environmental Quality 41:672–679

22. Szögi AA, Humenik FJ, Rice JM, Hunt PG (1997) Swine wastewater treatment by media filtration. Journal of Environmental Science & Health Part B 32:831–843

23. Arias CA, Brix H, Johansen N-H (2003) Phosphorus removal from municipal wastewater in an experimental two-stage vertical flow constructed wetland system equipped with a calcite filter. Water Science and Technology 48:51–58

24. Søvik AK, Kløve B (2005) Phosphorus retention processes in shell sand filter systems treating municipal wastewater. Ecological engineering 25:168–182

25. Shilton AN, Elmetri I, Drizo A, et al (2006) Phosphorus removal by an 'active'slag filter–a decade of full scale experience. Water Research 40:113–118

26. Ádám K, Søvik AK, Krogstad T (2006) Sorption of phosphorous to Filtralite-PTM—The effect of different scales. Water Research 40:1143–1154

27. Weber D, Drizo A, Twohig E, et al (2007) Upgrading constructed wetlands phosphorus reduction from a dairy effluent using electric arc furnace steel slag filters. Water Science and Technology 56:135–143

28. Dobbie KE, Heal KV, Aumonier J, et al (2009) Evaluation of iron ochre from mine drainage treatment for removal of phosphorus from wastewater. Chemosphere 75:795–800

29. Kõiv M, Liira M, Mander Ü, et al (2010) Phosphorus removal using Ca-rich hydrated oil shale ash as filter material–the effect of different phosphorus loadings and wastewater compositions. Water Research 44:5232–5239

30. Agrawal SG, King KW, Moore JF, et al (2011) Use of industrial byproducts to filter phosphorus and pesticides in golf green drainage water. Journal of environmental quality 40:1273–1280

31. Penn CJ, McGrath JM (2011) Predicting phosphorus sorption onto steel slag using a flow-through approach with application to a pilot scale system. Journal of Water Resource and Protection 3:235

32. Bryant RB, Buda AR, Kleinman PJ, et al (2012) Using flue gas desulfurization gypsum to remove dissolved phosphorus from agricultural drainage waters. Journal of environmental quality 41:664–671

33. Kirkkala T, Ventelä A-M, Tarvainen M (2012) Long-term field-scale experiment on using lime filters in an agricultural catchment. Journal of Environmental Quality 41:410–419

34. Liu J, Davis AP (2013) Phosphorus speciation and treatment using enhanced phosphorus removal bioretention. Environmental science & technology 48:607–614

35. Wang Z, Bell GE, Penn CJ, et al (2014) Phosphorus reduction in turfgrass runoff using a steel slag trench filter system. Crop Science 54:1859–1867

36. Penn CJ, Bell G, Wang Z, et al (2014) Improving the ability of steel slag to filter phosphorus from runoff. Turfgrass Environ Res online 13:1–5

37. Claveau-Mallet D, Lida F, Comeau Y (2015) Improving phosphorus removal of conventional septic tanks by a recirculating steel slag filter. Water Quality Research Journal 50:211–218

38. Klimeski A, Uusitalo R, Turtola E (2015) Variations in phosphorus retention by a solid material while scaling up its application. Environmental Technology & Innovation 4:285–298

39. Chavez RA, Brown GO, Coffman RR, Storm DE (2015) Design, construction and lessons learned from Oklahoma bioretention cell demonstration project. Applied engineering in agriculture 31:63–71

40. Sibrell PL, Kehler T (2016) Phosphorus removal from aquaculture effluents at the Northeast Fishery Center in Lamar, Pennsylvania using iron oxide sorption media. Aquacultural engineering 72:45–52

41. Penn C, Bowen J, McGrath J, et al (2016) Evaluation of a universal flow-through model for predicting and designing phosphorus removal structures. Chemosphere 151:345–355

42. Yin H, Yan X, Gu X (2017) Evaluation of thermally-modified calcium-rich attapulgite as a low-cost substrate for rapid phosphorus removal in constructed wetlands. Water research 115:329–338

43. Vandermoere S, Ralaizafisoloarivony NA, Van Ranst E, De Neve S (2018) Reducing phosphorus (P) losses from drained agricultural fields with iron coated sand (-glauconite) filters. Water research 141:329–339

44. Baker MJ, Blowes DW, Ptacek CJ (1998) Laboratory development of permeable reactive mixtures for the removal of phosphorus from onsite wastewater disposal systems. Environmental science & technology 32:2308–2316

45. Geohring LD, Steenhuis TS, Brooks AS, et al (1999) Cost-effective phosphorus removal from secondary wastewater effluent through mineral adsorption. Final Report Prepared for the Town of Willisboro

46. Roseth R (2000) Shell sand: a new filter medium for constructed wetlands and wastewater treatment. Journal of Environmental Science & Health Part A 35:1335–1355

47. Agyei NM, Strydom CA, Potgieter JH (2002) The removal of phosphate ions from aqueous solution by fly ash, slag, ordinary Portland cement and related blends. Cement and concrete research 32:1889–1897

48. Bourke WS, Bilby S, Hamilton DP, McDowell RW (2005) Recent water improvement initiatives using melter slag filter materials. enviroNZ05–Water Matters 28–30

49. Drizo A, Forget C, Chapuis RP, Comeau Y (2006) Phosphorus removal by electric arc furnace steel slag and serpentinite. Water research 40:1547–1554

50. Boujelben N, Bouzid J, Elouear Z, et al (2008) Phosphorus removal from aqueous solution using iron coated natural and engineered sorbents. Journal of hazardous materials 151:103–110

51. Hartikainen SH, Hartikainen HH (2008) Phosphorus retention by phlogopite-rich mine tailings. Applied Geochemistry 23:2716–2723

52. Sibrell PL, Montgomery GA, Ritenour KL, Tucker TW (2009) Removal of phosphorus from agricultural wastewaters using adsorption media prepared from acid mine drainage sludge. Water research 43:2240–2250

53. Penn CJ, Bryant RB, Callahan MP, McGrath JM (2011) Use of industrial by-products to sorb and retain phosphorus. Communications in Soil Science and Plant Analysis 42:633–644

54. Stoner D, Penn C, McGrath J, Warren J (2012) Phosphorus removal with by-products in a flow-through setting. Journal of environmental quality 41:654–663

55. Dunets CS, Zheng Y, Dixon M (2015) Use of phosphorus-sorbing materials to remove phosphate from greenhouse wastewater. Environmental technology 36:1759–1770

56. Mitrogiannis D, Psychoyou M, Baziotis I, et al (2017) Removal of phosphate from aqueous solutions by adsorption onto Ca (OH) 2 treated natural clinoptilolite. Chemical Engineering Journal 320:510–522

57. Lyngsie G, Katika K, Fabricius IL, et al (2019) Phosphate removal by iron oxide-coated diatomite: Laboratory test of a new method for cleaning drainage water. Chemosphere 222:884–890

58. Johansson L (1999) Industrial By-Products and Natural Substrata as Phosphorus Sorbents. Environmental Technology 20:309–316. https://doi.org/10.1080/09593332008616822

59. Kostura B, Kulveitova H, Leško J (2005) Blast furnace slags as sorbents of phosphate from water solutions. Water research 39:1795–1802

60. Ning P, Bart H-J, Li B, et al (2008) Phosphate removal from wastewater by model-La(III) zeolite adsorbents. Journal of Environmental Sciences 20:670–674. https://doi.org/10.1016/S1001-0742(08)62111-7

61. Yang J, Zhou L, Zhao L, et al (2011) A designed nanoporous material for phosphate removal with high efficiency. Journal of Materials Chemistry 21:2489–2494

62. Erickson AJ, Gulliver JS, Weiss PT (2012) Capturing phosphates with iron enhanced sand filtration. Water research 46:3032–3042

63. Claveau-Mallet D, Wallace S, Comeau Y (2012) Model of Phosphorus Precipitation and Crystal Formation in Electric Arc Furnace Steel Slag Filters. Environ Sci Technol 46:1465–1470. https://doi.org/10.1021/es2024884

64. (8) (PDF) Testing of reactive materials for phosphorus removal from water and wastewater-Comparative study. In: ResearchGate. https://www.researchgate.net/publication/261947055_Testing_of_reactive_materials_for_phosphorus_removal_from_water_and_wastewater-Comparative_study. Accessed 3 Nov 2019

65. Rittmann BE, Mayer B, Westerhoff P, Edwards M (2011) Capturing the lost phosphorus. Chemosphere 84:846–853. https://doi.org/10.1016/j.chemosphere.2011.02.001

66. Ahmad SZN, Hamdan R, Mohamed WAW, et al (2017) Comparisons Study of Phosphate Removal in Unaerated and Aerated High Calcium Steel Slag Filter System of Different pH Feed. MATEC Web Conf 103:06018. https://doi.org/10.1051/matecconf/201710306018

67. Steiner GR, Freeman RJ (1989) Configuration and substrate design considerations for constructed wetlands wastewater treatment. Constructed Wetlands for Wastewater Treatment: Municipal, Industrial and Agricultural Lewis Publishers, Chelsea Michigan 1989 p 363-377, 3 fig, 1 tab, 18 ref

68. Moshiri GA (2020) Constructed wetlands for water quality improvement. CRC Press

69. Bird SC, Drizo A (2010) EAF Steel Slag Filters for Phosphorus Removal from Milk Parlor Effluent: The Effects of Solids Loading, Alternate Feeding Regimes and In-Series Design. Water 2:484–499. https://doi.org/10.3390/w2030484

70. Johansson Westholm L (2006) Substrates for phosphorus removal—Potential benefits for on-site wastewater treatment? Water Research 40:23–36. https://doi.org/10.1016/j.watres.2005.11.006

71. Vohla C, Kõiv M, Bavor HJ, et al (2011) Filter materials for phosphorus removal from wastewater in treatment wetlands—A review. Ecological Engineering 37:70–89. https://doi.org/10.1016/j.ecoleng.2009.08.003

72. Mercado-Borrayo BM, González-Chávez JL, Ramírez-Zamora RM, Schouwenaars R (2018) Valorization of Metallurgical Slag for the Treatment of Water Pollution: An Emerging Technology for Resource Conservation and Re-utilization. J Sustain Metall 4:50–67. https://doi.org/10.1007/s40831-018-0158-4

73. Claveau-Mallet D, Comeau Y (2020) Chemical Clogging and Evolution of Head Losses in Steel Slag Filters Used for Phosphorus Removal. Water 12:1517. https://doi.org/10.3390/w12061517

74. Barca C, Gérente C, Meyer D, et al (2012) Phosphate removal from synthetic and real wastewater using steel slags produced in Europe. Water Research 46:2376–2384. https://doi.org/10.1016/j.watres.2012.02.012

75. Okochi NC (2013) Phosphorus Removal From Stormwater Using Electric Arc Furnace Steel Slag. Thesis, Faculty of Graduate Studies and Research, University of Regina

76. Hosseini S, Soltani SM, Fennell PS, et al (2016) Production and applications of electric-arc-furnace slag as solid waste in environmental technologies: a review. Environmental Technology Reviews 5:1–11. https://doi.org/10.1080/21622515.2016.1147615

77. Wang LK, Shammas NK, Hung Y-T (2016) Waste treatment in the metal manufacturing, forming, coating, and finishing industries. CRC Press

78. Proctor DM, Fehling KA, Shay EC, et al (2000) Physical and Chemical Characteristics of Blast Furnace, Basic Oxygen Furnace, and Electric Arc Furnace Steel Industry Slags. Environ Sci Technol 34:1576–1582. https://doi.org/10.1021/es9906002

79. Johansson Westholm L (2010) The Use of Blast Furnace Slag for Removal of Phosphorus from Wastewater in Sweden—A Review. Water 2:826–837. https://doi.org/10.3390/w2040826

80. Al-Reasi HA, Wood CM, Smith DS (2011) Physicochemical and spectroscopic properties of natural organic matter (NOM) from various sources and implications for ameliorative effects on metal toxicity to aquatic biota. Aquatic Toxicology 103:179–190. https://doi.org/10.1016/j.aquatox.2011.02.015

81. Wendling LA, Binet MT, Yuan Z, et al (2013) Geochemical and ecotoxicological assessment of iron- and steel-making slags for potential use in environmental applications. Environmental Toxicology and Chemistry 32:2602–2610. https://doi.org/10.1002/etc.2342

82. Pratt C, Shilton A, Pratt S, et al (2007) Phosphorus Removal Mechanisms in Active Slag Filters Treating Waste Stabilization Pond Effluent. Environ Sci Technol 41:3296–3301. https://doi.org/10.1021/es062496b

83. Huaiwei Z, Xin H (2011) An overview for the utilization of wastes from stainless steel industries. Resources, Conservation and Recycling 55:745–754. https://doi.org/10.1016/j.resconrec.2011.03.005

84. Kriskova L, Pontikes Y, Cizer Ö, et al (2012) Effect of mechanical activation on the hydraulic properties of stainless steel slags. Cement and Concrete Research 42:778–788. https://doi.org/10.1016/j.cemconres.2012.02.016

85. Santos RM, François D, Mertens G, et al (2013) Ultrasound-intensified mineral carbonation. Applied Thermal Engineering 57:154–163. https://doi.org/10.1016/j.applthermaleng.2012.03.035

86. Santos RM, Van Bouwel J, Vandevelde E, et al (2013) Accelerated mineral carbonation of stainless steel slags for CO2 storage and waste valorization: Effect of process parameters on geochemical properties. International Journal of Greenhouse Gas Control 17:32–45. https://doi.org/10.1016/j.ijggc.2013.04.004

87. Zuo M, Renman G, Gustafsson JP, Renman A (2015) Phosphorus removal performance and speciation in virgin and modified argon oxygen decarburisation slag designed for wastewater treatment. Water Research 87:271–281. https://doi.org/10.1016/j.watres.2015.09.035

88. Turkdogan ET (1984) Physicochemical Aspects of Reactions in Ironmaking and Steelmaking Processes. Transactions of the Iron and Steel Institute of Japan 24:591–611. https://doi.org/10.2355/isijinternational1966.24.591

89. Gomez E, Rani DA, Cheeseman CR, et al (2009) Thermal plasma technology for the treatment of wastes: A critical review. Journal of Hazardous Materials 161:614–626. https://doi.org/10.1016/j.jhazmat.2008.04.017

90. Alsheyab MAT, Khedaywi TS (2013) Effect of electric arc furnace dust (EAFD) on properties of asphalt cement mixture. Resources, Conservation and Recycling 70:38–43. https://doi.org/10.1016/j.resconrec.2012.10.003

91. Drizo A, Comeau Y, Forget C, Chapuis RP (2002) Phosphorus Saturation Potential: A Parameter for Estimating the Longevity of Constructed Wetland Systems. Environ Sci Technol 36:4642–4648. https://doi.org/10.1021/es011502v

92. Khoshkhoo H, Sadeghi SHH, Moini R, Talebi HA (2011) An efficient power control scheme for electric arc furnaces using online estimation of flexible cable inductance. Computers & Mathematics with Applications 62:4391–4401. https://doi.org/10.1016/j.camwa.2011.10.009

93. Shi C (2004) Steel Slag—Its Production, Processing, Characteristics, and Cementitious Properties. Journal of Materials in Civil Engineering 16:230–236. https://doi.org/10.1061/(ASCE)0899-1561(2004)16:3(230)

94. Tsakiridis PE, Papadimitriou GD, Tsivilis S, Koroneos C (2008) Utilization of steel slag for Portland cement clinker production. Journal of Hazardous Materials 152:805–811. https://doi.org/10.1016/j.jhazmat.2007.07.093

95. Wang X, Cai Q-S (2006) Steel Slag as an Iron Fertilizer for Corn Growth and Soil Improvement in a Pot Experiment1 1Project supported by the National Natural Science Foundation of China (No. 30270800). Pedosphere 16:519–524. https://doi.org/10.1016/S1002-0160(06)60083-0

96. Stolaroff JK, Lowry GV, Keith DW (2005) Using CaO- and MgO-rich industrial waste streams for carbon sequestration. Energy Conversion and Management 46:687–699. https://doi.org/10.1016/j.enconman.2004.05.009

97. Huijgen WJJ, Witkamp G-J, Comans RNJ (2005) Mineral CO2 Sequestration by Steel Slag Carbonation. Environ Sci Technol 39:9676–9682. https://doi.org/10.1021/es050795f

98. Li H, Li Y, Gong Z, Li X (2013) Performance study of vertical flow constructed wetlands for phosphorus removal with water quenched slag as a substrate. Ecological Engineering 53:39–45. https://doi.org/10.1016/j.ecoleng.2013.01.011

99. Nehrenheim E, Waara S, Johansson Westholm L (2008) Metal retention on pine bark and blast furnace slag – On-site experiment for treatment of low strength landfill leachate. Bioresource Technology 99:998–1005. https://doi.org/10.1016/j.biortech.2007.03.006

100. Klimeski A, Chardon WJ, Uusitalo R, Turtola E (2012) Potential and limitations of phosphate retention media in water protection: a process-based review of laboratory and field-scale tests. Agricultural and Food Science 21:206–223

101. McDowell RW, Hawke MF (2006) Assessment of a novel technique to remove phosphorus from streamflow. Environment Bay of Plenty

102. Pratt C, Shilton A, Haverkamp RG, Pratt S (2009) Assessment of physical techniques to regenerate active slag filters removing phosphorus from wastewater. Water Research 43:277–282. https://doi.org/10.1016/j.watres.2008.10.020

103. Park J-H, Wang JJ, Kim S-H, et al (2017) Phosphate removal in constructed wetland with rapid cooled basic oxygen furnace slag. Chemical Engineering Journal 327:713–724. https://doi.org/10.1016/j.cej.2017.06.155

104. Reddy KR, Smith WH (1987) Aquatic plants for water treatment and resource recovery. Magnolia Publ. Inc Orlando, Fl

105. Mitsch WJ, Cronk JK (1992) Creation and Restoration of Wetlands: Some Design Consideration for Ecological Engineering. In: Lal R, Stewart BA (eds) Soil Restoration: Soil Restoration Volume 17. Springer, New York, NY, pp 217–259

106. Newbold JD, Elwood JW, O'Neill RV, Sheldon AL (1983) Phosphorus Dynamics in a Woodland Stream Ecosystem: A Study of Nutrient Spiralling. Ecology 64:1249–1265. https://doi.org/10.2307/1937833

107. Diazo A, Reddy KR, Moore PA (1994) Solubility of inorganic P in stream water as influenced by pH and Ca concentration. Water Research 28:1755–1763

108. Kadlec RH (1997) An autobiotic wetland phosphorus model. Ecological Engineering 8:145–172. https://doi.org/10.1016/S0925-8574(97)00257-7

109. Greenway M, Woolley A (1999) Constructed wetlands in Queensland: Performance efficiency and nutrient bioaccumulation. Ecological Engineering 12:39–55. https://doi.org/10.1016/S0925-8574(98)00053-6

110. Reddy KR, Kadlec RH, Flaig E, Gale PM (1999) Phosphorus Retention in Streams and Wetlands: A Review. Critical Reviews in Environmental Science and Technology 29:83–146. https://doi.org/10.1080/10643389991259182

111. Seo DC, Cho JS, Lee HJ, Heo JS (2005) Phosphorus retention capacity of filter media for estimating the longevity of constructed wetland. Water Research 39:2445–2457. https://doi.org/10.1016/j.watres.2005.04.032

112. Gerritse RG (1993) Prediction of travel times of phosphate in soils at a disposal site for wastewater. Water Research 27:263–267. https://doi.org/10.1016/0043-1354(93)90084-U

113. Park J-H, Kim S-H, Delaune RD, et al (2016) Enhancement of phosphorus removal with near-neutral pH utilizing steel and ferronickel slags for application of constructed wetlands. Ecological Engineering 95:612–621. https://doi.org/10.1016/j.ecoleng.2016.06.052

114. Chazarenc F, Brisson J, Comeau Y (2007) Slag columns for upgrading phosphorus removal from constructed wetland effluents. Water Sci Technol 56:109–115. https://doi.org/10.2166/wst.2007.499

115. Pratt C, Shilton A (2010) Active slag filters—simple and sustainable phosphorus removal from wastewater using steel industry byproduct. Water Sci Technol 62:1713–1718. https://doi.org/10.2166/wst.2010.389

116. Fausey NR, Brown LC, Belcher HW, Kanwar RS (1995) Drainage and water quality in Great Lakes and cornbelt states. Journal of Irrigation and Drainage Engineering 121:283–288

117. Skaggs RW, Brevé MA, Gilliam JW (1994) Hydrologic and water quality impacts of agricultural drainage∗. Critical Reviews in Environmental Science and Technology 24:1–32. https://doi.org/10.1080/10643389409388459

118. Eidman V (1997) Minnesota farmland drainage: Profitability and concerns. Minnesota Agricultural Economist 688:1–7

119. Sharpley A, Tunney H (2000) Phosphorus Research Strategies to Meet Agricultural and Environmental Challenges of the 21st Century. Journal of Environmental Quality 29:176–181. https://doi.org/10.2134/jeq2000.00472425002900010022x

120. Correll DL (1998) The Role of Phosphorus in the Eutrophication of Receiving Waters: A Review. Journal of Environmental Quality 27:261–266. https://doi.org/10.2134/jeq1998.00472425002700020004x

121. Schindler DW, Hecky RE, Findlay DL, et al (2008) Eutrophication of lakes cannot be controlled by reducing nitrogen input: results of a 37-year whole-ecosystem experiment. Proceedings of the National Academy of Sciences 105:11254–11258

122. Baker JL, Campbell KL, Johnson HP, Hanway JJ (1975) Nitrate, Phosphorus, and Sulfate in Subsurface Drainage Water. Journal of Environmental Quality 4:406–412. https://doi.org/10.2134/jeq1975.00472425000400030027x

123. Gentry LE, David MB, Royer TV, et al (2007) Phosphorus Transport Pathways to Streams in Tile-Drained Agricultural Watersheds. Journal of Environmental Quality 36:408–415. https://doi.org/10.2134/jeq2006.0098

124. King KW, Williams MR, Macrae ML, et al (2015) Phosphorus Transport in Agricultural Subsurface Drainage: A Review. Journal of Environmental Quality 44:467–485. https://doi.org/10.2134/jeq2014.04.0163

125. Smith DR, King KW, Johnson L, et al (2015) Surface Runoff and Tile Drainage Transport of Phosphorus in the Midwestern United States. Journal of Environmental Quality 44:495–502. https://doi.org/10.2134/jeq2014.04.0176

126. Zhang TQ, Tan CS, Zheng ZM, Drury CF (2015) Tile Drainage Phosphorus Loss with Long-Term Consistent Cropping Systems and Fertilization. Journal of Environmental Quality 44:503–511. https://doi.org/10.2134/jeq2014.04.0188

127. Sonzogni WC, Chapra SC, Armstrong DE, Logan TJ (1982) Bioavailability of Phosphorus Inputs to Lakes. Journal of Environmental Quality 11:555–563. https://doi.org/10.2134/jeq1982.00472425001100040001x

128. Sellner B (2016) Evaluating Steel Byproducts and Natural Minerals for Phosphate Adsorption from Agricultural Subsurface Drainage. Electronic Theses and Dissertations

129. Mendes D, Renato L (2020) Edge-of-Field Technologies for Phosphorus Retention from Agricultural Drainage Discharge. Applied Sciences 10:634. https://doi.org/10.3390/app10020634

130. Oguz E (2004) Removal of phosphate from aqueous solution with blast furnace slag. Journal of Hazardous Materials 114:131–137. https://doi.org/10.1016/j.jhazmat.2004.07.010

131. Kim E-H, Lee D-W, Hwang H-K, Yim S (2006) Recovery of phosphates from wastewater using converter slag: Kinetics analysis of a completely mixed phosphorus crystallization process. Chemosphere 63:192–201. https://doi.org/10.1016/j.chemosphere.2005.08.029

132. Drizo A, Cummings J, Weber D, et al (2008) New Evidence for Rejuvenation of Phosphorus Retention Capacity in EAF Steel Slag. Environ Sci Technol 42:6191–6197. https://doi.org/10.1021/es800232r

133. Chen X, Sun X, Xu P, et al (2020) Optimal regulation of N/P in horizontal sub-surface flow constructed wetland through quantitative phosphorus removal by steel slag fed. Environ Sci Pollut Res 27:5779–5787. https://doi.org/10.1007/s11356-019-06696-5

134. Pratt C, Shilton A, Haverkamp R g., Pratt S (2011) Chemical techniques for pretreating and regenerating active slag filters for improved phosphorus removal. null 32:1053–1062. https://doi.org/10.1080/09593330.2010.525749

135. Sellner B, Hua G, Ahiablame L, et al (2016) Evaluating Filter Materials for Phosphate Adsorption from Agricultural Subsurface Drainage. In: 2016 ASABE Annual International Meeting. American Society of Agricultural and Biological Engineers, p 1

136. Zeng F (2017) Phosphorus Retention and Regeneration of EAF Steel Slag and a Synthetic Iron Oxyhydroxide. The Ohio State University

137. Xie J, Lin Y, Li C, et al (2015) Removal and recovery of phosphate from water by activated aluminum oxide and lanthanum oxide. Powder Technology 269:351–357. https://doi.org/10.1016/j.powtec.2014.09.024

138. Triantafyllidis KS, Peleka EN, Komvokis VG, Mavros PP (2010) Iron-modified hydrotalcite-like materials as highly efficient phosphate sorbents. Journal of Colloid and Interface Science 342:427–436. https://doi.org/10.1016/j.jcis.2009.10.063

139. Wendling L, Loimula K, Korkealaakso J, et al (2017) StormFilter material testing summary report: Performance of stormwater filtration systems

140. Sengupta S, Pandit A (2011) Selective removal of phosphorus from wastewater combined with its recovery as a solid-phase fertilizer. Water Research 45:3318–3330. https://doi.org/10.1016/j.watres.2011.03.044

141. Kunaschk M, Schmalz V, Dietrich N, et al (2015) Novel regeneration method for phosphate loaded granular ferric (hydr)oxide – A contribution to phosphorus recycling. Water Research 71:219–226. https://doi.org/10.1016/j.watres.2015.01.001

142. Kuzawa K, Jung Y-J, Kiso Y, et al (2006) Phosphate removal and recovery with a synthetic hydrotalcite as an adsorbent. Chemosphere 62:45–52. https://doi.org/10.1016/j.chemosphere.2005.04.015

143. Urano K, Tachikawa H (1992) Process development for removal and recovery of phosphorus from wastewater by a new adsorbent. 3. Desorption of phosphate and regeneration of adsorbent. Industrial & engineering chemistry research 31:1510–1513

144. Yamada H, Kayama M, Saito K, Hara M (1986) A fundamental research on phosphate removal by using slag. Water Research 20:547–557. https://doi.org/10.1016/0043-1354(86)90018-7

145. Yamada H, Kayama M, Saito K, Hara M (1987) Suppression of phosphate liberation from sediment by using iron slag. Water Research 21:325–333. https://doi.org/10.1016/0043-1354(87)90212-0

146. Mann RA, Bavor HJ (1993) Phosphorus Removal in Constructed Wetlands Using Gravel and Industrial Waste Substrata. Water Sci Technol 27:107–113. https://doi.org/10.2166/wst.1993.0027

147. Mann RA (1997) Phosphorus adsorption and desorption characteristics of constructed wetland gravels and steelworks by-products. Soil Res 35:375–384. https://doi.org/10.1071/s96041

148. Pratt C, Shilton A (2009) Suitability of adsorption isotherms for predicting the retention capacity of active slag filters removing phosphorus from wastewater. Water Sci Technol 59:1673–1678. https://doi.org/10.2166/wst.2009.163

149. Valero MAC, Johnson M, Mather T, Mara DD (2009) Enhanced phosphorus removal in a waste stabilization pond system with blast furnace slag filters. Desalination and Water Treatment 4:122–127. https://doi.org/10.5004/dwt.2009.366

150. Mcgrath JM, Penn CJ, Coale FJ (2013) A modelling approach to the design of in situ agricultural drainage filters. Soil Use and Management 29:155–161. https://doi.org/10.1111/j.1475-2743.2011.00381.x

151. Bowen JM (2015) Design, Quantification, and Demonstration of Large Scale Phosphorus Removal Structures in Oklahoma

152. DeSutter TM, Pierzynski GM, Baker LR (2006) Flow-Through and Batch Methods for Determining Calcium-Magnesium and Magnesium-Calcium Selectivity. Soil Science Society of America Journal 70:550–554. https://doi.org/10.2136/sssaj2005.0065N

153. US EPA O (2014) Water Quality Standards Handbook. In: US EPA. https://www.epa.gov/wqs-tech/water-quality-standards-handbook. Accessed 3 Nov 2019

154. Xie J, Wang Z, Fang D, et al (2014) Green synthesis of a novel hybrid sorbent of zeolite/lanthanum hydroxide and its application in the removal and recovery of phosphate from water. Journal of Colloid and Interface Science 423:13–19. https://doi.org/10.1016/j.jcis.2014.02.020

155. Ghisellini P, Ripa M, Ulgiati S (2018) Exploring environmental and economic costs and benefits of a circular economy approach to the construction and demolition sector. A literature review. Journal of Cleaner Production 178:618–643. https://doi.org/10.1016/j.jclepro.2017.11.207

156. Gonzalez JM, Penn CJ, Livingston SJ (2020) Utilization of Steel Slag in Blind Inlets for Dissolved Phosphorus Removal. Water 12:1593. https://doi.org/10.3390/w12061593

157. Lindsay WL (1979) Chelate equilibria. Chemical equilibria in soils 238–263

158. Barrett PH (1953) Relationships between alkalinity and adsorption and regeneration of added phosphorus in fertilized trout lakes. Transactions of the American Fisheries Society 82:78–90

159. LaFlamme BD, Murray JW (1987) Solidsolution interaction: The effect of carbonate alkalinity on adsorbed thorium. Geochimica et Cosmochimica Acta 51:243–250

160. Penn CJ, Camberato JJ (2019) A Critical Review on Soil Chemical Processes that Control How Soil pH Affects Phosphorus Availability to Plants. Agriculture 9:120. https://doi.org/10.3390/agriculture9060120

161. Sakadevan K, Bavor HJ (1998) Phosphate adsorption characteristics of soils, slags and zeolite to be used as substrates in constructed wetland systems. Water Research 32:393–399. https://doi.org/10.1016/S0043-1354(97)00271-6

162. Johansson L, Gustafsson JP (2000) Phosphate removal using blast furnace slags and opoka-mechanisms. Water Research 34:259–265. https://doi.org/10.1016/S0043-1354(99)00135-9

163. Naylor S, Brisson J, Labelle MA, et al (2003) Treatment of freshwater fish farm effluent using constructed wetlands: the role of plants and substrate. Water Sci Technol 48:215–222. https://doi.org/10.2166/wst.2003.0324

164. Cha W, Kim J, Choi H (2006) Evaluation of steel slag for organic and inorganic removals in soil aquifer treatment. Water Research 40:1034–1042. https://doi.org/10.1016/j.watres.2005.12.039

165. Lan YZ, Zhang S, Wang JK, Smith RW (2006) Phosphorus removal using steel slag. Acta Metallurgica Sinica (English Letters) 19:449–454. https://doi.org/10.1016/S1006-7191(06)62086-3

166. Pratt C, Shilton A, Pratt S, et al (2007) Effects of Redox Potential and pH Changes on Phosphorus Retention by Melter Slag Filters Treating Wastewater. Environ Sci Technol 41:6585–6590. https://doi.org/10.1021/es070914m

167. McDowell RW, Hawke M, McIntosh JJ (2007) Assessment of a technique to remove phosphorus from streamflow. New Zealand Journal of Agricultural Research 50:503–510. https://doi.org/10.1080/00288230709510318

168. Xiong J, He Z, Mahmood Q, et al (2008) Phosphate removal from solution using steel slag through magnetic separation. Journal of Hazardous Materials 152:211–215. https://doi.org/10.1016/j.jhazmat.2007.06.103

169. Xue Y, Hou H, Zhu S (2009) Characteristics and mechanisms of phosphate adsorption onto basic oxygen furnace slag. Journal of Hazardous Materials 162:973–980. https://doi.org/10.1016/j.jhazmat.2008.05.131

170. Ling H, Yongqiang S Phosphorus Removal in Sewage by Mixed Steel Slag Fillings

171. Bowden LI, Jarvis AP, Younger PL, Johnson KL (2009) Phosphorus Removal from Waste Waters Using Basic Oxygen Steel Slag. Environ Sci Technol 43:2476–2481. https://doi.org/10.1021/es801626d

172. Lee MS, Drizo A, Rizzo DM, et al (2010) Evaluating the efficiency and temporal variation of pilot-scale constructed wetlands and steel slag phosphorus removing filters for treating dairy wastewater. Water Research 44:4077–4086. https://doi.org/10.1016/j.watres.2010.05.020

173. Li Y, Liu Y, Du G (2010) Removal of Phosphate from Wastewater Using Steel Slag Modified by High Temperature Activation. In: 2010 4th International Conference on Bioinformatics and Biomedical Engineering. pp 1–5

174. Chazarenc F, Filiatrault M, Brisson J, Comeau Y (2010) Combination of Slag, Limestone and Sedimentary Apatite in Columns for Phosphorus Removal from Sludge Fish Farm Effluents. Water 2:500–509. https://doi.org/10.3390/w2030500

175. Miller RL, Jensen BJ, Munns BT, Cardon GE (2010) Use of Steel Slag to Reduce Phosphorus Loading in Animal Waste Handling Systems. In: International Symposium on Air Quality and Manure Management for Agriculture Conference Proceedings, 13-16 September 2010, Dallas, Texas. American Society of Agricultural and Biological Engineers, p 1

176. Xiong J, Qin Y, Mahmood Q, et al (2011) Phosphorus removal from secondary effluents through integrated constructed treatment system. Marine Pollution Bulletin 63:98–101. https://doi.org/10.1016/j.marpolbul.2011.04.020

177. Wu J, He F, Xu D, et al (2011) Phosphorus removal by laboratory-scale unvegetated vertical-flow constructed wetland systems using anthracite, steel slag and related blends as substrate. Water Sci Technol 63:2719–2724. https://doi.org/10.2166/wst.2011.573

178. Wang G, Qiu L, Zhang S, et al Hydrothermal Modification of Granular Steel Slag for Phosphate Removal. In: 2011 5th International Conference on Bioinformatics and Biomedical Engineering

179. Wang Z (2012) Phosphorus Reduction in Runoff Using a Steel Slag Trench Filter System

180. Lee C-G, Park J-A, Kim S-B (2012) Phosphate removal from aqueous solutions using slag microspheres. Desalination and Water Treatment 44:229–236. https://doi.org/10.1080/19443994.2012.691738

181. Claveau-Mallet D, Wallace S, Comeau Y (2013) Removal of phosphorus, fluoride and metals from a gypsum mining leachate using steel slag filters. Water Research 47:1512–1520. https://doi.org/10.1016/j.watres.2012.11.048

182. Klimeski A, Uusitalo R, Turtola E (2014) Screening of Ca- and Fe-rich materials for their applicability as phosphate-retaining filters. Ecological Engineering 68:143–154. https://doi.org/10.1016/j.ecoleng.2014.03.054

183. Barca C, Meyer D, Liira M, et al (2014) Steel slag filters to upgrade phosphorus removal in small wastewater treatment plants: Removal mechanisms and performance. Ecological Engineering 68:214–222. https://doi.org/10.1016/j.ecoleng.2014.03.065

184. Wang JT, Yu YZ, Gao LL (2014) Adsorption removal of Phosphorus from wastewater by Steel slag filter material. In: Advanced Materials Research. Trans Tech Publ, pp 827–830

185. Tang JX, Sun LN, Yun YP, et al (2014) Adsorption of phosphate in aqueous solution with steel slag. In: Applied Mechanics and Materials. Trans Tech Publ, pp 401–404

186. Liu Z, Qiu LP, Zhang LX (2014) Start-up Characteristics of Biological Aerated Filter with Composite Steel Slag Media for Nitrogen and Phosphorus Removal. In: Applied Mechanics and Materials. Trans Tech Publ, pp 939–942

187. Hussain SI, Blowes DW, Ptacek CJ, Olding D (2014) Phosphorus Removal from Lake Water Using Basic Oxygen Furnace Slag: System Performance and Characterization of Reaction Products. Environmental Engineering Science 31:631–642. https://doi.org/10.1089/ees.2014.0074

188. Yu J, Liang W, Wang L, et al (2015) Phosphate removal from domestic wastewater using thermally modified steel slag. Journal of Environmental Sciences 31:81–88. https://doi.org/10.1016/j.jes.2014.12.007

189. Han C, Wang Z, Yang H, Xue X (2015) Removal kinetics of phosphorus from synthetic wastewater using basic oxygen furnace slag. Journal of Environmental Sciences 30:21–29. https://doi.org/10.1016/j.jes.2014.11.003

190. Yun Y, Zhou X, Li Z, et al (2015) Comparative research on phosphorus removal by pilot-scale vertical flow constructed wetlands using steel slag and modified steel slag as substrates. Water Sci Technol 71:996–1003. https://doi.org/10.2166/wst.2015.059

191. Wang H, Shen S, Liu L, et al (2015) Effective adsorption of phosphate from wastewaters by big composite pellets made of reduced steel slag and iron ore concentrate. Environmental Technology 36:2835–2846. https://doi.org/10.1080/09593330.2015.1050069

192. Wu J, Xu D, He F, et al (2015) Comprehensive evaluation of substrates in vertical-flow constructed wetlands for domestic wastewater treatment. Water Practice and Technology 10:625–632. https://doi.org/10.2166/wpt.2015.077

193. Ping X, Liyun Y, Aikebaier R, Hao B (2016) The Removal of Phosphate and Ammonia Nitrogen from Wastewater Using Steel Slag. In: Jha A, Wang C, Neelameggham NR, et al (eds) Energy Technology 2015: Carbon Dioxide Management and Other Technologies. Springer International Publishing, Cham, pp 165–172

194. Zhang C, Tan S, Li J, Peng C (2015) Polishing of Secondary Effluent by a Two-Stage Vertical-Flow Constructed Wetland. Pol J Environ Stud 24:923–928. https://doi.org/10.15244/pjoes/23868

195. Blanco I, Molle P, Sáenz de Miera LE, Ansola G (2016) Basic Oxygen Furnace steel slag aggregates for phosphorus treatment. Evaluation of its potential use as a substrate in constructed wetlands. Water Research 89:355–365. https://doi.org/10.1016/j.watres.2015.11.064

196. Han C, Wang Z, Yang W, et al (2016) Effects of pH on phosphorus removal capacities of basic oxygen furnace slag. Ecological Engineering 89:1–6. https://doi.org/10.1016/j.ecoleng.2016.01.004

197. Kõiv M, Mahadeo K, Brient S, et al (2016) Treatment of fish farm sludge supernatant by aerated filter beds and steel slag filters—effect of organic loading rate. Ecological Engineering 94:190–199. https://doi.org/10.1016/j.ecoleng.2016.05.060

198. Lu S, Zhang X, Wang J, Pei L (2016) Impacts of different media on constructed wetlands for rural household sewage treatment. Journal of Cleaner Production 127:325–330. https://doi.org/10.1016/j.jclepro.2016.03.166

199. Ge Y, Wang XC, Dzakpasu M, et al (2016) Characterizing phosphorus removal from polluted urban river water by steel slags in a vertical flow constructed wetland. Water Sci Technol 73:2644–2653. https://doi.org/10.2166/wst.2016.118

200. Afnizan WMW, Hamdan R, Othman N (2016) Study of The Maximum Uptake Capacity on Various Sizes of Electric Arc Furnace Slag in Phosphorus Aqueous Solutions. IOP Conf Ser: Mater Sci Eng 136:012060. https://doi.org/10.1088/1757-899X/136/1/012060

201. Christianson LE, Lepine C, Sibrell PL, et al (2017) Denitrifying woodchip bioreactor and phosphorus filter pairing to minimize pollution swapping. Water Research 121:129–139. https://doi.org/10.1016/j.watres.2017.05.026

202. Park T, Ampunan V, Maeng S, Chung E (2017) Application of steel slag coated with sodium hydroxide to enhance precipitation-coagulation for phosphorus removal. Chemosphere 167:91–97. https://doi.org/10.1016/j.chemosphere.2016.09.150

203. Postila H, Karjalainen SM, Kløve B (2017) Can limestone, steel slag or man-made sorption materials be used to enhance phosphate-phosphorus retention in treatment wetland for peat extraction runoff with low phosphorous concentration? Ecological Engineering 98:403–409. https://doi.org/10.1016/j.ecoleng.2016.05.042

204. Claveau-Mallet D, Boutet É, Comeau Y (2018) Steel slag filter design criteria for phosphorus removal from wastewater in decentralized applications. Water Research 143:28–37. https://doi.org/10.1016/j.watres.2018.06.032

205. Zuo M, Renman G, Gustafsson JP, Klysubun W (2018) Phosphorus removal by slag depends on its mineralogical composition: A comparative study of AOD and EAF slags. Journal of Water Process Engineering 25:105–112. https://doi.org/10.1016/j.jwpe.2018.07.003

206. Li J, Wu B, Zhou T, Chai X (2018) Preferential removal of phosphorus using modified steel slag and cement combination for its implications in engineering applications. Environmental Technology & Innovation 10:264–274. https://doi.org/10.1016/j.eti.2018.02.007

207. Hamdan R, Arshad NANM, Ahmad SZN (2018) The Effects of PO 4 3-Removal from Aqueous Solution with Varied Concentrations of Metal Oxides in Steel Slag Filter System. Journal of Physical Science 29:71–80

208. Wang J, Wang X, Qiu L, et al (2018) Study on Key Factors of Adsorption of Phosphorus by Steel Slag Filter Based on Response Surface Method. E3S Web Conf 53:03050. https://doi.org/10.1051/e3sconf/20185303050

209. Bailey SB, Chu ML, Cooke RA (2018) Mitigating tile drainage phosphorus using phosphorus sorbing materials in a continuous flow through pilot system. In: 2018 ASABE Annual International Meeting. American Society of Agricultural and Biological Engineers, p 1

210. Sellner BM, Hua G, Ahiablame LM, et al (2019) Evaluation of industrial by-products and natural minerals for phosphate adsorption from subsurface drainage. Environmental Technology 40:756–767. https://doi.org/10.1080/09593330.2017.1407364

211. Mohd Arshad NAN, Hamdan R, Rimin W, Ernastia Yaftha E (2020) Aerated and unaerated steel slag filter systems as polishing unit for phosphorus removal from textile industrial effluent. Materials Today: Proceedings 31:372–377. https://doi.org/10.1016/j.matpr.2020.06.573

212. Claveau-Mallet D, Seltani H, Comeau Y (2020) Phosphorus Removal and Carbon Dioxide Capture in a Pilot Conventional Septic System Upgraded with a Sidestream Steel Slag Filter. Water 12:275. https://doi.org/10.3390/w12010275

213. Edgar M, Ray H, Grubb DG, et al (2020) Removal of Phosphate and Nitrate from Impacted Waters via Slag-Driven Precipitation and Microbial Transformation. Journal of Sustainable Water in the Built Environment 6:04020007. https://doi.org/10.1061/JSWBAY.0000914

214. Penn C, Livingston S, Shedekar V, et al (2020) Performance of Field-Scale Phosphorus Removal Structures Utilizing Steel Slag for Treatment of Subsurface Drainage. Water 12:443. https://doi.org/10.3390/w12020443

215. Wang L, Penn C, Huang C, et al (2020) Using Steel Slag for Dissolved Phosphorus Removal: Insights from a Designed Flow-Through Laboratory Experimental Structure. Water 12:1236. https://doi.org/10.3390/w12051236

Appendix

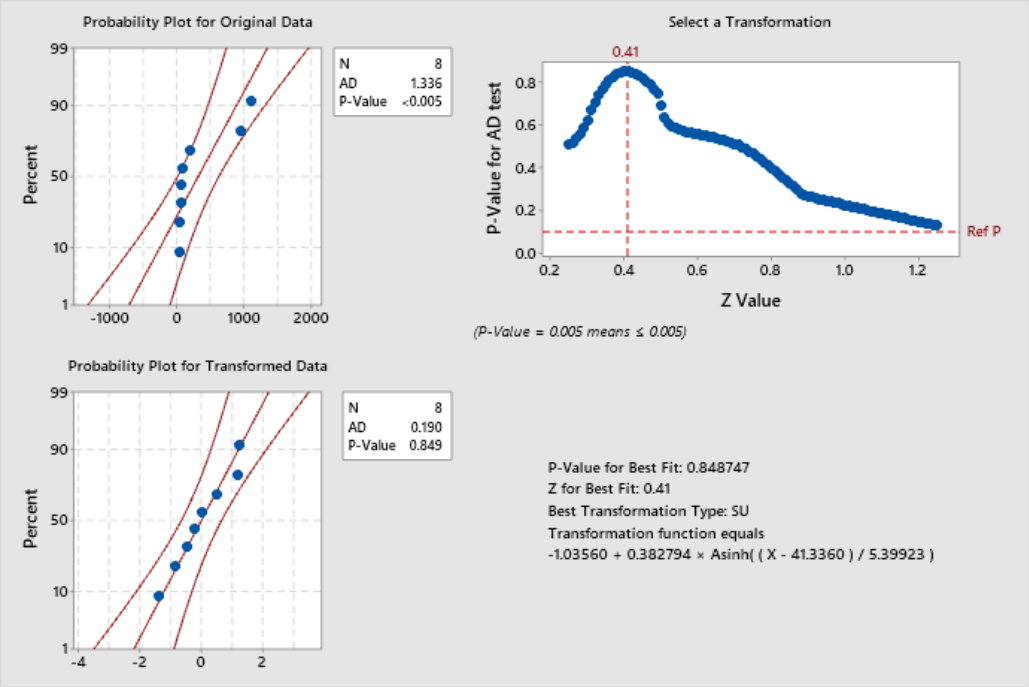

Figure S 1. Data transformation for the effect of bicarbonate concentration on P removal of Al-treated slag

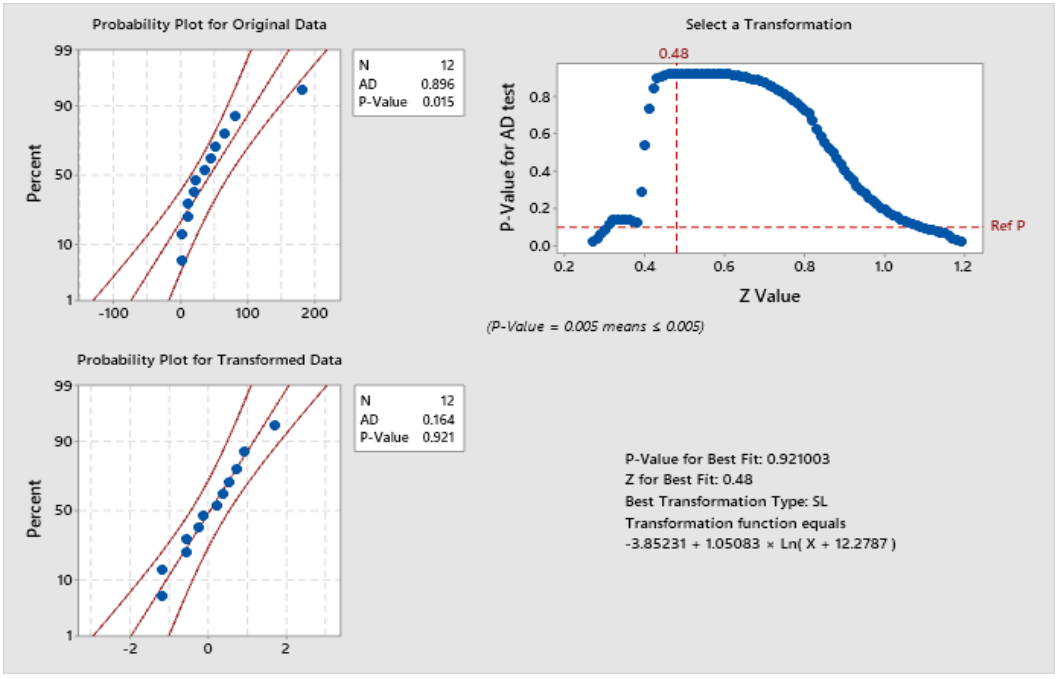

Figure S 2. Data transformation for the effect of Al treatment on P removal of slag for bicarbonate-rich inflow solution

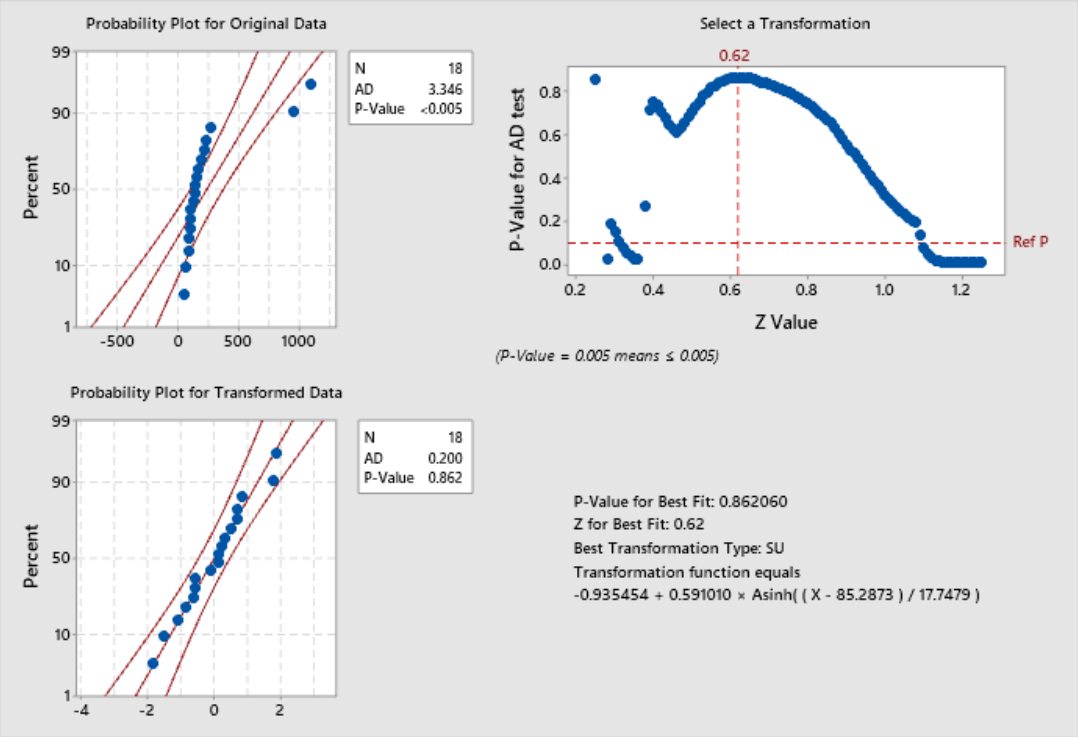

Figure S 3. Data transformation for the effect of incubation time and solution on Al-treated slag

Table S 1. A chronological order of research about application of steel slag as PSM

Year	Type of slag	P removal experiment	Factors studied	CaO%	Maximum DP removal performance		Reference
					P removal capacity (mg/g)	Removal efficiency %	
1986	Steel slag	Batch	pH, T, competing ions, porosity of slag	40.5-42.3	0.034	-	[144]

1987	Steel slag	Aquarium with sediment	Dosage of slag	40.5-42.3	-	98.8	[145]
1993	BFS	Batch	-	42	0.42	-	[146]
1997	BFS, Steel slag	Batch and Column	Type of slag, particle size	-	0.38	-	[147]
1998	BFS, Steel slag	Batch	Oxalate extractable Fe and Al	35-45	44.2	-	[161]
1999	BFS	Batch	Crystalline structure, particle size	35	0.7	-	[58]
2000	BFS	Batch	Crystalline structure, particle size	33.4-35	0.65	-	[162]
2002	EAF	Batch and Column	Physical regeneration treatment	33.2	1.35	-	[91]
2002	Steel slag	Column	Cp, pH, T, particle size, FR	33	60	-	[47]
2003	EAF	CW	pH	-	-	91	[163]
2005	BFS	Batch	Crystalline structure, pH	-	18.94	-	[59]

2006	EAF	Column	PSM composition	30.4	>2.2	-	[49]
2006	BOF	Column	-	32.14	-	100	[164]
2006	Melter slag	WWTP	-	15.9	1.23 (TP)	-	[25]
2006	Steel slag	Batch	pH, CT, Cp	48.43	18	-	[165]
2007	Melter slag	Batch	Redox potential, pH	-	-	-	[166]
2007	EAF	CW	flow regime, filter influent, pH	-	1.7	-	[27]
2007	EAF	Small/pilot-scale column	Scale of P removal setup	27.7	0.3-2	-	[114]
2007	Melter slag, EAF, BOF	Batch including P sock in runoff	-	-	2.6 to 4.5	-	[167]
2008	EAF, Melter slag	Column	Slag type, physical regeneration treatment	-	-	-	[132]
2008	Steel slag	Batch, column	Dosage of slag, pH, T	-	5.3	-	[168]

2009	Melter slag	WWTP	Drying, agitation, crushing of the slag granules	-	-	-	[102]
2009	BOF	Batch	pH, ion strengths	45.4	14.2		[169]
2009	Steel slag	Column	Composition of PSM	45.05	-	99.89	[170]
2009	Melter slag	Batch, waste stabilization pond	Scale of P removal setup	-	0.014 - 1.23	-	[148]
2009	BFS	Lab/pilot-scale waste stabilization pond	Scale of P removal setup	-	30	-	[149]
2009	BOF	Batch, column	pH, Cp, particle size, ionic strength	42-44	8.39	-	[171]
2010	EAF	Pilot-scale CW	Treatment configuration (hybrid or integrated)	30	-	>99	[172]
2010	Melter slag	WWTP	Physical and chemical	-	1.23	-	[115]

			regeneration treatment				
2010	Modified steel slag	Batch, column	Dosage of slag, pH, CT, Cp	49.58	11.12	-	[173]
2010	EAF	CW	Treatment configuration, TSS loading, feeding regime, physical regeneration treatment	-	-	76.11	[69]
2010	EAF	Column	Composition of PSM	-	1.7	-	[174]
2010	EAF	Column	T, organic content	-	-	63-71	[175]
2011	Steel slag	Integrated CTS with CW	-	-	-	96.4	[176]
2011	Steel slag	Lab-scale CW	Composition, treatment configuration	36.13	-	96.2	[177]
2011	Modified steel slag	Batch	Dosage of slag, CT, pH, Cp	40.9	-	99.4	[178]
2011	Melter slag	Batch	Source of solution,	-	-	100	[134]

			chemical regeneration treatment				
2011	EAF	Batch, column, pilot-scale pond filter	Cp, RT	-	0.059	38	[31]
2012	EAF, BOF	Batch	pH, Cp, source of solution	23.8 – 52.9	0.28 - 2.49	-	[74]
2012	EAF	Column	pH, HRT, water velocity	30	3.9	-	[63]
2012	EAF	Batch, P removal structure for suburban runoff	RT	-	0.259	-	[21]
2012	EAF	Trench filter for runoff	Composition of PSM		0.0083	43	[179]
2012	Converter slag	Batch, column	pH, competing ion	40.7	2.27-10.95	-	[180]
2012	Steel slag	Column	Cp, RT	-	-	-	[54]
2013	EAF	Column	Treatment configuration, slag source	28.8-31.7	8.26	99.9	[181]

2013	EAF	Batch, column	Cp, pH, T, dosage of slag, particle size	24.97	-	95	[75]
2013	EAF	Ditch filter	Cp, RT	-	-	-	[150]
2014	Steel slag	Column	Weathering	-	16	-	[182]
2014	EAF, BOF	Lab-scale horizontal flow	Slag type, particle size, composition of PSM	24.9 – 44.1	-	99	[183]
2014	Steel slag	Batch	pH, Cp, CT	-	-	-	[184]
2014	EAF	Field-scale trench	Presence of fertilizer	-	-	49.2	[35]
2014	Steel slag	Batch	-	-	9.4	-	[185]
2014	Steel slag	Field-scale biological aerated filter	-	-	-	90	[186]
2014	BOF	Pilot-scale column	-	33-40	-	96.1-99.9	[187]
2015	AOD	Batch	Cp, dosage of slag, slag modification treatment	-	1.3-27.5	97.8	[87]
2015	Steel slag	Batch, domestic WW reactor	Slag modification treatment	49.75	13.62	-	[188]

2015	BOF	Batch	Cp, T, particle size, pH, dosage of slag	47.08	-	-	[189]
2015	Converter slag	Batch, pilot-scale CW	Slag modification treatment, HRT, Cp	34.51-36.47	9.5 - 12.7	-	[190]
2015	EAF	Full-scale septic tank	Recirculation	40.6	1.9	-	[37]
2015	BOF	Batch, column	Cp, HRT	38.3	8.8	99	[55]
2015	Converter slag	Batch, column	T	-	2.46	-	[191]
2015	Steel slag	CW	-	-	-	-	[192]
2015	Steel slag	Batch	Particle size, dosage of slag, pH, RT, Cp	53.04	1.39	99	[193]
2015	Steel slag	CW	Composition of PSM	-	-	-	[194]
2016	BOF	Batch, column	-	-	0.12-8.78	99	[195]
2016	BOF	Batch	pH	47.08	21-30	-	[196]
2016	EAF	Pilot-scale aerated filter bed	Organic loading rate, HRT	-	-	85-98	[197]

2016	BFS, BOF	Batch	Composition of PSM, preparation process of slag	36.7 – 44.3	0.61 – 3.23	-	[113]
2016	Steel slag	CW	-	-	-	-	[198]
2016	BOF	Batch, lab-scale CW	Organic matter	37.8	0.95 - 3.15	-	[199]
2016	EAF	Batch	Particle size	-	-	-	[200]
2016	EAF	Batch, column	T, CT, pH, competing ions, chemical regeneration treatment	-	1.5	-	[128, 135]
2016	EAF	Column, pond filter, Poultry farm runoff filter, Golf course runoff filter, Runoff interception trenches, Ditch filter structures,	Cp, RT, particle size	-	-	-	[41]

		Storm water basin filter					
2017	BFS	Batch, column	Treatment configuration	-	-	-	[201]
2017	Ladle furnace slag	Batch, column	Slag modification treatment, particle size	-	-	-	[202]
2017	BOF	Batch, column, field-scale CW	Scale of P removal setup	-	-	98-99	[203]
2017	BOF	Batch, small-scale CW	CT, pH, particle size, dosage of slag, scale of P removal setup	36.7	0.146 – 3.57	-	[103]
2017	EAF	Column	Aeration, pH	49.5	-	-	[66]
2017	EAF	Batch, column	HRT, chemical regeneration treatment	-	-	-	[136]
2018	EAF	Batch, column, barrel reactor	Particle size	30	-	-	[204]

2018	EAF, AOD	Column	Mineralogical composition	-	-	-	[205]
2018	Modified steel slag	Batch, column	pH	41.09	21.7	96-98.2	[206]
2018	Steel slag	-	pH, aeration	20.4	-	-	[207]
2018	Steel slag	-	Dosage of slag, pH, RT,	57.78	-	-	[208]
2018	BFS	Pilot-scale reactor for tile	Slag modification treatment, CT	-	-	9.54	[209]
2018	EAF	Batch, column, stormwater filtration	Particle size	-	-	-	[19]
2019	EAF	Batch	T, pH, concentration of nitrate, sulphate, and dissolved organic carbon	-	1.68	-	[210]
2020	Steel slag	Column	Aeration	-	-	55-86	[211]
2020	Steel slag	CW	Dosage of slag, Cp, physical regeneration treatment	43.15	2.98	-	[133]

2020	EAF	Column	Source of solution (organic, inorganic)	30	-	-	[73]
2020	EAF	Pilot-scale septic system	-	30	105	-	[212]
2020	BOF	Column	Particle size, mulch presence	-	-	90-100	[213]
2020	EAF	Subsurface blind inlet, ditch	RT	-	-	55 - 37	[214]
2020	EAF	Horizontal flow column	Cp, dosage of slag, RT	28-55	0.061	-	[215]
2020	EAF	Blind inlet	Particle size	-	-	45	[156]

Curriculum Vitae

Summary of Qualifications

- Interdisciplinary materials science researcher with 6+ years of experience in conducting research in topics such as materials informatics and data science in processing, manufacturing, and characterization of advanced materials including metal matrix composite, metallic foams, self-healing, self-lubricating and self-cleaning materials, surface alloying, corrosion and protection, adsorbents, and nano materials
- Author of 15+ peer-reviewed publications
- 3+ years of experience in teaching undergraduate-level courses including Statistics, Metal Casting Engineering, Methods Engineering, Computer Aided Design

Education

2015 – 2021	Ph.D. in Engineering Major: Industrial & Manufacturing Engineering Minor: Materials Science & Engineering University of Wisconsin Milwaukee, USA **GPA: 4/4** Dissertation title: *Applying a statistical approach to develop a sustainable technology for capturing phosphorous from an agricultural tile drainage system using by-product phosphorous sorbing materials (PSM)* Faculty Advisor: Dr. Hamid Seifoddini
2009 - 2012	M.Sc. in Materials Science & Engineering Sharif University of Technology, Kish Island, Iran **GPA: 4/4** Thesis title: *Investigation and optimization of Ni-P-Zn electrolesss alloy coatings* Faculty Advisors: Dr. Saeed Reza Allahkaram, Dr. Abolghasem Dolati
2004 - 2009	B.Sc. in Materials Science & Engineering IKIU University, Qazvin, Iran

Academic Experiences

- **Graduate Student Researcher**, Centers for Composites and Advanced Materials Manufacture, Department of Materials Science & Engineering, University of Wisconsin – Milwaukee, Nov 2015 – May 2016, Oct 2018 – May 2021

    - Project title: "Surface Texturing, Alloying and Compositing During Manufacturing of Components for Improving Corrosion Resistance of Water Industry

Components", NSF I/UCRC funded project (#1540032), PI: Pradeep K. Rohatgi, Ph.D.

- Led and executed corrosion studies on the surface-alloyed samples
- Drafted four under review journal papers as the first or co-author
- File a US provisional patent as a co-inventor

- Project title: "Scum deposition in pipes, fouling in heat exchangers, and odor generation in Milwaukee Metropolitan Sewage District (MMSD) components", funded by MMSD, PI: Pradeep K. Rohatgi, Ph.D.
  - Conducted comprehensive literature review

- Project title: "Advanced Design and Novel In-situ Synthesis of Self-cleaning and Wear Resistant Metallic Surfaces for Water Industry Components", NSF funded project (#1331532), PI: Pradeep K. Rohatgi, Ph.D.
  - Developed machine learning models to predict surface wettability of different aluminum and iron alloys and composites
  - Drafted eight published/under publications peer-reviewed papers about the results of machine learning and wettability studies
  - Trained and supervised two undergraduate student researchers

- Project title: "Self-healing Corrosion and Wear Resistant Coatings for Components Used in Water Industry", NSF I/UCRC funded project, PI: Pradeep K. Rohatgi, Ph.D.
  - Executed corrosion studies on the developed coatings

- **Graduate Teaching Assistant**, Department of Industrial & Manufacturing Engineering, University of Wisconsin – Milwaukee, Jan 2016 – Jan 2018, Jan 2019 – Jan 2021
  Courses taught:
  - *Introductory Statistics for Physical Sciences and Engineering Students*
  - *Methods Engineering*
  - *Engineering Drawing & Computer Aided Design/Drafting*
  - *Introduction to Engineering*
- **Research Associate Intern,** National Soil Erosion Laboratory, Purdue University, West Lafayette, Indiana, Aug 2019 **–** Sep 2019, Jan 2020 – Feb 2020

  - Project title: "Removing phosphorus from drainage water with phosphorus removal structures", PI: Chad Penn, Ph.D.
    - Studied the effect of tile drainage parameters on phosphorous removal of steel slag
    - Supervised undergraduate student researcher

- **Graduate Research Assistant**, Water Technology Accelerator, University of Wisconsin - Milwaukee, Jan 2018 – Jan 2019
    - Project title: "Advancing Systematic and Fundamental Changes in Agricultural, Water Resources Management", funded by Great Lake Protection Fund (GLPF), PI: Marcia Silva, Ph.D.
        - Led a research team including eight undergraduate/graduate student researchers
        - Developed and supervised a pilot-scale production of functionalized zeolite by lanthanum oxide for phosphorous removal (the developed filter material was later licensed by Zeolite Australia PTY LTD)
        - Designed a prototype of phosphorous removal structure
        - Led field studies on the performance of phosphorous removal technology

- **Graduate Student Researcher**, Advanced Analysis Facility, Department of Materials Science & Engineering, University of Wisconsin – Milwaukee, Jun 2016 – Sep 2016

    - Project title: "Galvanic corrosion of the components used in household water system", funded by private industries in Milwaukee, PI: Benjamin Church, Ph.D.
        - Executed corrosion studies
        - Trained and supervised a graduate student researcher

Publications

Journal Papers

1. **A. Kordijazi**, S. Behera, D. Patel, P. Rohatgi, M. Nosonovsky, Predictive analysis of wettability of Al-Si based multiphase alloys and aluminum matrix composites by machine learning and physical modelling, *Langmuir* (IF: 3.56), 2021 https://doi-org.ezproxy.lib.uwm.edu/10.1021/acs.langmuir.1c00358

2. M. Hasan, **A. Kordijazi**, P. Rohatgi, M. Nosonovsky, Triboinformatics for friction and wear prediction of Al-Graphite composites using machine learning methods, *Journal of Tribology* (IF: 1.83), 2021, https://doi.org/10.1115/1.4050525

3. H. Sadabadi, S. Allahkaram, **A. Kordijazi**, O. Akbarzadeh, P. Rohatgi, Influence of fuel ratio on synthesis and characterization of LaCoO3 perovskite nanoparticles by sol-gel auto-combustion method, *Engineering Reports*. 2020, e12335. https://doi.org/10.1002/eng2.12335

4. **A. Kordijazi**, H. Roshan, A. Dhingra, M. Povolo, P. Rohatgi, M. Nosonovsky, Machine Learning Methods to Predict Wetting Properties of Iron-Based Composites, *Surface Innovation* (IF: 2.84), (2020), 9(2-3), 111-119 https://doi.org/10.1680/jsuin.20.00024

5. **A. Kordijazi**, S. Behera, S. Suri, R. Zhongying, M. Povolo, N. Salowitz, P. Rohatgi, Data-Driven Modeling of Wetting Angle and Corrosion Resistance of Hypereutectic Cast Aluminum-Silicon Alloys Based on Physical and Chemical Properties of Surface, *Surfaces and Interfaces* (IF: 3.72), 20 (2020), 100549. https://doi.org/10.1016/j.surfin.2020.100549

6. O. Akbarzadeh, N. Zabidi, G. Wang, **A. Kordijazi**, H. Sadabadi, S. Moosavi, A. Babadi, N. Hamizi, Y. Wahab, M. Rahman, S. Sagadevan, Z. Chowdhury, M. Johan, Effect of pressure, H_2/CO ratio and reduction conditions on Co-Mn/CNT bimetallic catalyst performance in Fischer-Tropsch reaction, *Symmetry* (IF: 2.64), (2020), 12(5), 698

7. **A. Kordijazi**, D. Wiess, S. Das, S. Behera, H. Roshan and P. Rohatgi, Effect of solidification time on microstructure, wettability and corrosion properties of A205-T7 aluminum alloys, *International Journal of Metalcasting* (IF:1.4), (2021), 15(1), 2-12 https://doi.org/10.1007/s40962-020-00457-8

8. S. Das, **A. Kordijazi,** O. Akbarzadeh, P. Rohatgi, An innovative process for dispersion of graphene nanoparticles and nickel spheres in A356 alloy using pressure infiltration technique, *Engineering Reports*, (2020) e12110

9. O. Akbarzadeh, N. Zabidi, Z. Merican, S. Sagadevan, **A. Kordijazi**, S. Das, A. Babadi, M. Rahman, N. Hamizi, Y. Wahab and M. Johan, Effect of manganese on Co-Mn/CNT bimetallic catalyst performance in Fischer-Tropsch reaction, *Symmetry* (IF: 2.64), 11 (2019) 1328

10. **A. Kordijazi**, Optimization of Ni-P-Zn electroless bath and investigation of corrosion resistance of as-plated coatings, *Materials Research Express* (IF: 1.92), 6 (2019) 096565

Upcoming Journal Papers

1. **A. Kordijazi**, T. Zhao, J. Zhang, K. Alrfou, P. Rohatgi, Application of Machine Learning in Design, Synthesis, and Characterization of Metal Matrix Composites: Current Status and Emerging Applications, *JoM*, Status: *Accepted*

2. K. Rane, M. Beining, S. Behera, **A. Kordijazi**, A. Kumar, Sand casting of surface-alloyed Butterfly Valve with improved hardness and corrosion resistance by incorporating metal powders in-mold coatings, *International Journal of Metalcasting*, Status: *Accepted*

3. K. Rane, **A. Kordijazi**, S. Behera, P. Rohatgi, Laboratory scale casting technique for surface alloying of WCB steel to improve hardness and corrosion resistance, *Journal of Materials Processing Technology*, Status: *Under review*

4. K. Rane, S. Behera, **A. Kordijazi**, A. Kumar, B. Church, R. Dasgupta, P. Rohatgi, Residual stress, adhesion, hardness, and corrosion resistance of surface alloyed layer formed during sand casting of mild steel, *Results in Surfaces and Interfaces*, Status: *Under review*

5. M. Hasan, **A. Kordijazi**, P. Rohatgi, M. Nosonovsky, Triboinformatic modeling dry friction and wear of aluminum base alloys using machine learning algorithms, *Tribology International*, Status: *Under review*

6. J. Zhao, **A. Kordijazi**, C. Valensa, H. Roshan, P. Rohatgi, Flexural Properties of AISI 8630 Steel Foams through Experimental and Simulated Tests, Status: *To be submitted*

7. H. Sadabadi, S. Allahkaram, **A. Kordijazi**, P. Rohatgi, Synthesis of self-healing coatings loaded by nano/microcapsules: A review, Status: *To be submitted*

8. **A. Kordijazi**, M. Beining, K. Rane, S. Behera, P. Rohatgi, Surface alloying of internal surfaces of low carbon steel during sand casting by adding Ni, Ni+Cr, and 316L stainless steel powders to coatings on cores, Status: *To be submitted*

9. **A. Kordijazi**, H. Seifoddini, C. Penn, A statistical approach to study performance of electric arc furnace steel slag as a sustainable phosphorous sorbing material used for agricultural tile drainage system, Status: *To be submitted*

10. O. Akbarzadeh, N. Zabidi, A. Babadi, S. Moosavi, I. Badruddin, **A. Kordijazi**, Y. Wahab, N. Hamizi, S. Sagadevan, T. Khan, S. Kamangar, M. Johan, Effect of temperature, syngas space velocity and catalyst stability on Co-Mn/CNT bimetallic catalyst performance in Fischer-Tropsch reaction, *Chemical Physics Letters*, 2020, Status: *To be submitted*

Book chapter

1. O. Akbarzadeh, **A. Kordijazi**, S. Sagadevan, S. Moosavi, A. Babadi, Y. Wahab, N. Hamizi, Z. Chowdhury, *Syngas to Green Fuel Conversion: Nanocatalysis Approach*, in Advanced Heterogeneous Catalysts Volume 1: Applications at the Nano-Scale, Chapter 18, pp 545-579, ACS Symposium Series V 1359; American Chemical Society: Washington, DC, 2020., DOI: 10.1021/bk-2020-1359.ch018

Conference Proceedings and Presentations

Published Proceedings

1. **A. Kordijazi**, D. Weiss, S. Das, P. Rohatgi, (2021) Manufacturing A206 Aluminum Alloy by Step Sand Casting: Effect of Solidification Time on Mechanical and Surface Properties of the Cast Samples Using Experimental and Simulation Results. In: Perander L. (eds) Light Metals 2021. The Minerals, Metals & Materials Series. Springer, Cham. https://doi-org.ezproxy.lib.uwm.edu/10.1007/978-3-030-65396-5_22

2. **A. Kordijazi**, S. Behera, O. Akbarzadeh, M. Povolo and P. Rohatgi, A statistical analysis to study the effect of silicon content, surface roughness, droplet size and elapsed time on wettability of hypoeutectic cast aluminum-silicon alloys, In: Tomsett A. (eds) Light Metals 2020. The Minerals, Metals & Materials Series. Springer, Cham

3. **A. Kordijazi**, M. Silva, Advancing systematic and fundamental changes in agricultural water resources management, 2018 IEEE Conference on Technologies for Sustainability (SusTech), p. 1-2

4. **A. Kordijazi**, "Electrochemical characteristics of an optimized Ni-P-Zn electroless composite coating", Advanced Materials Research, 1043 (2014) 124-128

Upcoming Proceedings

1. **A. Kordijazi**, S. Behera, A. Jamet, A. Fernández, P. Rohatgi, Predictive analysis of water wettability and corrosion resistance of secondary AlSi10MnMg(Fe) alloy manufactured by vacuum assisted high pressure die casting, 2021, AFS Transaction, Status: *Accepted*

2. H. Ullberg, K. Rane, **A. Kordijazi**, P. Rohatgi, Cast magnesium foam for energy absorption and bone regrowth, Metalcasting Congress 2021, American Foundry Society Status: *Accepted*

Oral Presentations

1. **A. Kordijazi**, P. Rohatgi, Manufacturing A206 Aluminum Alloy by Step Sand Casting: Effect of Solidification Time on Mechanical and Surface Properties of the Cast Samples Using Experimental and Simulation Results, TMS, Mar 2021, Virtual Meeting, Orlando, FL, USA

2. S. Behera, **A. Kordijazi**, P. Rohatgi, Predictive analysis of water wettability and corrosion resistance of secondary AlSi10MnMg(Fe) alloy manufactured by vacuum assisted high

pressure die casting, Metalcasting Congress, American Foundry Society, April 2021, Virtual Meeting, Milwaukee, WI, USA

3. **A. Kordijazi**, H. Roshan, P. Rohatgi, "Application of Artificial Neural Network and Statistical Modeling to Study Water Contact Angle of Ductile Iron: Iron-graphite Composite", MS&T, Nov 2020, Virtual Meeting, Pittsburgh, PA, USA

4. **A. Kordijazi**, M. Nosonovsky, P. Rohatgi, Artificial Intelligence/Machine Learning driven design and synthesis of anti-fouling and anti-corrosion surfaces on components used in the water industry, WEP NSF I/UCRC annual meeting, Nov 2020, Virtual Meeting, Milwaukee, WI, USA

5. **A. Kordijazi**, H. Roshan, P. Rohatgi, Intelligent Materials Manufacturing: Interdisciplinary filed between materials science and engineering, computer science, artificial intelligence, and industrial and manufacturing engineering, UWM Computer Science department's Meet & Greet event, Oct 2020, Virtual Meeting, Milwaukee, WI, USA

6. **A. Kordijazi**, S. Behera, O. Akbarzadeh, M. Povolo and P. Rohatgi, "A Statistical Analysis to Study the Effect of Silicon Content, Surface Roughness, Droplet Size and Elapsed Time on Wettability of Hypoeutectic Cast Aluminum-silicon Alloys", TMS, Feb 2020, San Diego, CA, USA

7. **A. Kordijazi**, K. Rane, S. Behera, P. Rohatgi, "Advanced design and novel in-situ synthesis of corrosion and fouling resistant surface on brass and other components used in water industry and design of experiment to predict their lifespan", WEP NSF I/UCRC annual meeting, Oct 2019, Milwaukee, WI, USA

8. **A. Kordijazi**, M. H. Manjilipour, "Corrosion Resistance of Ni-P-Zn Alloy Deposit Coated by a Sulfate Electroless Bath", TMS, Feb 2017, San Diego, CA, USA

9. **A. Kordijazi**, "Electrochemical characteristics of an optimized Ni-P-Zn electroless composite coating", International Conference on Engineering and Innovative Materials, Sep 2014, Kuala Lumpur, Malaysia

Invited Talks

1. P. Rohatgi, **A. Kordijazi**, AI/ML-driven design and synthesis of anti-fouling, anti-corrosion, and drag reducing materials and surfaces, Artificial Intelligence - Enabled Water-Energy Nexus (AIWEN) IUCRC workshop, Transforming the Water & Wastewater

Industry Through Artificial Intelligence, Co-organized by UChicago, Argonne, WUSL, NU, UWM, MU, Feb 2021, Virtual Meeting

2. **Kordijazi**, M. Silva, "Advancing Systematic and Fundamental Changes in Agricultural, Water Resources Management", 6th IEEE Conference on Technologies for Sustainability, Nov 2018, Long Beach, CA, USA

Patent

- P. Rohatgi, M. Beining, K. Rane, S. Behera, **A. Kordijazi**, Surface alloying of mild steels during casting, Filing Date: October 26, 2020, UWMRF Ref. OTT 1585, Status: *US Patent Pending*

Awards

- Chancellor's Graduate Student Award, University of Wisconsin Milwaukee, Jan 2021
- UWM Graduate Student Excellence Fellowship (GSEF), May 2020
- Chancellor's Graduate Student Award, University of Wisconsin Milwaukee, Mar 2020
- Chancellor's Graduate Student Award, University of Wisconsin Milwaukee, May 2019
- Chancellor's Graduate Student Award, University of Wisconsin Milwaukee, Apr 2018
- Chancellor's Graduate Student Award, University of Wisconsin Milwaukee, May 2017
- Chancellor's Graduate Student Award, University of Wisconsin Milwaukee, Sept 2015

Synergistic activities

Reviewer of 15+ submitted papers for publication in the following journals:

- Ceramics International, Elsevier
- Materials, MDPI
- Surface Innovations, ICE Publishing
- Sustainability, MDPI
- Coatings, MDPI
- International Journal of Metalcasting, Springer
- Electrochem, MDPI

Skills

Technical: Proficient in SEM, EDS, XRD, FTIR, Potentiostat, Electrochemical Impedance Spectroscopy, Spectrophotometer

Computer: Python, IBM SPSS Modeler, Minitab, SAS, AutoCAD, Procore